

Revista Portuguesa *de* Química

Nuclear Magnetic Resonance:
A noninvasive technique in the study
of life processes *in situ*

Twisted Intramolecular Charge Transfer
Reactions: The Role of the Solvent

Co-ordination Chemistry
with Macrocyclic Compounds

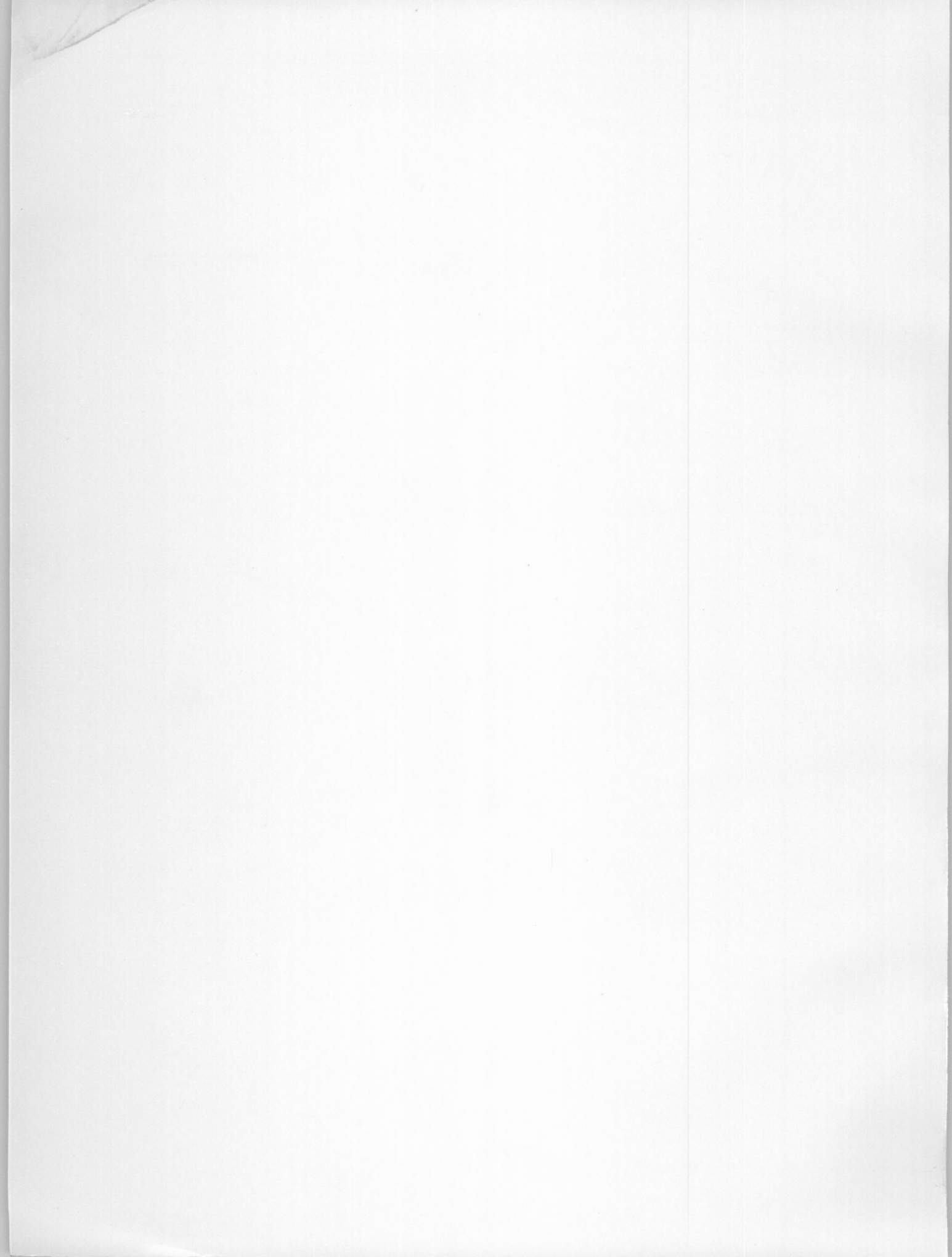
Biological Photosensitizers.
Phototoxic Agents of the Future?



SOCIEDADE
PORTUGUESA
DE QUÍMICA

THE JOURNAL OF
THE PORTUGUESE CHEMICAL SOCIETY

1995



ISSN 0035-0419

DEPÓSITO LEGAL: 79910/94

SGMG: 101240

DIRECTOR E COORDENADOR
DA COMISSÃO EDITORIAL
DIRECTOR AND THE EDITORIAL
BOARD COORDINATOR
Belarmino A. Salvado
Barata

COMISSÃO EDITORIAL
EDITORIAL BOARD

Carlos F.G.C. Gerales
Dep.de Bioquímica
Faculdade de Ciências e
Tecnologia
Universidade de Coimbra
3000 Coimbra

José da Costa Lima
Dep. de Química-Física
Faculdade de Farmácia
Universidade de Porto
Rua Aníbal Cunha, 164
4000 Porto

Carlos Crispim Romão
Instituto de Tecnologia
Química e Biológica
Rua da Quinta Grande, 6
Apartado 127
2780 Oeiras

Carlos Corrêa
Dep. de Química
Faculdade de Ciências
Universidade do Porto
4000 Porto

José Manuel Gaspar
Martinho
Dep. de Engenharia Química
Instituto Superior Técnico
1096 Lisboa Codex

Lélio Lobo
Dep. de Engenharia Química
Faculdade de Ciências
e Tecnologia
Universidade de Coimbra
3000 Coimbra

José J.C. Cruz Pinto
Dep. de Engenharia de
Polímeros
Universidade do Minho
4719 Braga Codex

José Ferreira Gomes
Dep. de Química
Faculdade de Ciências
Universidade do Porto
4000 Porto

Fernando Pina
Dep.de Química
Faculdade de Ciências e
Tecnologia
Universidade Nova de Lisboa
Quinta da Torre
2825 Monte da Caparica

Fernanda Madalena A. Costa
Departamento de Química
Faculdade de Ciências
Universidade de Lisboa
Rua Ernesto de Vasconcelos,
Bloco C1
1700 Lisboa

Propriedade da
Sociedade Portuguesa
de Química
Property of the Portuguese
Chemical Society
Av. da República, 37, 4º
1050 Lisboa, PORTUGAL
Tel.: (351-1) 793 46 37
Fax: (351-1) 755 23 49

DESIGN GRÁFICO DESIGN
Luís Moreira

FOTOCOMPOSIÇÃO TYPING
Cristina Moreira

Impresso na Facsimile,
Offset e Publicidade Lda

TIRAGEM CIRCULATION
2300 exemplares

PREÇO DE VENDA PRICE
1 000\$00 individual personal
2 000\$00 bibliotecas libraries



Publicação subsidiada pela
Junta Nacional de Investigação
Científica e Tecnológica

Nuclear Magnetic Resonance: 3 A noninvasive technique in the study of life processes *in situ*

Ressonância Magnética Nuclear: uma técnica
não invasiva para investigar processos
biológicos *in situ*

HELENA SANTOS, PAULA FARELEIRA,
ANA RAMOS, HELENA PEREIRA,
AND MANUELA MIRANDA

Twisted Intramolecular Charge 12 Transfer Reactions: The Role of the Solvent

Reacções Intramoleculares
de Transferência de Carga com Rotação:
O Papel do Solvente

JAMES T. HYNES

Co-ordination Chemistry 18 with Macrocyclic Compounds

Química de Coordenação
com Compostos Macrocíclicos

RITA DELGADO

Biological Photosensitizers. 30 Phototoxic Agents of the Future?

Fotosensibilizadores Biológicos.
Pesticidas no Futuro?

RALPH S. BECKER AND ANTÓNIO L. MAÇANITA

Nuclear Magnetic Resonance: a noninvasive technique in the study of life processes *in situ*

Ressonância Magnética Nuclear: uma técnica não invasiva para investigar processos biológicos *in situ*

HELENA SANTOS^{1*}, PAULA FARELEIRA^{1,2}, ANA RAMOS¹, HELENA PEREIRA¹, AND MANUELA MIRANDA¹

¹INSTITUTO DE TECNOLOGIA QUÍMICA E BIOLÓGICA, UNIVERSIDADE NOVA DE LISBOA, APARTADO 127, 2780 OEIRAS, PORTUGAL

²ESTAÇÃO AGRONÓMICA NACIONAL, INSTITUTO NACIONAL DE INVESTIGAÇÃO AGRÁRIA, QUINTA DO MARQUÊS, 2780 OEIRAS, PORTUGAL

One of the most attractive aspects of the application of Nuclear Magnetic Resonance to study cellular physiology derives from the noninvasive and nondestructive characteristics of this method; in fact, not only is it possible to monitor substrate consumption and end-product formation, but it is also possible to follow the changes in the concentrations of intracellular metabolites in the same sample. Furthermore, various aspects of the cellular processes can be probed with the different nuclides that can be detected by NMR. For instance, ³¹P-NMR allows monitoring of the energetic status of the cell and the transmembrane proton gradient, and allows measuring of enzyme kinetics *in vivo*, whereas the fate of individual carbon (or nitrogen) atoms through different metabolic pathways can be followed by ¹³C-NMR (or ¹⁵N-NMR); cation gradients as well as cation transport over the cell membrane can be measured with ²³Na- or ³⁹K-NMR in the presence of shift reagents.

A major drawback of *in vivo* NMR techniques is low sensitivity which forces the use of dense cell suspensions in order to increase the total intracellular space that is accessible to detection. However, in many cases these sensitivity limitations are by far overcome by the unique opportunity provided by these measurements to monitor a number of biochemical parameters without disturbing the cellular organization. Examples of our work on the application of this technique to study bacterial physiology *in vivo* are presented.

Um dos aspectos mais atraentes na aplicação de técnicas de Ressonância Magnética Nuclear (RMN) para estudar fisiologia celular deriva das suas características não-destrutivas e não-invasivas; de facto, não só é possível seguir consumo de substratos e formação de produtos finais, mas também, na mesma amostra, detectar variações nas concentrações de metabolitos intracelulares sem interferência nos processos biológicos. A variedade de núclídeos acessíveis a detecção por esta técnica permite a investigação de facetas complementares dos processos celulares. Por exemplo, a RMN de ³¹P permite avaliar o estado energético celular, medir pH intracelular, determinar gradientes protónicos transmembranares ou medir velocidades de reacções *in vivo*, enquanto que a detecção de ¹³C (ou ¹⁵N) permite determinar o percurso de átomos individuais de carbono (ou azoto) ao longo de diferentes vias metabólicas. O transporte de cátions, tais como sódio ou potássio, pode ser estudado usando RMN de ²³Na ou ³⁹K em presença de agentes de desvio apropriados. A maior limitação desta técnica deriva da sua baixa sensibilidade intrínseca, que impõe o uso de suspensões celulares densas com o objectivo de aumentar o espaço intracelular sujeito a detecção. Contudo, em muitos casos, estas limitações são em grande medida ultrapassadas pela oportunidade única que esta técnica oferece de avaliar uma variedade de parâmetros bioquímicos sem perturbação da estrutura e organização celulares. Neste artigo serão usados como ilustração das potencialidades desta metodologia, exemplos dos estudos sobre fisiologia bacteriana efectuados por esta equipa de investigação.

1. Introduction

Nuclear magnetic resonance spectroscopy (NMR) is one of the most powerful analytical methods available to chemists today, allowing, for example, the qualitative and quantitative characterization of chemical mixtures, the measurement of reaction rates in the steady state, the determination of the isotopic distribution within molecules or the determination of the three-dimensional structure of proteins. The tremendous improvement achieved in the performance of spectrometers in the last two decades has made it possible for biochemists to benefit from the capabilities of this technique for carrying out measurements directly on living systems [1-5].

One of the most attractive aspects of the application of this method in the study of cellular processes derives from its noninvasive and nondestructive characteristics: not only is it possible to monitor substrate consumption and end-products formation, but also to follow changes in the levels of intracellular metabolites in the same sample. Moreover, with the high number of nuclides available to NMR, different aspects of cellular processes can be probed by taking a multinuclear approach. For instance, ^{31}P -NMR allows monitoring the intracellular pH [6,7], the energetic status of the cell and the dynamics of intracellular phosphate pools [8]; in favourable cases, enzyme kinetics can be studied *in vivo* [9,10], and unique information on compartmentation can be obtained. By using ^{13}C -NMR, the fate of individual carbon atoms are traced and carbon fluxes through several pathways can be determined [1,11]. Similar kind of information is in principle available by using ^{15}N -NMR, but more severe sensitivity limitations occur in this case. Cation gradients as well as cation transport over the cell membrane are measured with ^{23}Na - or ^{39}K -NMR [12,13]; calcium levels can be measured indirectly by the very sensitive ^{19}F NMR with suitable fluorinated probes [14]. Provided that the required probe heads are available, all this information can be obtained for a single sample by interleaved acquisition of the signals due to different nuclei.

A major drawback of NMR is its intrinsic low sensitivity, which limits *in vivo* observations to metabolites present at concentrations of the order of 0.5 mM or higher. This limitation imposes the use of dense cell suspensions in order to increase the total intracellular space available to detection and, therefore, problems in gas or nutrients supply may arise [5]. However, the low sensitivity turns out as an advantage when the method is applied to complex mixtures such as living cells and tissues since it results in relatively simple spectra as only a few number of resonances are apparent. In many cases, the sensitivity limitations are by far overcome by the unique opportunity provided by these measurements to monitor a number of biochemical parameters without disturbing the cellular organization.

To date, the *in vivo* NMR field has expanded tremendously. The availability of wide bore horizontal magnets of a size sufficient to accommodate a human body has provided an entirely new clinical dimension in the NMR applications. It is now possible to produce metabolic maps with concentration profiles of the major metabolites present, for example, in heart or human brain. Despite the clinical importance of these new developments, commonly referred to as MRS (magnetic resonance spectroscopy) and MRI (magnetic resonance imaging), here we will focus on the applications of *in vivo* NMR to study cell systems, either in suspensions, or when immobilized.

2. Phosphorus-31 NMR studies of whole cells

Energy metabolism

^{31}P has been the most popular nucleus in the studies of biological systems by *in vivo* NMR. This is due to the high relative sensitivity of this nucleus allowing direct detection of many important phosphorylated metabolites as well as noninvasive measurements of intracellular pH, in experiments performed with intact cells, tissues, organs or even humans [15].

The intracellular levels of phosphorylated compounds intimately involved in energy metabolism, such as ATP, ADP and AMP, sugar phosphates or inorganic phosphate, have been assayed by ^{31}P -NMR in many different types of living cells [2,5,15,16]; these noninvasive measurements are particularly useful since the rapid turnover of the observed metabolites and, eventually, their compartmentation in different cellular structures, make the interpretation of the results obtained by classical extraction procedures difficult.

Intracellular metabolites may become unobservable by NMR techniques as a consequence of binding to macromolecular structures, localization in environments with high viscosity, or association with paramagnetic ions; in any of these cases, the resonances may become too broad to be detected. Therefore, the question concerning the observability of di- and triphosphonucleosides in whole cells by NMR is of great importance, specially when considering the consequences for the calculation of phosphorylation potentials [5,17]. Several authors share the opinion that only the freely mobile molecules are available to participate in metabolism and, consequently, the fractions detected by NMR represent the true chemical activity of these metabolites. It is now well established that, in several types of mammalian cells, ADP and Pi are largely unobservable by *in vivo* NMR [5,17-21]. For this reason, considerably higher phosphorylation potentials have been measured in some systems by *in vivo* NMR than by destructive analytical methods [20,22,23].

^{31}P -NMR is the only noninvasive method available to measure intracellular pH: it is possible to estimate pH

in different intracellular compartments and to determine the magnitude of transmembrane pH gradients formed during metabolism in a noninvasive way [15,24]. These measurements are most often made by utilizing inorganic phosphate as an intrinsic probe, although the resonances due to other phosphorus compounds, such as glucose-6-phosphate, 2,3-bisphosphoglycerate and polyphosphate have also been used [15, 24-26]. The application of the method relies on the fact that in aqueous solution the proton exchange between the several ionization species is fast, leading to the observation of a single resonance at a frequency which depends on the relative concentrations of the ionization species. Thereby, the chemical shift of the resulting resonance can be used to determine pH, provided that a reliable calibration curve is available [24,27]. The precision of the method is usually on the order of 0.05 pH unit whereas accuracy is on the order of 0.1-0.2 pH unit. This high precision allows accurate determinations of pH changes although absolute pH values may be affected by the poorer accuracy.

A large volume of work have been done over the last two decades based on pH measurements by NMR: pH homeostasis was demonstrated in a large number of different cell types [28-35]; distinction between different cellular compartments was possible, and the method was applied, for example, to study the pH regulation in cytosolic and vacuolar compartments in yeast and plant cells [36-38].

Typical ^{31}P spectra of a bacterial cell suspension (Figure 1) are characterized by the presence of resonances due to nucleoside triphosphates and nucleoside diphosphates (mainly ATP and ADP), inorganic phosphate, oxidized and reduced forms of nicotinamide adenine dinucleotides (NAD(P)^+ and NAD(P)H) and a complex broad signal due to phosphomonoesters (PME), such as glucose 6-phosphate, glycerophosphate or AMP. The presence of two distinct resonances in the inorganic phosphate region (1 to 3 ppm), assigned to the intracellular and the extracellular inorganic phosphate, reveals the existence of a pH gradient across the cell membrane; from the chemical shifts of these signals, values of 7.1 and 6.5 were inferred for the intracellular and the extracellular pH, respectively. As shown in trace A (Figure 1), high levels of nucleoside triphosphates are detected in cells in the absence of added external substrate: a value of approximately $6 \mu\text{mol} \cdot \text{g}$ (cells dry weight) $^{-1}$ was determined by quantitative ^{31}P -NMR. In this organism the full pool of NTP is detected by NMR. In the absence of an external substrate the energy source for NTP synthesis in this particular bacterium (*Desulfovibrio gigas*) is polyglucose, an endogenous carbon reserve which can be detected in living cells by natural abundance ^{13}C -NMR. When the metabolism of polyglucose was inhibited by addition of fluoride, an inhibitor of the glycolytic pathway, the energy status of the cells decreased drastically as demonstrated by the disappearance of the NTP resonances (Figure 1B); a

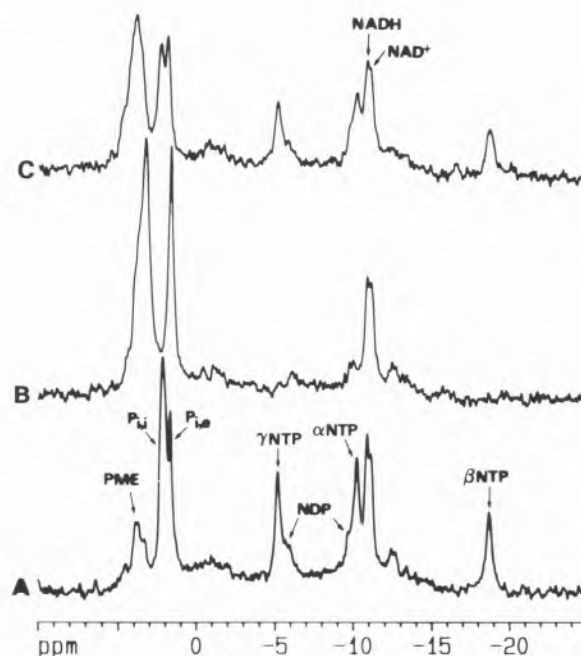


Figure 1 - *In vivo* ^{31}P -NMR spectra of a cell suspension of *Desulfovibrio gigas*. (A) initial spectrum under anaerobic conditions; (B) spectrum acquired after addition of 10 mM NaF to the cell suspension; (C) the argon atmosphere was switched to oxygen. Spectra were obtained at 202.5 MHz, at a probehead temperature of 33°C. PME, phosphomonoesters; $\text{P}_{i,i}$, intracellular inorganic phosphate; $\text{P}_{i,e}$, extracellular inorganic phosphate; NTP, nucleoside triphosphates.

concomitant increase in the intensity of the broad signal due to phosphomonoesters, indicating accumulation of phosphorylated metabolites of the glycolytic pathway, was also observed. Detailed analysis of perchloric acid extracts of cells treated with sodium fluoride showed that 3-phosphoglycerate and glycerol-3-phosphate were the two major intermediate metabolites that accumulated [39].

Most interesting is the observation that upon addition of an electron acceptor, such as oxygen, nitrite or thiosulfate, the synthesis of NTP would resume and consequently the energetic status of the cells would be nearly restored (Figure 1C). *D. gigas* is a strict anaerobe and, therefore, is unable to grow under aerobic conditions. However, as demonstrated by these experiments, it is capable of using oxygen for disposal of the reducing power derived from the utilization of internal carbon reserves, and thereby surviving under temporary aerobic conditions. In fact, not only is it able to utilize oxygen, but also the levels of cellular energization are enhanced by oxygen when aerobic and anaerobic conditions are compared. This can be appreciated in Figure 2 which illustrates an experiment where a cell suspension was subjected to repeated anaerobic/aerobic cycles: for a given cycle the levels of NTP are consis-

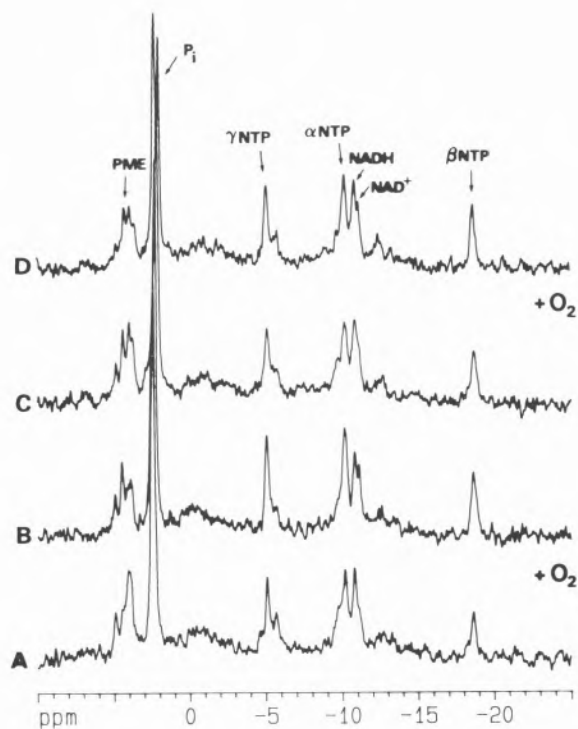


Figure 2 - Effects of alternating between anaerobic/aerobic conditions on the nucleoside triphosphates content of a cell suspension of *Desulfovibrio gigas*, as monitored by *in vivo* ^{31}P -NMR. Gases (argon or oxygen) were delivered directly to the cell suspension in the NMR tube. After acquisition of the first spectrum (A) under argon atmosphere, the gas phase was switched to oxygen and spectrum (B) was acquired; these anaerobic/aerobic cycles were repeated (spectra C-D). Spectra were obtained at 202.5 MHz, at a probehead temperature of 33°C. PME, phosphomonoesters; P_i , inorganic phosphate; NTP, nucleoside triphosphates.

tently higher when oxygen is delivered to the cells than when the cell suspension is made anaerobic by bubbling argon.

At this point it is worth stressing that the non-destructive characteristics of the NMR measurements allowed to monitor, for a single sample, changes in the levels of intracellular phosphorylated metabolites in response to different external conditions.

Detection of unusual phosphorylated metabolites

NMR provides a straightforward way for detecting the unexpected; this is a very important advantage in the studies involving living systems since unknown metabolites can be readily detected without need for separative techniques or special sample treatment. Several unusual metabolites were first detected by *in vivo* NMR. This was the case for cyclic 2,3-diphoglycerate, the unique compound detected in sev-

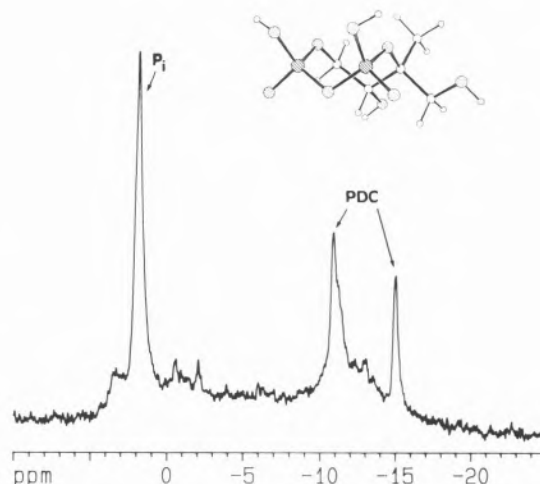


Figure 3 - *In vivo* ^{31}P -NMR spectrum of a cell suspension of *Desulfovibrio desulfuricans* ATCC 27774, showing the presence of high intracellular amounts of a novel phosphoric anhydride diester compound (3-methyl-1,2,3,4-tetrahydroxybutane-1,3-cyclic bisphosphate). The spectrum was obtained at 202.5 MHz, at 33°C. The inset shows the minimum-energy conformation found for the RS isomer of the compound. P_i , intracellular inorganic phosphate; $\text{P}_{i,e}$, extracellular inorganic phosphate; PDC, phosphoric anhydride diester compound.

eral strains of methanogenic archaea [40,41], and which was found to play an important role in the carbohydrate metabolism of these organisms. The presence of high amounts of a novel phosphorus-containing compound in *Desulfovibrio desulfuricans* was also revealed by *in vivo* ^{31}P -NMR [42]. The spectrum obtained from a cell suspension of this strain (Figure 3) is dominated by two strong resonances in the phosphoric anhydride diester region; the chemical shift of one of the phosphorus resonances (-14.8 ppm) is rather unusual in ^{31}P -NMR spectra of living systems, and immediately suggested the uncommon nature of this metabolite. Following extraction and partial purification, its structure and molecular conformation were fully elucidated using a combination of multinuclear NMR techniques [43], and the novel metabolite was identified as 3-methyl-1,2,3,4-tetrahydroxybutane-1,3-cyclic bisphosphate (inset in Figure 3). The intracellular concentration was found to be independent of the stage of growth, ruling out the possibility of being a phosphorus reserve material; so far the physiological role of this metabolite has not been elucidated.

3. Carbon-13 NMR in living systems

The major disadvantage of carbon-13 for NMR applications derives from the low receptivity of this nucleus which is due to a low natural abundance (1.1%) combined with a low absolute sensitivity. As a

consequence of this, the large majority of the metabolic studies utilizing this nuclide use isotopically enriched substrates. The major drawback of these experiments is related with the high cost of specifically labelled compounds; however, this disadvantage is by far overcome by the valuable information unravelled by these labelling studies which allow tracing a specific carbon atom through different metabolic pathways, identifying metabolic pathways and measuring carbon fluxes. The ^{13}C labelling/NMR detection approach allows the identification of intermediate metabolites and end-products without the need to use elaborate analytical and separation procedures and also provides details on the distribution of the label within the same molecule [11,44]. Current studies are directed towards obtaining information about *in vivo* metabolic rates and control of fluxes of central pathways such as glycolysis, gluconeogenesis, and the tricarboxylic acid cycle (TCA). Although most reactions of central pathways of metabolism are well established, there is a severe lack of information on *in vivo* regulation within the different organs and species. *In vivo* ^{13}C -NMR is an indispensable tool in these studies [11]. Examples of the utilization of this method are the determination of metabolic fluxes through the branch point of the TCA cycle and the glyoxylate shunt in *Escherichia coli* and yeast [45,46], the metabolism of pyridine nucleotides in *E. coli* and *Saccharomyces cerevisiae* [47], sugar transport processes in *Zymomonas mobilis* [48] or methanol metabolism in *Hansenula polymorpha* [49].

Labelling experiments and ^{13}C -NMR analysis have also proved very useful in biosynthetic studies. Substrates isotopically enriched on specific positions are provided to the cells and the ^{13}C enriched sites of biosynthetic molecules are identified. This approach has been used, for instance, in the elucidation of biosynthesis of aromatic compounds in yeast [50], antibiotic production by *Streptomyces parvulus* [51], alginate biosynthesis in *Pseudomonas aeruginosa* [52], isoprenoid synthesis in several bacteria [53], or nonactin biosynthesis from acetate, propionate and succinate by *Streptomyces* [54].

Although natural abundance ^{13}C -NMR is in general not useful in metabolic studies, it is the technique of choice for detection and identification of major metabolites, such as freely mobile carbon reserves or compatible solutes (small organic solutes that accumulate intracellularly in response to changes in salinity and/or temperature). In this latter area several novel organic solutes have been recently detected and characterized: *di-myo*-inositolphosphate in the hyperthermophile *Pyrococcus woesei* [55], β -mannosylglycerate in *Rhodothermus marinus* [56] and *Pyrococcus furiosus* [57].

Two examples of our own work were selected in order to illustrate the potentialities of *in vivo* ^{13}C -NMR to elucidate carbon metabolism: in the first one, lactic acid bacteria were the object of study, and information was withdrawn from the labelling pattern analysis of meta-

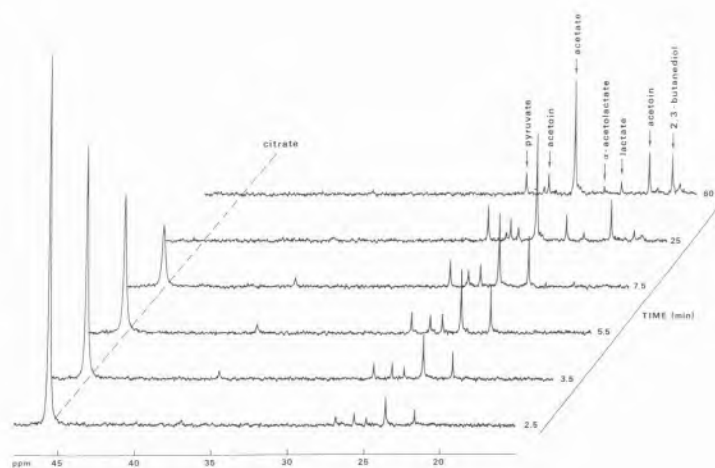


Figure 4 - ^{13}C -NMR spectra showing the time-course for the consumption of $[2,4\text{-}^{13}\text{C}]$ citrate (20 mM) by a cell suspension of *Lactococcus lactis* at pH 5.5. The spectra were obtained at 125.8 MHz, at a probehead temperature of 30°C . Each spectrum represents 30 s of accumulation.

bolites excreted to the external medium; the second example deals with polyphosphate accumulating bacteria where the flux of label is determined from analysis of intracellular carbon reserves *in vivo*.

Studies involving analysis of labelling patterns of extracellular compounds

Citrate is an important precursor of flavour compounds (acetate and diacetyl) in lactic acid bacteria, organisms playing an important role in the production of fermented foods, such as milk derivatives, olives or wine.

The metabolic pathway of citrate degradation by lactic acid bacteria was until recently subject of controversy, due to chemical instability of some of the intermediates in the catabolism, such as α -acetolactate. Two alternative pathways were proposed for the biosynthesis of flavour compounds: one involving the condensation of hydroxyethyl-thiamin pyrophosphate with acetyl-CoA and the other involving the condensation of two molecules of pyruvate to originate α -acetolactate. In the experiment shown in Figure 4, citrate labelled on carbons 2 and 4 was supplied to a cell suspension of *Lactococcus lactis*, and spectra were acquired consecutively until substrate exhaustion. Citrate was consumed at a rate of $180 \mu\text{mol} \cdot \text{min}^{-1} \cdot \text{g}$ (cells dry weight) $^{-1}$ and the label was found on the methyl groups of the end-products acetate, lactate, acetoin and 2,3-butanediol. Resonances due to labelled pyruvate and α -acetolactate were also transiently observed, indicating the existence of carbon flux through pyruvate, and demonstrating that α -acetolactate is in fact the intermediate metabolite in the production of acetoin and 2,3-butanediol [58].

Carbon 13 NMR was also successfully used to characterize the pathways of glucose [59] and citrate

[60] catabolism in *Oenococcus oeni*, a lactic acid bacterium involved in wine production. From the analysis of label present in the end-products (acetate, lactate and erythritol) derived from glucose selectively labelled on different carbon atoms, it was possible to elucidate the pathway for synthesis of erythritol by these wine bacteria [59].

Lactic acid bacteria involved in the production of fermented foods occur in complex media such as milk, meat and wine. Therefore, for the detailed characterization of the fermentation processes it is necessary to study the interactions between the catabolism of different substrates. The interpretation of results from experiments where multiple substrates are supplied is often difficult since the origin of carbon in the end-products cannot be exactly determined. Whenever different substrates are converted to a common intermediate metabo-

lite, the information supplied by analytical methods is insufficient to fully characterize the co-metabolic processes. This is the case for citrate and glucose metabolism in the homofermentative lactic acid bacterium *Lactococcus lactis*, where pyruvate is the central intermediate in the catabolic pathways of both sugar and citrate. By using glucose and citrate labelled on suitable positions, it is possible to determine precisely the origin of each carbon atom in the end-products. According to the metabolic pathways proposed for citrate and sugar catabolism in *L. lactis* (Figure 5), the utilization of [2,4-¹³C]citrate will produce [2-¹³C]acetate, [3-¹³C]lactate, and acetoin or 2,3-butanediol labelled on C-1 and C-4, whereas [1-¹³C]acetate, [2-¹³C]lactate and acetoin or 2,3-butanediol labelled on C-2 and C-3 are derived from the metabolism of [2-¹³C]glucose. The experiment was carried out and the extent of isotopic enrichment in the end-products evaluated from ¹H-NMR spectra of supernatant solutions obtained after centrifugation of the cell suspensions. The presence of an additional substrate caused a stimulation on the rate of citrate utilization and the pattern of end-products was changed; acetate, acetoin and 2,3-butanediol represented more than 80% of the end-products of citrate alone, however, when glucose was also added, 80% of the citrate was converted to lactate. Significant amounts of unlabelled acetate and lactate were found in these spectra, due to the utilization of endogenous reserve compounds even in the presence of exogenously added substrates.

The information derived from the above mentioned experiments can be obtained with certainty from other analytical methods only if all the end-products are determined, the carbon recoveries are 100% for each substrate, the metabolic pathways are well-known, and the contribution of endogenous reserve compounds is negligible [58].

Metabolic studies involving detection of intracellular components

In vivo ¹³C-NMR detection of intracellular pools of metabolites in bacterial suspensions metabolizing isotopically enriched substrates is often precluded by the low concentrations of metabolites and the small proportion of the sample volume occupied by intracellular space. A much more favourable situation is found with organs, such as liver, heart or brain, where many intermediates of glycolysis and the TCA cycle have been monitored *in vivo* [61-64]. Despite these unfavourable conditions, some examples of direct detection of glycolytic intermediates have been reported [65]. Here we will report on our studies on carbon metabolism by a mixed culture of polyphosphate accumulating bacteria obtained from a wastewater treatment plant at Beirilas. Conventional wastewater plants for biological phosphorus removal work on the basis of anaerobic/aerobic cycles. During the anaerobic stage

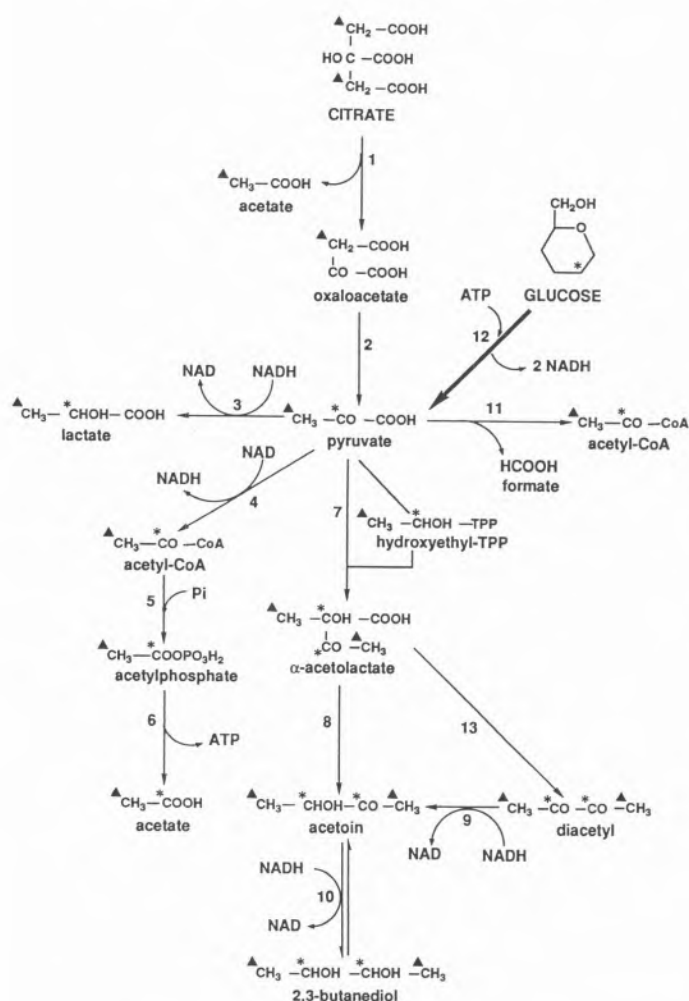


Figure 5 - Pathways of citrate and glucose metabolism in *Lactococcus lactis* showing the labelling pattern on the intermediates and end-products derived from the utilization of [2,4-¹³C]citrate (▲) and [2-¹³C]glucose (*).

inorganic phosphate is released by the biomass and carbon substrates (mainly short chain fatty acids) are taken up and stored as carbon reserves such as polyhydroxyalkanoates. In the aerobic stage carbon reserves are utilized while inorganic phosphate is taken up and intracellularly accumulated as polyphosphate [66]. Enrichment of activated sludge in polyphosphate accumulating microorganisms is only possible due to this metabolic coupling of polyphosphate hydrolysis with synthesis of carbon reserves under anaerobic conditions. In order to elucidate carbon/phosphorus metabolism in this biological system, acetate labelled with ^{13}C on the methyl group was provided to a cell suspension in the beginning of the first anaerobic stage, and the fate of label through anaerobic/aerobic cycles monitored *in vivo* by ^{13}C -NMR. It was possible to follow the flux of label from acetate to hydroxybutyrate /hydroxyvalerate co-polymer in the first anaerobic stage (Figure 6), then to monitor the conversion of these units into glycogen in a subsequent aerobic stage (Figure 7), and afterwards, by subjecting the same sludge to a second anaerobic stage, to observe the flux of labelled carbon from glycogen to the hydroxyvalerate and hydroxybutyrate units (not shown). The uptake/release of inorganic phosphate and the extracellular pH were monitored by ^{31}P -NMR in the same experiments (not shown here). The data provide an unequivocal demonstration of the involvement of glycogen in the biological phosphorus removal process. On the basis of these ^{13}C labelling data, a biochemical model for the synthesis of polyhydroxyalkanoates from acetate and glycogen was elaborated in which the tricarboxylic acid cycle is proposed as an additional source of reduction equivalents. According to this study, with 1 C-mol acetate 1.48 C-mol P(HB/HV) are synthesized, and 0.70 C-mol glycogen are degraded anaerobically, while 0.16 P-mol phosphate is released. In the aerobic stage 1 C-mol of P(HB/HV) is converted to 0.44 C-mol glycogen [67].

4. Proton NMR of living systems

Proton NMR spectra from small metabolites in living animals, perfused organs or cell suspensions should in theory be easily obtained, since the sensitivity of proton detection is much higher than that of ^{13}C or ^{31}P . Thus ^1H NMR methods should allow the detection of lower metabolite concentrations with improved time resolution when compared with ^{13}C detection, without the need of using labelled precursors. Despite these advantages, *in vivo* proton NMR has not been extensively used due to a narrow chemical shift window of ^1H and to interference from the large water signal in biological samples. At present, this can be overcome with special techniques that reduce the water resonance or selectively excite a given spectral region [15,44,68], and the number of useful *in vivo* NMR studies has increased considerably [69-71].

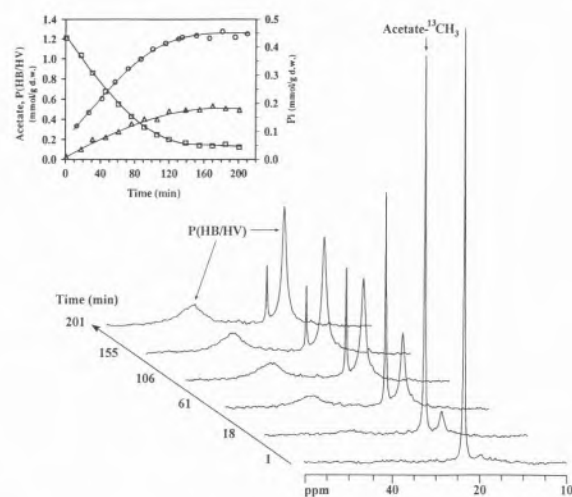


Figure 6 - Time course of phosphate release, acetate consumption and P(HB/HV) formation by activated sludge under anaerobic conditions as monitored by *in vivo* ^{13}C -NMR. The corresponding data are shown in the inset. The cell suspension was supplied with $[2\text{-}^{13}\text{C}]$ acetate at time zero. Spectra were acquired sequentially at the times indicated, alternating between phosphorus and carbon detection. Each spectrum represents 8 min of acquisition. The HB content was determined from the intensities of the resonances due to the methyl group of hydroxybutyrate at 19.7 ppm, after correction for signal saturation; Symbols: inorganic phosphate (\circ); acetate (\square); P(HB/HV) (\triangle). Resonance assignments: $\text{CH}_3(\text{B}_4)$ in P(HB/HV), 19.7 ppm; $\text{CH}_2(\text{B}_2, \text{V}_2)$ in P(HB/HV), 40 ppm; methyl group in $[2\text{-}^{13}\text{C}]$ acetate, 23.9 ppm.

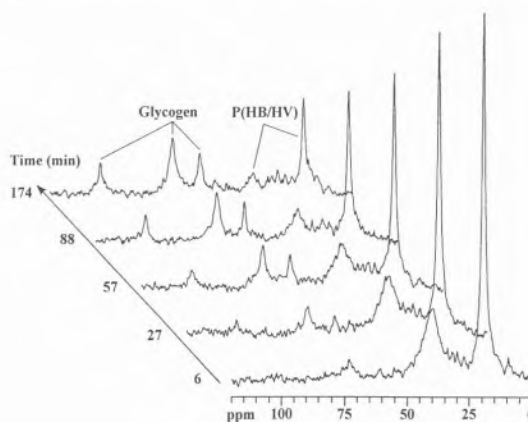


Figure 7 - Time course for the aerobic degradation of P(HB/HV) by activated sludge under aerobic conditions, as monitored *in vivo* by ^{13}C -NMR. Following the experiment shown in Figure 6, oxygen was provided at time zero and spectra were acquired sequentially at the times indicated, alternating between phosphorus and carbon detection. The decrease of resonances due to P(HB/HV) at 19.7 and 40 ppm and the build-up of glycogen (C_1 at 100.2 ppm, C_2+C_5 at 71.7 ppm and C_6 at 61.1 ppm) are clearly observed. The values represented for glycogen refer to the amounts directly detected by NMR.

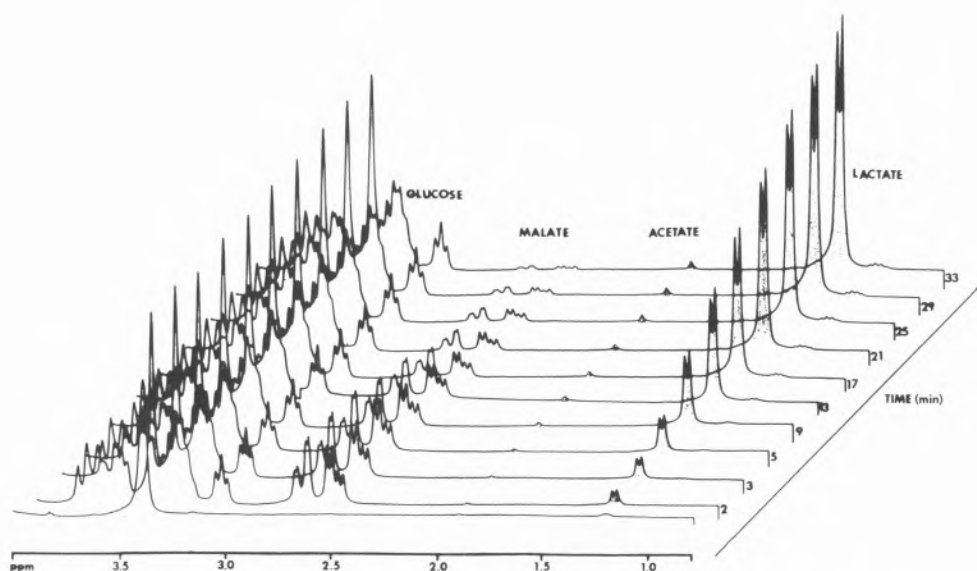


Figure 8 - Time-course for the consumption of L-malate plus glucose (45 mM each) at pH 3.5 by a cell suspension of *Oenococcus oeni* as monitored by $^1\text{H-NMR}$ (300.1 MHz).

$^1\text{H-NMR}$ is also an ideal analytical technique to monitor, on line, kinetics of product formation and substrate consumption. An example is shown in Figure 8 where this technique was used to measure the activity of the malolactic enzyme in a cell suspension of *Oenococcus oeni*. Malolactic fermentation consists of the decarboxylation of L-malate to L-lactate and CO_2 , and its rate is commonly measured by manometric techniques. However, the evaluation of malolactic activity as a function of released CO_2 is only possible when carbon dioxide is not produced by other metabolic reactions. In this experiment, (Figure 8) L-malate was supplied to a cell suspension of *O. oeni* and spectra were acquired consecutively until malate exhaustion. The rate of malolactic fermentation was easily determined by integration of the relevant resonances. Furthermore, when mixed substrates are used the extent of their utilization can also be evaluated from the production of acetic acid which is readily detected by proton NMR (Miranda, M., Veiga-da-Cunha, M., Loureiro-Dias, M. C. and Santos, H., unpublished results).

5. Concluding remarks

Although metabolic studies by NMR have begun only in the 1970s, the field has expanded rapidly and is presently making major contributions to the understanding of metabolic biochemistry in relation to cell physiology. Despite the enormous progress, NMR is unlikely to replace existing methods for metabolic analysis, mainly due to intrinsic insensitivity; however, *in vivo* NMR remains as an indispensable complement because of its valuable noninvasive characteristics.

Acknowledgments

H.S. would like to stress the essential contribution of Professor António V. Xavier for the establishment of this research line in Portugal which began in 1986 on his own suggestion.

References

1. R.G. Shulman, T.R. Brown, K. Ugurbil, S. Ogawa, S.M. Cohen, J.A. den Hollander, *Science* **205** (1979) 160.
2. J.K.M. Roberts, O. Jardetzky, *Biochim. Biophys. Acta* **639** (1981) 53.
3. D.G. Gadian, *Nuclear Magnetic Resonance and its Applications to Living Systems*, Oxford University Press, Clarendon, Oxford, 1982.
4. M. Bárány, T. Glonek, *Methods Enzymol.* **85** (1982) 625.
5. R.S. Balaban, *Am. J. Physiol.* **246** (Cell Physiol. 15) (1984) C10.
6. J.L. Slonczewsky, B.P. Rosen, J.R. Alger, R.M. Macnab, *Proc. Natl. Acad. Sci. U.S.A.* **78** (1981) 6271.
7. K. Nicolay, R. Kaptein, K.J. Hellingwerf, W.N. Konings, *Eur. J. Biochem.* **116** (1981) 191.
8. J.K.M. Roberts, in: *Nuclear Magnetic Resonance*; H.F. Linskens, J.F. Jackson, Eds.; Modern Methods of Plant Analysis, New Series, Vol.2; Springer-Verlag: Berlin, 1986; pp. 43-59.
9. K.M. Brindle, *Prog. Nucl. Magn. Reson. Spectrosc.* **20** (1988) 257.
10. H. Degani, *Quart. Magn. Reson. Biol. Med.* **2** (1995) 53.
11. R.E. London, *Progr. Nucl. Magn. Reson. Spectrosc.* **20** (1988) 337.
12. R.K. Gupta, P. Gupta, R.D. Moore, *Ann. Rev. Biophys. Bioeng.* **13** (1984) 221.
13. C.S. Springer, Jr., *Annu. Rev. Biophys. Biophys. Chem.* **16** (1987) 375.
14. O. Ben-Yoseph, P.G. Morris, H. Bachelard, *Quart. Magn. Reson. Biol. Med.* **1** (1994) 117.
15. P. Lundberg, E. Harmsen, C. Ho, H.J. Vogel, *Anal. Biochem.* **191** (1990) 193.
16. E.J. Fernandez, D.S. Clark, *Enzyme Microb. Technol.* **9** (1987) 259.
17. E. Murphy, S.A. Gabel, A. Funk, R.E. London, *Biochemistry* **27** (1988) 526.
18. M. Stubbs, D. Freeman, B.D. Ross, *Biochem. J.* **224** (1984) 241.

19. F. Desmoulin, P.J. Cozzone, P. Cannoni, *Eur. J. Biochem.* **162** (1987) 151.
20. C.C. Cuningham, C.R. Malloy, G.K. Radda, *Biochim. Biophys. Acta* **885** (1986) 12.
21. S.M. Hutson, G.D. Williams, D.A. Berkich, K.F. LaNoue, *R.W. Briggs, Biochemistry* **31** (1992) 1322.
22. J.K.M. Roberts, A.N. Lane, R.A. Clark, R.H. Nieman, *Arch. Biochem. Biophys.* **240** (1985) 712.
23. H. Santos, P. Fareleira, R. Toci, J. LeGall, H.D. Peck Jr., A.V. Xavier, *Eur. J. Biochem.* **180** (1989) 421.
24. R.J. Gillies, J.R. Alger, J.A. den Hollander, R.G. Shulman, in: *Intracellular pH: its Measurement, Regulation and Utilization in Cellular Functions*; Alan R. Liss Inc.: New York, 1982; pp. 79-104.
25. P.E. Pfeffer, W.V. Gerasimowicz, in: *Nuclear Magnetic Resonance in Agriculture*; P.E. Pfeffer, W.V. Gerasimowicz, Eds.; CRC Press Inc.: New York, 1989, pp. 3-70.
26. M.C. Loureiro-Dias, H. Santos, *Arch. Microbiol.* **153** (1990) 384.
27. R. B. Moon, J. H. Richards, *J. Biol. Chem.* **248** (1973) 7276.
28. J.M. Salhany, T. Yamane, R.G. Shulman, S. Ogawa, *Proc. Natl. Acad. Sci. USA* **72** (1975) 4966.
29. J.L. Slonczewski, B.P. Rosen, J.R. Alger, R.M. Macnab, *Proc. Natl. Acad. Sci. USA* **78** (1981) 6271.
30. T. Kallas, F.W. Dahlquist, *Biochemistry* **20** (1981) 5900.
31. J.K.M. Roberts, D. Wemmer, P.M. Ray, O. Jardetzky, *Plant Physiol.* **69** (1982) 1344.
32. M. Satre, J.-B. Martin, *Biochem. Biophys. Res. Commun.* **132** (1985) 140.
33. R.R. Kay, D.G. Gadian, S.R. Williams, *J. Cell Sci.* **83** (1986) 165.
34. M. Ginzburg, R.G. Ratcliffe, T.E. Southon, *Biochim. Biophys. Acta* **969** (1988) 225.
35. H. Santos, P. Fareleira, J. LeGall, A. V. Xavier, *Methods Enzymol.* **243** (1994) 543.
36. G. Navon, R.G. Shulman, T. Yamane, T.R. Eccleshall, K.-B. Lam, J. J. Baronofsky, J. Marmor, *Biochemistry* **18** (1979) 4487.
37. J.K.M. Roberts, P.M. Ray, N. Wade-Jardetzky, O. Jardetzky, *Nature* (London) **283** (1980) 870.
38. P. Brodelius, H.J. Vogel, *J. Biol. Chem.* **260** (1985) 3556.
39. H. Santos, P. Fareleira, A.V. Xavier, L. Chen, M.-Y. Liu, J. LeGall, *Biochem. Biophys. Res. Commun.* **195** (1993) 551.
40. R.J. Seely, D.E. Fahrney, *J. Biol. Chem.* **258** (1983) 10835.
41. S. Kanodia, M.F. Roberts, *Proc. Natl. Acad. Sci. USA* **80** (1983) 5217.
42. H. Santos, P. Fareleira, C. Pedregal, J. LeGall, A.V. Xavier, *Eur. J. Biochem.* **201** (1991) 283.
43. D.L. Turner, H. Santos, P. Fareleira, I. Pacheco, J. LeGall, A.V. Xavier, *Biochem J.* **285** (1992) 387.
44. J.R. Alger, in: *NMR in Living Systems*; T. Axenrod and G. Ceccarelli, Eds. D. Reidel Publishing Company, Dordrecht, 1986; pp 231-264.
45. K. Walsh, D.E. Koshland Jr., *J. Biol. Chem.* **259** (1984) 9646.
46. B. Sumegi, M.T. McCammon, D. Sherry, D.A. Keys, L. McAllister-Henn, P.A. Srere, *Biochemistry* **31** (1992) 8720.
47. C.J. Unkefer, R.E. London, *J. Biol. Chem.* **259** (1984) 2311.
48. S.M. Schobert, A.A. de Graaf, *Anal. Biochem.* **210** (1993) 123.
49. J.G. Jones, E. Bellion, *Biochem. J.* **280** (1991) 475.
50. T. Ogino, C. Garner, J.L. Markley, K.M. Herrmann, *Proc. Natl. Acad. Sc. USA* **79** (1982) 5828.
51. L. Inbar, A. Lapidot, *J. Bacteriol.* **173** (1991) 7790.
52. A. Narbad, M.J.E. Hewlins, P. Gacesa, N.J. Russel, *Biochem. J.* **267** (1990) 579.
53. M. Rohmer, M. Knani, P. Simonin, B. Sutter, H. Samh, *Biochem. J.* **295** (1993) 517.
54. D.M. Ashworth, J.A. Robinson, D.L. Turner, *J. Chem. Soc., Chem. Commun.* (1982) 491.
55. S. Scholz, J. Sonnenbichler, W. Schafer, R. Hensel, *FEBS Lett.* **306** (1992) 239.
56. O.C. Nunes, C.M. Manaia, M.S. da Costa, H. Santos, *Appl. Environ. Microbiol.* **61** (1995) 2351.
57. L.O. Martins, H. Santos, *Appl. Environ. Microbiol.* **61** (1995) 3299.
58. A. Ramos, K.N. Jordan, T.M. Cogan, H. Santos, *Appl. Environ. Microbiol.* **60** (1994) 1739.
59. M. Veiga da Cunha, P. Firme, M.V. SanRomão, H. Santos, *Appl. Environ. Microbiol.* **58** (1992) 2271.
60. A. Ramos, J.S. Lolkema, W.N. Konings, H. Santos, *Appl. Environ. Microbiol.* **61** (1995) 1303.
61. L.B. Pasternack, D.A. Laude, Jr., D.R. Appling, *Biochemistry* **33** (1994) 7166.
62. C.T. Evans, B. Sumegi, P.A. Srere, A.D. Sherry, C.R. Malloy, *Biochem. J.* **291** (1993) 927.
63. J.F. Mason, D.L. Rothman, K.L. Behar, R.G. Shulman, *J. Cereb. Blood Flow Metab.* **12** (1992) 434.
64. C.R. Malloy, A.D. Sherry, F.M.H. Jeffrey, *J. Biol. Chem.* **263** (1988) 6964.
65. J.A. denHollander, K. Ugurbil, R.G. Shulman, *Biochemistry* **25** (1986) 212.
66. G. W. Fuhs, M. Chen, *Microbiol. Ecol.* **2** (1975) 119.
67. H. Pereira, P.C. Lemos, M.A.M. Reis, J.P.S.G. Crespo, M.J.T. Carrondo, H. Santos, *Water Research*, in press.
68. M. Gussoni, A. Vezzoli, F. Greco, R. Consonni, M. Pegna, H. Molinari, L. Zetta, *Quart. Magn. Reson. Biol. Med.* **1** (1994) 9.
69. W. Chen, E.J. Novotny, X.-H. Zhu, D.L. Rothman, R.G. Shulman, *Proc. Natl. Acad. Sci. USA* **90** (1993) 9896.
70. W. Chen, M.J. Avison, G. Bloch, R.G. Shulman, *Magn. Reson. Med.* **31** (1994) 576.
71. R.G. Shulman, A.M. Blamire, D.L. Rothman, G. McCarthy, *Proc. Natl. Acad. Sci. USA* **90** (1993) 3127.

Twisted Intramolecular Charge Transfer Reactions: The Role of the Solvent

Reacções Intramoleculares de Transferência de Carga com Rotação: O Papel do Solvente

JAMES T. HYNES

DEPARTMENT OF CHEMISTRY AND BIOCHEMISTRY - UNIVERSITY OF COLORADO, BOULDER, CO 80309-0315, U.S.A.

The title topic is reviewed in the context of the excited electronic state photoreaction of dimethylaminobenzonitrile in solution and a recent theoretical study by Fonseca et al. in which a two-dimensional perspective, involving a twist coordinate and a solvent coordinate, is used to understand the reaction.

A revisão das reacções referidas em título é feita no contexto da fotoreacção do estado electrónico excitado do dimetilaminobenzonitrilo em solução. O estudo teórico recente de Fonseca et al., no qual é apresentada uma perspectiva bidimensional, considerando uma coordenada para a reacção e outra para o solvente é usado na compreensão da reacção.

1. Introduction

Over twenty years ago, Grabowski et al. [1] introduced the Twisted Intramolecular Charge Transfer (TICT) conceptual framework to explain, via a photoreaction, the dual fluorescence [2] of electronically excited dimethylaminobenzonitrile (DMABN) in polar solvents. Since that time, the dual fluorescence phenomenon — which has been found to occur in a wide variety of molecules in which the electron donor and electron acceptor units are joined by a single bond [3-5] — has been most frequently interpreted via the TICT picture [3-14]. Such excited electronic state electron transfer reactions, aside from their intrinsic interest, form an important reaction class in which — as opposed to, e.g., ground electronic state, outer sphere electron transfer reactions [15], the electron transfer is supposed to be coupled to a large amplitude nuclear coordinate motion in the molecule — a twisting motion. There has been considerable work on TICT since the initial efforts [3-14, 16-27], and there are a number of excellent reviews detailing the scope and characteristics of TICT reactions [5].

But, as will be described below, there remain various questions as to how to view and to describe TICT reactions in solution, and even fundamental questions about the identity of the reaction coordinate. The present review is focused on a recent theoretical study by Fonseca et al. [20] of TICT for DMABN in solution and aims to shed light on some of these issues. The focus is on DMABN, the classic TICT molecule, and the role of the solvent in the TICT reaction.

2. TICT and the Role of the Solvent

It is useful to first briefly review the original TICT concept in the context of the DMABN dual fluorescence. The picture is that a fluorescent, locally excited (LE) state, in which the molecule is nearly planar, is produced as a result of photoexcitation. This state is the origin of the normal fluorescence. In polar solvents, a twisting in the dihedral angle between the dimethylamino group and the benzonitrile plane, accompanied by a charge transfer from the amino group to the ring system, produces the twisted charge transfer state, as indicated in Fig. 1. (The twisting would break any conjugation between the two groups, and localize the transferred charge.) The latter state, with a nearly perpendicular geometry, is responsible for the additional, "anomalous" fluorescence at lower energies.

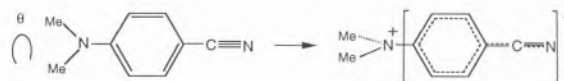


Figure 1. The excited state DMABN reaction in the TICT picture.

That the solvent is important for the DMABN TICT reaction is established by the fact that the anomalous fluorescence is absent for DMABN in the gas phase and in nonpolar, low polarizability solvents. In polar solvents, the anomalous fluorescence is continually red-shifted with increasing solvent polarity [5], indicating increasing solvent stabilization of the charge transferred product state produced in the photoreaction.

A further role of the solvent — a slowing of the photoreaction in solvents of increasing viscosity [5] — was used to support the notion that a large amplitude nuclear twisting motion (opposed by the solvent) is central to the reaction process. Over the years, this solvent viscosity effect has been regarded as a primary experimental support for the TICT picture, but it is very important to appreciate, in view of the discussion below, that there is other experimental evidence supporting the essential role of the intramolecular twisting motion. For example, molecular compounds with bridges, such that the twisting of the amino group is precluded or severely inhibited, do not display the anomalous fluorescence band [5].

So far, everything seems clear and consistent. We now turn to various experimental results which cloud this simple and attractive picture.

As noted above, the notion of the key participation of the solute twisting motion in the TICT reaction was supported by an observed slowing of the reaction in solvents of increasing viscosity, and various inverse power law dependencies of the rate constant on the solvent viscosity have since been established [11]. In the simplest interpretation, the reaction coordinate would be the twist angle of the DMABN solute, and the inverse solvent viscosity effect would be interpreted as a solvent dynamical frictional effect on that motion.

An alternate possibility arose from the striking findings by Kosower and Huppert [27] in their studies of ICT (intramolecular charge transfer) aryl sulfonates in alcohol solvents. In particular, the reaction rate correlated linearly with the inverse longitudinal dielectric relaxation time of the solvent τ_L . This work was quite influential in many subsequent solvation dynamics studies, but for the present purposes, it can be identified as the initial source of a different perspective for ICT systems in general and possibly TICT systems: the reaction coordinate is a solvent collective coordinate — measuring the state of the electrical, orientational polarization of the solvent, and the inverse τ_L dependence is a solvent dynamical frictional effect on that motion. (The larger is τ_L the slower is the orientational motion of the solvent molecules, and the slower is motion along the solvent coordinate.)

In this latter connection, the subsequent studies of Fonseca, Barbara and coworkers [18] on the excited state ICT reaction of bianthryl in solution are particularly germane. A key feature of bianthryl in the present context is that the molecule is *pre-twisted* in the ground electronic state, due to steric repulsions between the two anthracene rings joined by a carbon-carbon single bond. Fonseca, Barbara and coworkers were able to successfully describe the kinetics and solvent dependence on the excited state bianthryl ICT reaction via a picture in which the reaction coordinate is the solvent, with solvent dynamical effects correlated with τ_L giving a frictional suppression of the reaction rate. No twisting was required in the description.

One possibility then is that, in the general TICT case, the reaction coordinate is the solvent, and not the solute twist. However, this is not very plausible for the general case. For example, the bianthryl example above features a crucial pretwist in the ground state, thus presumably reducing the need for extensive further twisting in the excited state. In addition, Su and Simon [13] found that the rate constant for TICT formation in cold alcoholic solvents could exceed the inverse τ_L value of the solvent, i.e., reaction was faster than solvation dynamics; this is an impossible situation if the reaction coordinate is the solvent coordinate. Finally, there remains the previously mentioned solvent viscosity dependence, favoring the twist as the reaction coordinate.

Finally, to the two contrasting scenarios above, must be added a third, based on the experimental results of Eisenthal and coworkers [11] on DMABN kinetics in a series of nitrile solvents. These workers observed a linear correlation between the logarithm of the rate constant with the solvent polarity scale $E_T(30)$, the rate accelerating in more polar solvents. This was interpreted as a static solvent polarity effect on the free energy barrier height for the reaction, a barrier lowering as the solvent polarity increases. Further, when rate measurements were performed in a series of nitrile solvents and solvent mixtures where the solvent polarity — as measured by $E_T(30)$ — was held constant, the reaction rate was found to be essentially *independent* of the solvent viscosity [11]. (A similar conclusion will hold with respect to τ_L .) The picture here would be that the reaction coordinate is the DMABN twist angle, but the motion in that coordinate is not significantly frictionally opposed by the solvent viscosity. In addition, solvent dynamics plays no role, but there is a strong *static* solvent effect on the activation free energy barrier height for the reaction.

In summary then, the experimental results reviewed briefly here paint quite different (and even mutually inconsistent) pictures of the solvent role in the DMABN TICT photoreaction. We now describe how the theoretical study of Ref. 20 can help to clarify the situation.

3. A Two-dimensional View of TICT

A significant issue to be resolved, in view of the discussion above is the identity of the reaction coordinate for the DMABN TICT photoreaction, with the two opposing, limiting views being that it is either the twist coordinate or a solvent coordinate. The approach adopted by Fonseca et al. [20] was to theoretically examine the photoreaction free energy surface in these two dimensions simultaneously and to find the reaction coordinate in that two-dimensional space. This approach allows the possibility, in principle, that either limiting case could emerge, but is not *a priori* biased in favor of either limit, and indeed allows for the possibility that some more complicated mixed coordinate could emerge.

The initial focus of Ref. 20, also adopted here, is on the DMABN reaction in acetonitrile solvent, a representative of the dipolar, aprotic solvent class. The reaction is then examined for different solvent polarities within this solvent class, and finally attention is turned to the situation for hydroxylic hydrogen-bonding solvents such as the alcohols.

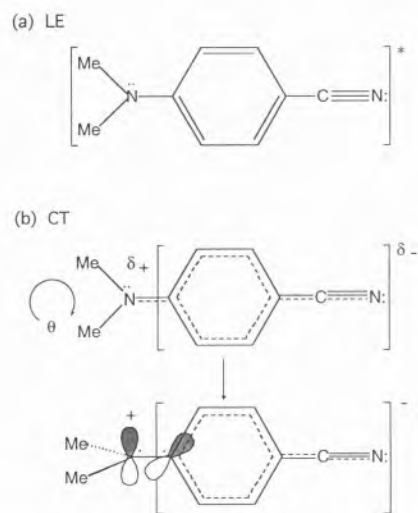


Figure 2. The LE and CT VB states.

The theoretical description [20] has several key ingredients, very briefly described here. The first is a simplified two valence bond (VB) state description for the DMABN electronic structure in solution. These two states — whose energies and dipole moments are approximately extracted from an earlier *ab initio* gas phase study by Kato and Amatatsu [16] — are, respectively, a low polarity LE state ψ_{LE} and a highly polar charge transfer (CT) state ψ_{CT} , whose dipole moment increases with increasing twist angle θ within the DMABN molecule (see Fig. 2). These two VB states are coupled by an electronic resonance coupling $\beta(\theta)$, which declines with increasing twist θ , as the overlap between ψ_{LE} and ψ_{CT} diminishes. Their contribution to the wave function

$$\Psi = c_{LE} \psi_{LE} + c_{CT} \psi_{CT}$$

describing the DMABN electronic structure has to be found as a function of the two coordinates of the problem: the DMABN twist angle θ and a solvent coordinate s . The latter is a gauge of the collective dielectric polarization in the solvent, treated in the dielectric continuum description. Small values of s correspond to solvent polarization appropriate to equilibrium with the LE state, while large values correspond to equilibrium with the fully twisted CT state. It is important to stress

that the solvent is *not* assumed to be in equilibrium with the instantaneous charge distribution in the DMABN solute. Rather, s is an independent variable, and is allowed to adopt values corresponding to nonequilibrium solvent polarizations; indeed, this is absolutely necessary to have a two-dimensional description.

With these ingredients, a Schrödinger equation is solved to determine both the VB weights [$c_{LE}(\theta, s)$, $c_{CT}(\theta, s)$] and the nonequilibrium free energy surface $G(\theta, s)$ for the reaction system in the excited electronic state. The photoreaction transition state is found by locating the saddle point on the surface, which gives activation free energy ΔG^\ddagger for the reaction, and the reaction rate constant is determined as the Transition State Theory value on this two dimensional surface [20]. For the moment, we focus on the overall free energetics and activation free energetics for the DMABN photoreaction, and return below to the issue of the reaction coordinate.

The first results of the theoretical description above are estimates for the thermodynamic reaction free energy ΔG_{rxn} and the kinetic signatures, the rate constant k and the barrier height ΔG^\ddagger . These compare reasonably well with the values inferred from experimental extrapolation [20] (e.g., ΔG^\ddagger is estimated theoretically as ≈ 2 kcal/mol, while the extrapolation from experiments for DMABN in other nitrile solvents is ≈ 1.9 kcal/mol.) These estimates were sufficiently reasonable for CH_3CN solvent to inquire from the theoretical formulation what the effect of changing the solvent would be (but still within the dipolar aprotic solvent class, for which the dielectric continuum solvent description is most plausible).

In the continuum model employed, the solvent polarity is varied by varying the solvent static dielectric constant. When this is done, an approximately linear correlation is found between the activation free energy ΔG^\ddagger and the overall reaction free energy ΔG_{rxn} . This behavior is in perfect accord with the trend established experimentally by Eisenthal and coworkers [11] for DMABN in nitrile solvents. Thus, with increasing solvent polarity, as the reaction becomes less endothermic or more exothermic in free energy terms, the activation free energy barrier drops. (Thus, in a sense, the long appreciated solvent stabilization of the CT product state is transmitted to the barrier.) This pronounced static solvent effect can be analyzed more deeply [20] to display behavior completely consistent with the Hammond postulate. As the solvent polarity increases, the transition state is “earlier” and moves to smaller twist angles, i.e., the transition state more closely resembles the reactant. The percentage CT character of the transition state also declines with increasing solvent polarity, in a completely consistent fashion [20].

We next turn to the reaction coordinate, or more generally the reaction path on the two dimensional free energy surface for DMABN in acetonitrile. This path is the solution phase analogue [28] of the intrinsic reaction path introduced by Fukui [29] for gas phase reactions,

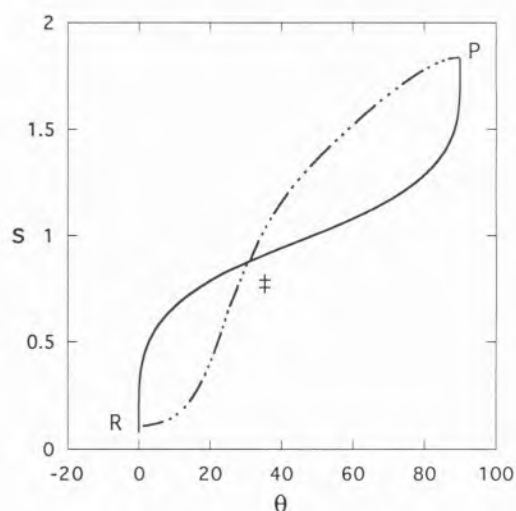


Figure 3. Reaction paths in acetonitrile (—) and in methanol (---).

and is the steepest descent path on the surface from the transition state, leading back to the LE reactant and forward to the CT product. It is found that, in the vicinity of the transition state, this path lies mainly in the direction of the twist coordinate, which is thus the approximate reaction coordinate for the TICT reaction (see Fig. 3). That this should be so for DMABN in acetonitrile is a consequence of the fact that (in mass-weighted coordinates) the gradient of the free energy surface is steeper in the twist angle direction than it is in the solvent coordinate direction. The latter is in part determined by the solvent frequency (which can be determined from the initial "inertial" time dependence in time dependent fluorescence [30]), which is low on the scale set by the frequency associated with the twist angle gradient. In this sense, acetonitrile is a "slow" solvent — there is almost no time for the solvent to move in the rapid passage through the saddle point, transition state region, and the reaction coordinate is the twist. (The solvent reorganization necessary for the reaction to occur takes place early in the reaction path, *before* the critical passage through the transition state region [20]).

Armed with this result, one can understand why, as observed experimentally for DMABN in nitrile solvents [11], there should be a negligible rate dependence on the solvent viscosity, even though the reaction coordinate is the twist. According to Grote-Hynes (GH) theory [31], which has been found to be highly successful in describing a wide variety of reaction classes in solution [32], the solvent frictional influence on the transition state passage is determined by events on the very short time scale ω_b^{-1} associated with the frequency ω_b of the reaction barrier (within a mass factor, the latter is the absolute magnitude of the curvature of the free energy barrier in the transition state neighborhood). For

DMABN in acetonitrile and similar solvents, the barrier frequency is sufficiently high, and the critical time scale sufficiently short, that no slower, longer time solvent motions — which are responsible for the solvent's viscosity — can play any significant role in slowing the reaction. (The same argument applies to any τ_L dependence, which while it would not enter directly since the reaction coordinate is the DMABN twist and not the solvent coordinate, is nonetheless conceivable in practice [33].)

In summary, the theoretical study of DMABN in acetonitrile and similar dipolar, aprotic solvents [20] is in every way consistent with the experimental results of the Eisenthal group [11] on DMABN TICT kinetics in nitrile solvents: there is a strong static solvent polarity effect on the photoreaction barrier height, but not a significant dynamical solvent viscosity (or τ_L) effect on the rate. The reaction coordinate is the twist.

But what of other solvents, in particular hydroxylic solvents like the alcohols? Here the experimental evidence reviewed in the second section appeared to favor a different picture. To understand the situation there, Fonseca et al [20] performed a model study in which, all things remaining the same as for acetonitrile solvent, the solvent frequency for acetonitrile was replaced by the solvent frequency for methanol. The latter is almost four times the former, reflecting the fact that on a short time scale, methanol is a "fast" solvent due to the rapid small amplitude inertial motion of the OH group [34]. (On a longer time scale, methanol is a slower solvent than is acetonitrile, due to slow dynamics of hydrogen bond breaking; but in the first instance it is the short time behavior of the solvent that is critical here.) Now, in contrast to the "slow" acetonitrile solvent situation, methanol is fast, the gradient in the solvent coordinate is large, and the reaction coordinate is essentially in the solvent coordinate! [20] (See Fig. 3).

This key observation, which was possible due to the two-dimensional perspective, indicates that TICT photoreaction dynamics can be quite different in the hydrogen-bonding alcohol solvents. Whether the fact that the reaction coordinate is now the solvent coordinate will in turn lead to a τ_L solvent dynamical influence on the rate awaits further elucidation, but some preliminary remarks can be made here.

All other things being equal, the alcohols tend to be highly polar solvents. In view of the strong solvent polarity-reaction barrier height correlation noted above, this implies that there can be very low reaction barriers for DMABN in these solvents, and thus low barrier frequencies. In such a case, with the reaction coordinate being the solvent coordinate, the GH theory arguments above would lead to the conclusion that now there is enough time during the transition state passage for longer time solvent dynamical friction effects to play an important retarding role for the reaction rate. Thus now a τ_L dependence should be expected [35].

In the limit where there is no longer any barrier, one will have a more complex situation: there will no longer be a well-defined rate constant, i.e., there will be complex nonexponential kinetics [5, 12, 13, 36]. We say no more about this here, but we point out that in cold, alcoholic solvents, the lower temperature will itself increase the effective polarity of the solvent and assist in obliterating any barrier for the photoreaction. Again, the static solvent effect for the reaction will be the key.

4. Concluding Remarks

The DMABN TICT reaction thus appears to be one where the role of the solvent is a multi-faceted one: statically influencing the reaction energetics and kinetic barrier heights, altering the character of the reaction coordinate, and sometimes dynamically opposing the passage in that reaction coordinate over the reaction barrier. It is difficult to name another reaction where such a rich and often bewildering variety is displayed.

The work [20] briefly and qualitatively summarized here is only a beginning, and much more remains to be done, not only for DMABN but also for other TICT (or potentially TICT) molecules. Among the most pressing tasks, we would list the following. First, a more accurate vacuum electronic structure needs to be incorporated in the description. Indeed, new gas-phase calculations are now available [26] and show some differences from earlier work [16] on which Ref. 20 was based. We expect only quantitative, rather than qualitative, differences to result in the solution phase (where the reaction actually occurs), but this must be verified. Second, the alcoholic solvents need to have a complete, quantitative treatment to unravel the rich and complex kinetic behavior projected above. Finally, the entire treatment should be generalized to have a molecular, rather than a continuum, description of the solvent. But whatever these future studies reveal, it seems for the moment safe to say that a two-dimensional perspective and the static solvent effect on the barrier height will both remain at the core of TICT reaction analysis for some time to come.

Acknowledgments

The original work on which the present is based was supported in part by NSF grants CHE90-1707 (T. Fonseca) and CHE88-07852 (JTH) and a PRF grant (H.J. Kim). The present work was supported in part by NSF grant CHE93-12267. The late Teresa Fonseca was responsible for initiating the TICT work and provided many of its key ideas. Some sense of her very special spirit can be found in the memorial issues of the *Journal of Molecular Liquids* in which the TICT work described here appears.

References

1. K. Rotkiewicz, K. H. Grellmann and Z. R. Grabowski, *Chem. Phys. Lett.* **19** (1973) 315; **21** (1973) 212.
2. E. Lippert, W. Lüder, F. Mol., W. Nägele, H. Boos, H. Prigge and I. Siebold-Blankenstein, *Angew. Chem.* **73** (1961) 695.
3. (a) Z. R. Grabowski, K. Rotkiewicz, A. Siemiarzczuk, D. J. Cowley and W. Baumann, *Nouv. J. Chim.* **3**, 443 (1979); (b) J. Lipiński, H. Chojnacki, Z. R. Grabowski and K. Rotkiewicz, *Chem. Phys. Lett.* **70** (1980) 449; (c) D. Huppert, S. D. Rand, P. M. Rentzepis, P. F. Barbara, W. S. Struve and Z. R. Grabowski, *J. Chem. Phys.* **75** (1981) 5714; (d) Z. R. Grabowski and J. Dobkowski, *Pure Appl. Chem.* **55** (1983) 245.
4. (a) W. Rettig, G. Wermuth and E. Lippert, *Ber. Bunsenges Phys. Chem.* **83** (1979) 692; (b) W. Rettig and E. Lippert, *J. Mol. Structure* **61** (1980) 17.
5. (a) W. Rettig, *Angew. Chem., Int. Ed. Engl.* **25** (1986) 971; (b) E. Lippert, W. Rettig, V. Bonāic-Koutecký, G. Heisel and A. Miehé, *Adv. Chem. Phys.* **68** (1987) 1; (c) J. Michl and V. Bonāic-Koutecký, *Electronic Aspects of Organic Photochemistry* (Wiley, New York, 1990); (d) W. Rettig, in *Dynamics and Mechanisms of Photoinduced Transfer and Related Phenomena*, edited by N. Mataga, T. Okada and H. Masuhara (Elsevier, B. V., 1992).
6. E. Lippert, W. Lüder and H. Boos, in *Advances in Molecular Spectroscopy*, edited by A. Mangini (Pergamon, Oxford, 1962).
7. O. S. Khali, R. H. Hofeldt and S. P. McGlynn, *Chem. Phys. Lett.* **17** (1972) 479; *J. Lumin.* **6** (1973) 229.
8. N. Nakashima, H. Inoue, N. Mataga and C. Yamanaka, *Bull. Chem. Soc. Jpn.* **46** (1973) 2288; N. Nakashima and N. Mataga, *Bull. Chem. Soc. Jpn.* **46** (1973) 3016.
9. E. M. Kosower and H. Dodiuk, *J. Am. Chem. Soc.* **98** (1976) 924.
10. R. J. Visser and C. A. G. O. Varma, *J. Chem. Soc. Faraday Trans. II* **76** (1980) 453; R. J. Visser, C. A. G. O. Varma, J. Konijnenberg, P. C. M. Weisenborn, *J. Mol. Structure* **114** (1984) 105.
11. (a) Y. Wang and K. Eiseenthal, *J. Chem. Phys.* **77** (1982) 6076; (b) J. Hicks, M. T. Vandersall, Z. Babarogic and K. Eiseenthal, *Chem. Phys. Lett.* **18** (1985) 116; (c) J. Hicks, M. Vandersall, E. V. Sitzmann and K. Eiseenthal, *Chem. Phys. Lett.* **135** (1987) 413.
12. F. Heisel and J. A. Miehé, *Chem. Phys.* **98** (1985) 233; F. Heisel, J. A. Miehé and J. M. G. Martinho, *Chem. Phys.* **98** (1985) 243; F. Heisel and J. A. Miehé, *Chem. Phys. Lett.* **128** (1986) 323.
13. (a) S.-G. Su and J. D. Simon, *J. Chem. Phys.* **89** (1988) 908; (b) *J. Phys. Chem.* **93** (1989) 753.
14. O. Kajimoto, M. Futakami, T. Kobayashi and K. Yamasaki, *J. Phys. Chem.* **92** (1988) 1347.
15. For some general reviews, M. D. Newton and N. Sutin, *Ann. Rev. Phys. Chem.* **35** (1984) 437; R. A. Marcus and N. Sutin, *Biochim. Biophys. Acta* **811** (1985) 265.
16. S. Kato and Y. Amatatsu, *J. Chem. Phys.* **92** (1990) 7241.
17. (a) G. J. Moro, P. L. Nordio and A. Polimeno, *Mol. Phys.* **68** (1989) 1131; (b) G. K. Schenter and C. B. Duke, *Chem. Phys. Lett.* **176** (1991) 563.
18. P. F. Barbara, T. J. Kang, W. Jarzaba and T. Fonseca, in *Perspectives in Photosynthesis*, edited by J. Jortner and B. Pullman (Reidel, Dordrecht, 1990); T. J. Kang, W. Jarzaba, P. F. Barbara and T. Fonseca, *Chem. Phys.* **149** (1990) 81.
19. K. Bhattacharyya and M. Chowdhury, *Chem. Rev.* **93** (1993) 507.
20. T. Fonseca, H. J. Kim, and J. T. Hynes, *J. Mol. Liq.* **60** (1994) 161.
21. W. Rettig and V. Bonāic-Koutecký, *Chem. Phys. Lett.* **62** (1979) 115, and J. P. LaFemina, C. B. Duke and A. Paton, *J. Chem. Phys.* **87** (1987) 2151.

22. J. A. Warren, E. R. Bernstein and J. I. Seeman, *J. Chem. Phys.* **88** (1988) 871; V. H. Grassian, J. A. Warren, E. R. Bernstein and H. V. Secor, *J. Chem. Phys.* **90** (1989) 3994.
23. R. Howell, H. Petek, D. Phillips and K. Yoshihara, *Chem. Phys. Lett.* **183** (1991) 249.
24. K. A. Zachariasse, T. von der Haar, A. Hebecker, U. Leinhos and W. Kühnle, *Pure Appl. Chem.* **65** (1993) 1745.
25. O. Kajimoto, H. Yokoyama, Y. Ooshima and Y. Endo, *Chem. Phys. Lett.* **179** (1991) 455.
26. L. Serrano-Andrés, M. Merchán, B. O. Roos and R. Lindh, *J. Am. Chem. Soc.* **117** (1995) 3189.
27. See, e.g., E. M. Kosower and D. Huppert, *Ann. Rev. Phys. Chem.* **37** (1986) 127.
28. S. Lee and J. T. Hynes, *J. Chem. Phys.* **88** (1988) 6953.
29. K. Fukui, *J. Phys. Chem.* **74** (1970) 4161; *Acc. Chem. Res.* **14** (1981) 363.
30. M. Maroncelli, *J. Chem. Phys.* **94** (1991) 2084; E. A. Carter and J. T. Hynes, *J. Chem. Phys.* **94** (1991) 5961.
31. R. F. Grote and J. T. Hynes, *J. Chem. Phys.* **74** (1980) 2715.
32. See, e.g., A. Staib, D. Borgis and J. T. Hynes, *J. Chem. Phys.* **102** (1995) 2487 and references therein.
33. G. van der Zwan and J. T. Hynes, *J. Chem. Phys.* **76** (1982) 2993.
34. T. Fonseca and B. M. Ladanyi, *J. Phys. Chem.* **95** (1991) 2116.
35. T. Fonseca and M. Cunha, *Chem. Phys. Lett.* **155** (1989) 385; T. Fonseca, *J. Chem. Phys.* **91** (1989) 2869.
36. T. Fonseca and B. M. Ladanyi, in *Ultrafast Reaction Dynamics and Solvent Effects*, edited by Y. Gauduel and P. Rossky (AIP, New York, 1994), p. 380.

Co-ordination Chemistry with Macrocyclic Compounds

Química de Coordenação com Compostos Macroscíclicos

RITA DELGADO

INSTITUTO DE TECNOLOGIA QUÍMICA E BIOLÓGICA, RUA DA QUINTA GRANDE, 2780 OEIRAS, PORTUGAL AND INSTITUTO SUPERIOR TÉCNICO, 1096 LISBOA CODEX PORTUGAL

A brief review from the origins of macrocycles to supramolecular chemistry was undertaken, emphasising the relevant aspects for the co-ordination chemistry and the most interesting applications. The author's work on N-acetate derivatives of macrocyclic compounds was summarised, and the analytical and medical applications of this type of ligands was stressed.

1. Macrocycles and Polymacrocycles

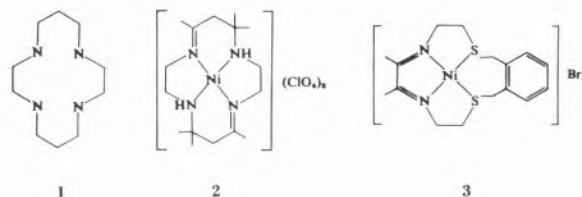
Macrocyclic compounds are synthetic or natural polydentate ligands, containing their donor atoms incorporated in a cyclic backbone or/and in substituents attached to it. They contain at least three donor atoms and the ring should have a minimum of nine atoms. The co-ordination chemistry of these compounds has now become a major subdivision of inorganic chemistry [1], while the active search for new types of macrocycles and the number of their applications has systematically increased since their discovery. Moreover, there is such a fascination for the macrocyclic compounds, that all of us who work with them become subdued by their intrinsic beauty and the unexpectedness of their structures.

The increase of data collected by Izatt *et al.* may give us an idea of the expanding scope of this field: in 1974, the 33 page article referred 197 macrocycles [2]; in 1985, the article consisted of 68 pages and 255 macrocycles are mentioned [3], and in 1991, the 364 pages of the article included the data determined for 1588 macrocycles [4]. It should be emphasised that Izatt *et al.* collected thermodynamic and kinetic data relative to macrocyclic interactions and did not mention all the macrocyclic compounds so far synthesised. Gokel and Korzeniowski report the syntheses of about 2100 macrocyclic compounds in their book published in 1982 [5]. Nowadays the future of this area still seems promising, as from the traditional Co-ordination to the Supramolecular Chemistry; it has enlarged our vision and imagination on the co-ordination chemistry field.

The earliest known examples of metal complexes of macrocyclic ligands were observed in natural sub-

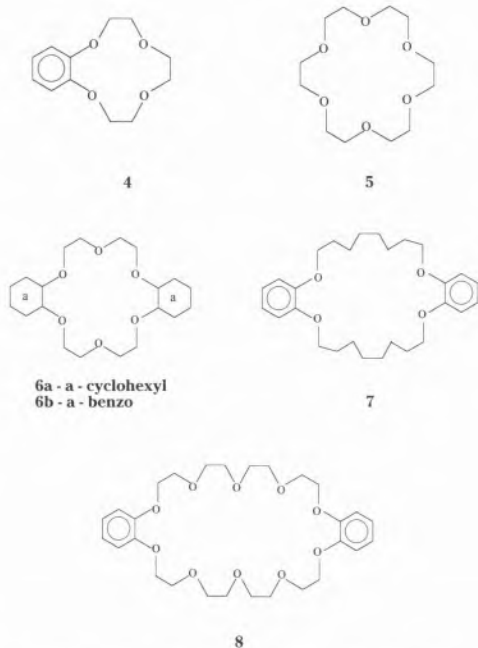
Neste artigo faz-se uma breve revisão dos compostos macrocíclicos desde a origem até à química supramolecular, salientando os aspectos significativos para a química de coordenação e as aplicações mais interessantes. Sumariza-se ainda o trabalho em que a autora tem estado envolvida no que respeita aos macrociclos com substituintes acetato nos átomos de azoto bem como as aplicações analíticas e médicas deste tipo de ligandos.

stances, such as the porphyrin ring of the iron-containing haem proteins, the related (partially reduced) chlorin complex of magnesium in chlorophyll, or the corrin ring of vitamin B₁₂ (a cobalt complex), and in some synthetic highly conjugated phthalocyanines, used mainly as dyestuffs or pigments [1,6,7]. *Cyclam* (1,4,8,11-tetraazacyclotetradecane, **1**), was obtained for the first time in 1936, as a by-product in very small yield [8], but its metal complexes were prepared and studied only in mid-1960. In the early sixties, Curtis [9] and Busch [10], working independently, synthesised some macrocyclic complexes containing nitrogen, **2**, and nitrogen and sulphur donor atoms, **3**, respectively, and new series were developed afterwards, although with restricted expansion. It was the publication of Pedersen's work on crown-ethers (macrocyclic-polyethers) in 1967, that truly opened a new era on macrocyclic chemistry [11].

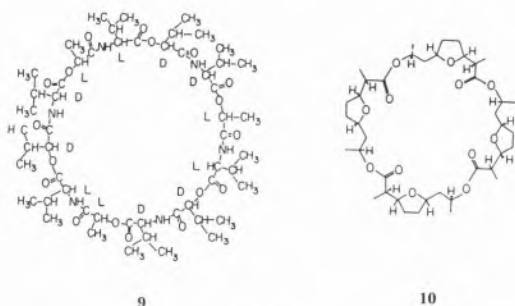


Pedersen reported syntheses of over 50 cyclic polyethers where the size of the rings, the number of oxygen atoms, and the number and type of substituent groups are varied. **4-8** are some examples. After that, a fast progress ensued in the following decades, not only for crown-ethers, but also for macrocycles containing all kind of donor atoms (mainly nitrogen, but also sulphur, phosphorus, and mixed donor atoms). New and more gene-

ral synthetic processes were reported for macrocyclic compounds containing nitrogen atoms, which strongly contributed for the interest in this field [12].



The discovery in 1964 that certain naturally occurring antibiotic ionophores such as valinomycin **9**, nonactin **10**, monensin, and others, exhibiting alkali specificity, were capable of active transport of metal ions across membranes, was a starting point for a large number of studies of alkali and alkaline-earth cations selectivity of biological and model systems. Unlike the synthetic macrocycles, these antibiotics exhibit special metal selectivity despite their very large size [7,13].



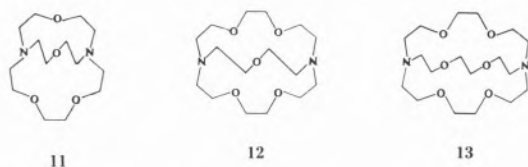
The intense interest on macrocyclic compounds was related to their unusual affinity for certain metal ions, their ability to bind selectively some cations in preference to others, the inertia to decomposition of some complexes, and the capacity of some of those ligands to solubilize inorganic salts in non-aqueous media [11]. Macrocyclic ligands typically contain central hydrophilic cavities with electronegative or electropositive binding atoms and an exterior flexible skele-

ton exhibiting a hydrophobic behaviour. Their hydrophobic exteriors allow them to solubilize ionic substances in non-aqueous solvents and in membrane media. The most spectacular fact, at that time, was the dissolution of potassium permanganate in benzene by an 18-crown-6, **5**, reported by Pedersen [11]. Particularly interesting is the strong affinity shown by the crown-ethers for alkali and alkaline-earth metal ions and for transition metal ions by polyazamacrocycles. The selective binding of some of their metal complexes allows them to be attractive for many applications, such as ion storage and transport *in vivo*, solvent extraction of metals, the development of metal-ion selective reagents for analytical applications or of new chromatographic materials for separation of metal ions. Macrocyclic compounds in general offer a unique way of carrying out many ionic reactions in non-aqueous solvents, as for example: oxidation of olefins to carboxylic acids in benzene or toluene at room temperature by complexed potassium permanganate with the cyclic polyether dicyclohexyl-18-crown-6, **6a**; more efficient saponification of esters by complexed potassium hydroxide with a crown-ether in toluene than by potassium hydroxide itself in propanol; or by phase transfer catalysis, which allows the development of reactions between reagents contained in two different phases [1,13-15].

In the first studies on the co-ordination chemistry of macrocyclic ligands, crown-ethers and tetraazamacrocycles, it was recognised that these ligands co-ordinate most strongly those metal ions whose ionic crystal radius best matches the size of the cavity formed by the ring upon complexation. This complementarity rule means that bond energies between cation and ligand will be greatest when all donor atoms can fully participate. In this case, the macrocyclic structure restricts ligand adaptation so that the macrocycle would exhibit a so-called *peak selectivity* for size [15]. If the macrocyclic ring is too large, the metal ion would "fall through" the cavity and not take full advantage of the available binding interactions, while if the ring is too small the metal ion would achieve only limited penetration or require some distortion of the ligand away from its equilibrium conformation with consequent energy-loss [1,13-15]. This behaviour is the basis of the *macrocyclic effect*, which can be quantified by the ratio between the stability constants of the complexes of the macrocyclic ligand over an analogous acyclic ligand bearing the same set of binding sites, with a given cation, in a given solvent, at a given temperature. However, the *hole-size selectivity rule* often does not hold [13,15]. Complementarity (size and shape) provides the minimal requirement for strong affinity [16]. Other effects are also important in determining selectivity and stability patterns. Differences in stability depend also upon the level of *preorganisation* of the ligand into its optimal binding conformations [15]. In Lehn's words "this level of preorganization is related to both the solvation state and the equilibrium solution conformation, which are

functions of each other and are difficult to predict" [15]. Or, in Busch's words, "an additional stereochemical contribution to the complexation affinity... is determined by topological and rigidity constraints. Topological and rigidity constraints are the design factors available for arbitrarily enhancing affinity" [16]. In general, when no problems of complementarity exist, the increase of topological and flexibility constraint leads to increases in binding affinities.

It follows from the above considerations that the introduction of other bridges on simple or mono-macrocycles should present certain advantages if more selective ligands were required. This point was soon confirmed by the work of Lehn *et al.* [17] through the synthesis of macrobicyclic polyethers containing three polyether strands joined by two bridgehead nitrogen atoms, forming a bicyclic ligand (**11-13** are some examples), a logical extension of crown-ether chemistry.



These compounds having three-dimensional cavities, which can accommodate metal ions of suitable size, were called *cryptands* and the corresponding complexes,

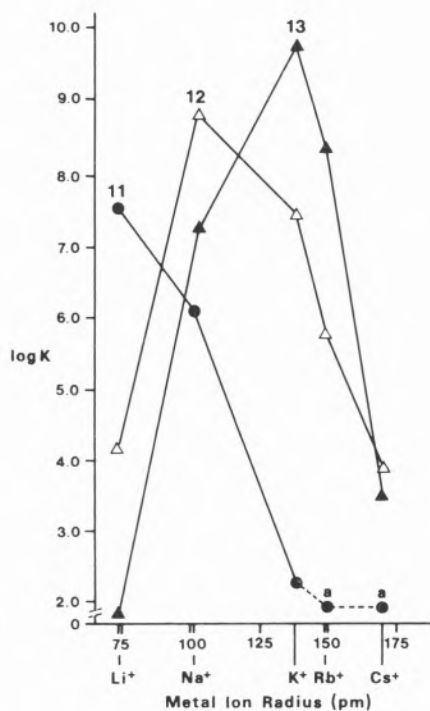
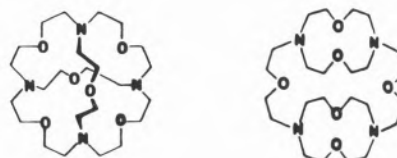


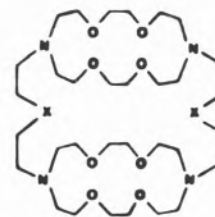
Figure 1. Selectivity of *cryptands*: stability constants (log K) of some *cryptands* (**11-13**) with alkali metal ions *versus* cation radius. **a** - values reported to be less than 2.0.

cryptates. It was found that on proceeding across a series of these ligands of ever increasing size, each of the alkali metal ion is in turn preferentially bound, the cation located in each selectivity peak having an ionic radius very close to the ligand cavity size (Figure 1) [18].

Macrocyclic compounds containing two bridges, like **14**, would be expected to induce even more rigidity and to show enhanced peaks of selectivity and affinity for metal ions than the *criptand* series. This macrotricyclic presents a spherical cavity, though larger than would be necessary for alkaline metal ions. It will play however an important role in supramolecular chemistry, owing to special affinity for NH₄⁺, as will be shown in the following section. Other macrotricyclics have been synthesised as well (**15** and **16**, are examples) which can bind more than one metal ion forming di- or polynuclear complexes, or be suitable receptors for molecular recognition.

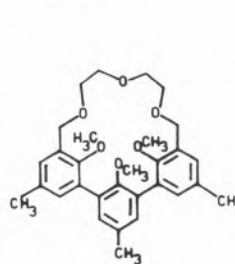


14 15

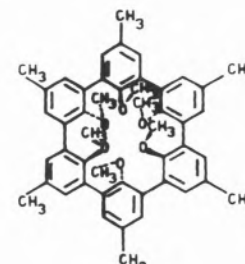


16

An entirely different design of macrocyclic ligands has been developed [19] with the same objectives, namely to get rigid compounds: cavitands, spherands and carcerands, **17**, **18**. These ligands exhibit rigid cavities in tridimensional arrays approaching spherical geometry. For example, **18** has a small cavity and does bind strongly to lithium and sodium, among alkali metal ions [19].



17



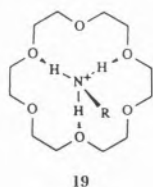
18

2. Supramolecular Chemistry

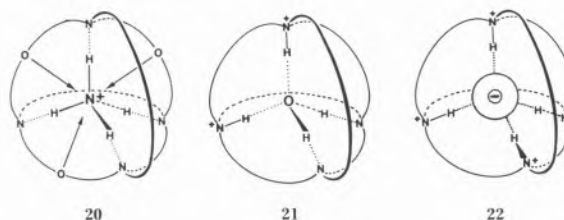
The association of two or more species by non-covalent bonds constituted what has been designated by *supramolecular chemistry* or *host-guest chemistry*, and extends the Fischer's "lock and key" concept from steric fit to other molecular properties [15,20, 21]. Among macrocycles there is a vast number of molecules that can act as *receptors* or *host* molecules for the complexation of inorganic or organic anions and cations or neutral molecules - *substrate* or *guest* molecule. Some of them are able to modify significantly the properties of the substrates upon complexation, as found in many natural systems like enzymes. The structures of the associates are governed by relatively weak forces such as ion-dipole and dipole-dipole interactions, hydrogen-bonds, van der Waals interactions, etc. [1,14-16,21-24]. The association is characterised by similar thermodynamic and kinetic constants as used in classical co-ordination chemistry. Supramolecular chemistry may be considered generalised co-ordination chemistry. It extends the classical field of metal co-ordination chemistry to all kinds of substrates or guests: cationic, anionic and neutral species of an inorganic, organic or biological nature [16,20,21]. For the "recognition" and binding of the receptor to a potential substrate, the two species must complement each other in size, shape and binding sites. This behaviour has been observed for many natural molecules, including enzymes and drugs and also for smaller natural products, such as cyclodextrins and antibiotics. Such selective complexation of ions is the basis for the extraction of ions or neutral molecules and, if accompanied by transport of the complex across a lipophilic membrane, provides the basis for ion-selective electrodes, which have been developed not only for metal ions but also for many other ionic species. If, in addition to the binding sites, the receptor bears reactive sites that may transform the bound substrate, it could be an interesting catalytic reagent. Therefore, the functional properties of such an association cover molecular recognition, catalysis and transport. Other areas of interest are model systems for enzymes, including the activation of small molecules like O₂, CO, CO₂ and N₂ [1,14-16,21-24].

As it is not my goal in this paper to develop this theme, but only to mention this important and active field of the macrocyclic chemistry, I will summarise this point using some examples from the literature [1,14,15]:

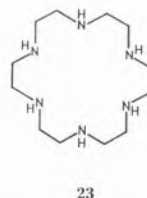
• The alternating oxygen atoms of an 18-membered crown-ether ring are appropriately spaced to form hydrogen bonds with each of the three N-H bonds of an ammonium ion, **19**.



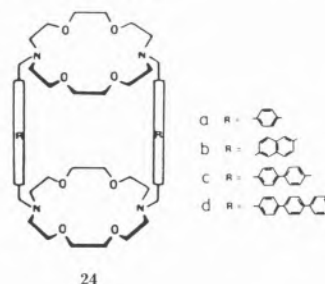
• The receptor **14** presents a spherical recognition site with an octahedron of oxygen sites superimposed on a tetrahedron of nitrogen sites in appropriate positions for NH₄⁺, **20**. The complementary between cavity size and the nature and arrangement of the co-ordination sites gives this ligand the highest affinity for NH₄⁺ and among the alkali metal ions, for Rb⁺. The cavity of this macrocycle in its diprotonated form is also adequate for the complexation of a neutral molecule, like H₂O **21**, or of anions (halides) in its tetraprotonated form, **22**. A remarkable Cl⁻/Br⁻ selectivity >10³ was observed in this last case.



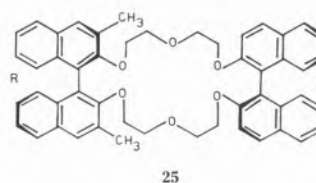
• The hexacyclen **23** complexes a large variety of anions, its triprotonated form co-ordinate polycarboxylate anions (citrate³⁻, succinate²⁻, malonate²⁻, etc.) and its tetraprotonated form complexes inorganic anions (Cl⁻, NO₃⁻, Br⁻, ClO₄⁻, IO₃⁻, etc.).



• The architecture of the macrotricyclic **24** displays good length selectivity for linear diammonium $\overset{+}{N}H_3 - (CH_2)_n - \overset{+}{N}H_3$.

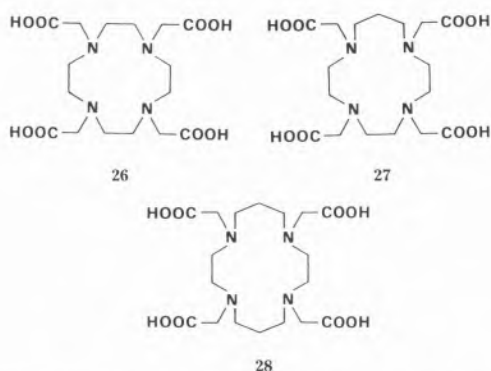


• Crown-ethers incorporating chiral binaphthyl units **25**, show high chiral discrimination on interaction with particular racemic amine salts.



3. Polyazamacrocycles with N-acetate Arms - Cyclic Complexones

My interests in the world of macrocyclic chemistry started with my PhD work when my supervisor - Prof. Fraústo da Silva - suggested me to repeat the work published three years earlier by Stetter and Frank [25]. Their work consisted on the synthesis and the stability constants determination of the metal complexes (alkaline-earth and divalent first-row transition metal ions) of N-acetate derivatives of three tetraazamacrocycles, DOTA **26**, TRITA **27** and TETA **28**. The astonishing though not unlikely fact for macrocyclic compounds



stated on the Stetter *et al.* very short paper was an inversion of the usual order of stability constants of Ca^{2+} and Sr^{2+} TRITA complexes. It was to be expected for the complexes of these metal ions, held together mainly by electrostatic interactions, that stability would follow the order of the ionic potential. The published values were 8.06 for the Ca^{2+} and 11.7 for the Sr^{2+} complexes, in log units, respectively [25]. If confirmed, this fact would be very important for the removal of radioactive ^{89}Sr and ^{90}Sr from the human body. Since ^{90}Sr is one of the most dangerous and abundant fission products, having a radioactive half-life of 28 years and a long biological half-life, it is readily assimilated into the body lodging in the bones. Nevertheless, although it were important to verify that these N-tetraacetate tetraazamacrocycles could exhibit specific selectivity for the alkaline-earth metal ions, we soon became aware that another type of macrocycles managed to invert the usual stability order of the complexes of these metal ions. In fact, the *criptand*, **13**, presents the following stability constants for the complexes: Ca^{2+} , 4.4, Sr^{2+} , 8.0 and Ba^{2+} , 9.5 (values in log units, determined in aqueous solution at 25 °C and ionic strength 0.1 M) [26]. It is one of those cases where the hole-size selectivity rule does hold and certainly one fact that strongly contributed for the Nobel Prize awarded to Jean-Marie Lehn in 1987 (the prize was shared with two other big names of the macrocyclic field, C. J. Pedersen and D. J. Cram). Also, it was confirmed in experiments made with rats, that 80% of ^{85}Sr was

removed 72 hours after injection of the radioactive element using the *criptant* **13**, while the remaining radioactivity was found in the skeleton [27].

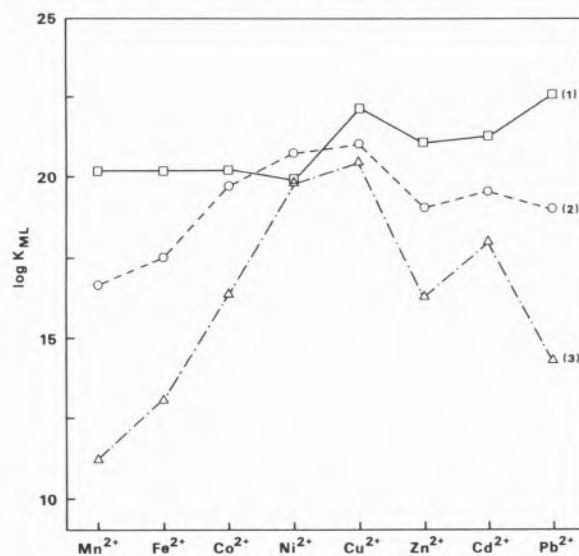


Figure 2. Stability constants of the metal complexes of N-tetracetate tetraazamacrocycles (log K) along the first row transition metal ions, Cd^{2+} and Pb^{2+} : (1) DOTA; (2) TRITA and (3) TETA [28b].

In spite of our lack of confirmation of the most intriguing data included in the Stetter and Frank report, our work was not in vain. In fact, it allowed the determination of a series of more accurate thermodynamic data, namely, protonation constants [28a,b] and protonation sequence of the ligands [29], stability constants of metal complexes for a series of mono- and divalent metal ions (alkali and alkaline-earth, first-row transition metal ions, Cd^{2+} and Pb^{2+}) [28a,b], enthalpy changes for the metal complexations [30] and some structural studies in aqueous solution by EPR and NMR spectroscopic techniques [31,32], very useful for the later development of many analytical and medical applications.

The appending of arms on the macrocyclic compounds, specially when additional ligating groups are introduced such as acetates, can greatly modify the properties of the metal complexes of the macrocycles, namely the stability, the selectivity, the solubility, the kinetics of formation or dissociation of complexes and the reactivity. In fact, in the case of the DOTA-TETA metal complexes, all the acetate groups are located on the same side of the plane formed by the four nitrogen atoms of the ring, building up a kind of cage where the metal ions will be encapsulated. This cage is quite rigid for the macrocycle of small size, DOTA, and to fit inside, the metal ions must be first stripped off of their hydration shells, before co-ordinating to the nitrogen and carboxylate oxygen atoms of the macrocycle [28a,b, 30].

All these ligands lead to stable complexes with both alkaline-earth and transition metal ions and, also, with

lanthanide ions [33,34] and other trivalent metal ions, like Ga^{3+} , Fe^{3+} and In^{3+} [35], particularly DOTA which forms by far the most stable Ca^{2+} and lanthanide complexes. The stability of the complexes of the alkaline-earth ions decreases abruptly with the increase in the size of the tetraaza ring of the ligands, none being particularly favoured by the increase of the size of the cavity of the macrocycle. However, the complexes of the divalent transition metal ions have very close stabilities, which are not specially high when compared with linear complexes. The rigid cage of DOTA exhibits such a conformation that the size of the transition metal ion does not make much difference, which means that there is no selectivity for these metal ions, all the complexes having constants between *ca.* 20 (for Mn^{2+} or Fe^{2+}) and *ca.* 22 (for Cu^{2+} or Pb^{2+}), values in log units. The increased flexibility of TRITA and TETA allows a better discrimination of the metal ions, TETA having a behaviour almost as a non-cyclic ligand following the Irving-Williams series, *cf.* Figure 2. These observations were interpreted and later confirmed by NMR studies in solution [32,36-38] and by some crystal X-ray structure determinations [38-44], as arising from the co-ordination of all the donor atoms in the complexes of the alkaline-earth metal ions, while not all the donor atoms of the macrocycle are involved in the complexes of the transition metal ions.

Crystal structural data for alkaline-earth metal complexes are not available, nevertheless the related structures involving lanthanide ions should give transferable information, as lanthanide ions also form complexes through mainly non-directional electrostatic interactions, while the ionic radius of Ca^{2+} is of the same order of magnitude of that of some trivalent lanthanides. The X-ray structure of the Eu^{3+} complex of DOTA, $\text{Na}[\text{Eu}(\text{DOTA})(\text{H}_2\text{O})].4\text{H}_2\text{O}$ [39] shows a nine co-ordinate metal ion linked to the four nitrogens of the macrocycle, and its four carboxylate oxygens atoms, as well as to one water molecule. The co-ordination polyhedron is a distorted capped square antiprism, Figure 3. The metal ion lies between the two planes of the four nitrogen and the four oxygens, which are nearly parallel to each other. NMR studies in solution were in good agreement with the structure, suggesting that the lantha-

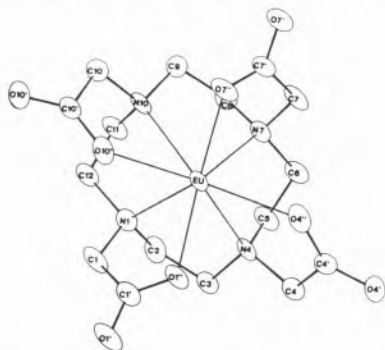


Figure 3. Crystal X-ray structure of $\text{Na}[\text{Eu}(\text{DOTA})(\text{H}_2\text{O})].4\text{H}_2\text{O}$ [39].

nide DOTA complexes are unusually rigid. The crystal structure analysis of the Tb^{3+} complex of TETA, $\text{Na}[\text{Tb}(\text{TETA})].6\text{H}_2\text{O}.1/2\text{NaCl}$ [40], has shown that this ligand also wraps itself around the lanthanide ion but in a different manner than that described for the DOTA complex. The TETA ring is more flexible and can wrap in a more effective, although more distorted way. The Tb^{3+} ion is eight co-ordinated, being also linked to the four nitrogen atoms and the four carboxylate oxygen atoms of the ligand, and the co-ordination polyhedron in this case is a severely distorted dodecahedron, Figure 4.

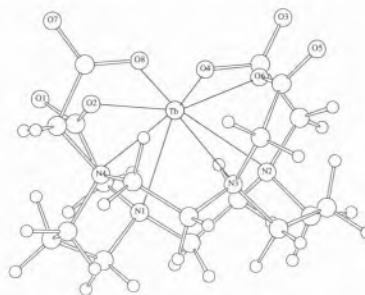


Figure 4. Crystal X-ray structure of $\text{Na}[\text{Tb}(\text{TETA}).6\text{H}_2\text{O}.1/2\text{NaCl}$ [40, 88].

X-ray structures of $[\text{Ni}(\text{H}_2\text{DOTA})]$ and $[\text{Cu}(\text{H}_2\text{DOTA})]$ [38] have shown that the four N-atoms of the macrocycle and two of the carboxylate oxygen atoms are bound to the metal ion, whereas the other two carboxylates are protonated and not involved in the co-ordination. Two nitrogen and two oxygen atoms define a plane in which the metal ions is located. The other two nitrogen atoms of the ring are in axial positions. A *cis*-octahedral geometry is observed, the macrocycle being folded along the axis passing through two opposed nitrogen atoms and takes a *trans-I* conformation according to the nomenclature of Bosnich [45], Figure 5. The Cu^{2+}

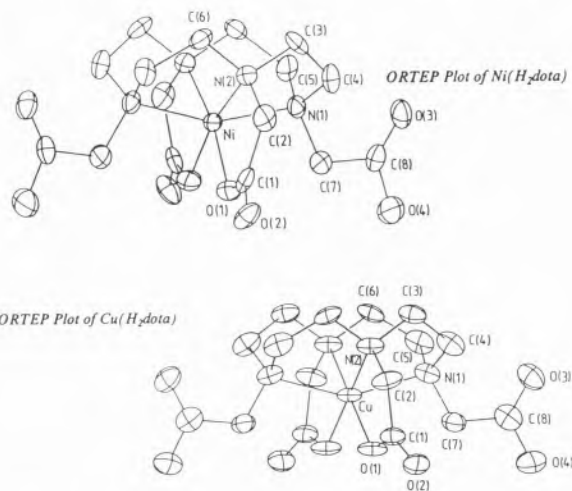


Figure 5. Crystal X-ray structures of $[\text{Ni}(\text{H}_2\text{DOTA})]$ and $[\text{Cu}(\text{H}_2\text{DOTA})]$ [38].

complex is more distorted than the Ni²⁺ one, which is only slightly distorted. Studies in solution carried out by Kaden et al. [38] have also shown that the co-ordination geometry for [Cu(DOTA)]²⁻ or [Ni(DOTA)]²⁻ are very similar to those of the corresponding diprotonated species. The structure of a [Cu(TETA)]²⁻ (Figure 6) complex has also shown two

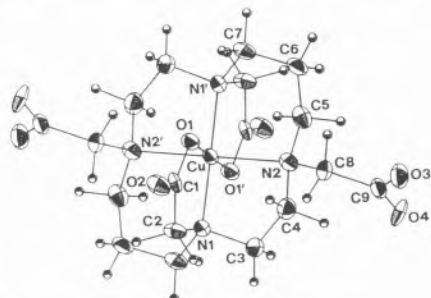
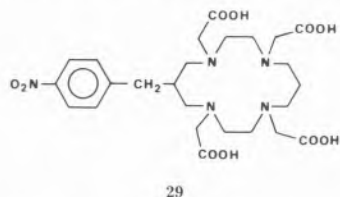


Figure 6. Crystal X-ray structure of Ba[Cu(TETA)] [44].

non-co-ordinated acetate groups: the Cu²⁺ has a distorted octahedral environment with the four amino nitrogen atoms in a plane and two apical acetate oxygen donors [44]; the Cu atom is situated exactly in the N4 plane of the macrocycle, which thus takes a *trans*-III configuration, according to the Bosnich nomenclature [45]. In this case the 14-membered ring is able to encompass the metal ion and does not need to fold as happens with the 12-membered ring. However, this structure is in contrast with that of a Cu²⁺ complex of a C-substituted analogue of TETA **29** [43] in which the metal ion is situated in a N₂O₂ plane, and the two nitrogen atoms linked to the two non-co-ordinated acetate groups are in axial positions.



DOTA and TETA also form binuclear complexes with transition metal ions, M₂L, whose stability constants have been determined [28b] and crystal structures of some Cu and Ni complexes have been determined [41,42,43], but their description is not essential for the continuation of this discussion.

4. Applications of N-tetraacetate tetraazamacrocyclic ligands

Analytical applications

The most interesting applications of those macrocyclic compounds are found in analytical and medical fields. The selectivity shown by TETA for some alkaline-earth metal ions, owing to the very low stabil-

ties of the Mg²⁺ and Ba²⁺ complexes, allows the use of this ligand for the semimicro determination of calcium in the presence of other alkaline-earth metals in natural and synthetic water samples; the end-point detection can be achieved amperometrically with Zn(en)₃²⁺ as indicator. When strontium is present in concentrations similar to that of calcium, two distinct end-point are obtained, but, if the concentrations are substantially different, calcium and strontium appear to be titrated together [46] (constants are 1.97 for Mg²⁺, 8.32 for Ca²⁺, 5.73 for Sr²⁺ and 3.85 for Ba²⁺, in log units [28a]). DOTA will be an interesting alternative to EGTA for the simultaneous potentiometric direct titration of calcium and magnesium [28a]. The very high molar absorptivity of the Cu²⁺ complex of TRITA, the stability of the colour of the complex and the wide range of pH at which the complex formation is completed make this ligand a convenient reagent for the fast and easy spectrophotometric determination of copper in metal alloys, without interference of nickel and cobalt [31].

Medical applications

More interesting, however, has been the use of those ligands in medical and pharmaceutical applications. In fact, in contrast with the analytical ones, the medical applications only require small amounts of ligands, which is more convenient, considering the long and tedious synthesis of these macrocycles. They are used, in the metal complexes form, as contrast-enhancing agents in nuclear magnetic resonance imaging (MRI), and as radiopharmaceuticals for diagnostic or therapeutical uses.

Lanthanides or radionuclides used in those experiments are toxic elements, so for safety reasons they should preferably be administered intravenously as a co-ordination complex and its premature release in the body should be prevented, as it leads to their accumulation in the liver, bone, and bone marrow. The biodistribution of the complex will principally be determined by its shape, charge, lipophilicity and redox properties. The most important condition for this kind of experiments is the stability of the complex *in vivo* and its integrity in the biological medium. Some of the properties requested for the complexes are:

- 1) They should have high stability constants, because the complex may be administered in very diluted concentrations if radiopharmaceuticals are used (about 10⁻¹⁰ M or less) and should not dissociate or transfer to thermodynamic competing ligands present in biological media, such as albumin or transferrin. Serum proteins will be present in great stoichiometric excess over the artificial ligand, so metal ions can be lost by mass action effects alone; also metal ions present *in vivo*, like Fe³⁺, can compete with the radioactive metal for the ligand.
- 2) Kinetic inertia or very slow dissociation, and resistance to acid and cation promoted dissociation *in*

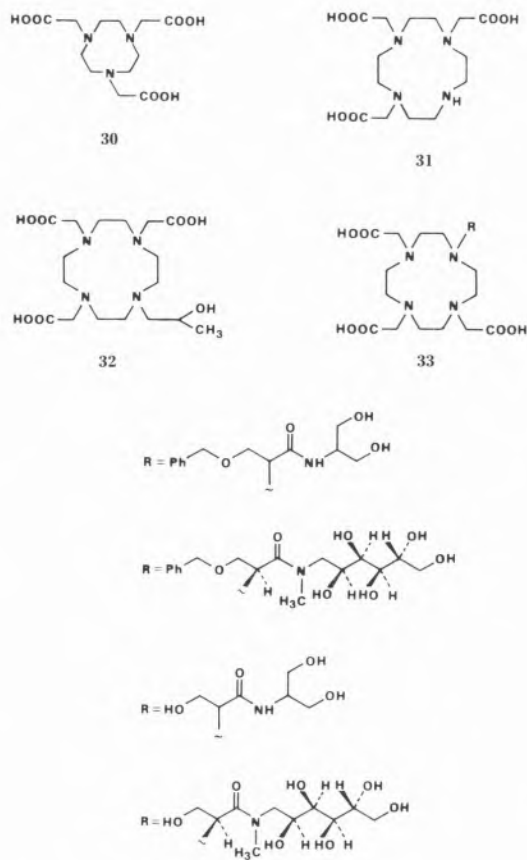
in vivo, particularly important as the complex need to cross low pH regions, such as the stomach and the liver, and some cations like, Ca^{2+} and Zn^{2+} , exist in relatively high concentrations.

- 3) Fast rate formation of the complex when radionuclides of short half-life are used.
- 4) Other important conditions are: the oxidation state of the metal in the complex should be stable to resist to electron transfer; the complex should be neutral for best passive diffusion into cells and a combination of charge neutrality, sufficient lipophilicity and low molecular weight is desired, if the complex needs to penetrate the blood-brain barrier, or even the nuclear membrane of a cell [47-50].

MRI contrast agents

In recent years MRI has been recognised as a powerful diagnostic tool in clinical practices. It is a tomographic technique giving three-dimensional images in the form of slices of tissues [50] and relies on detecting the spatially localised NMR signals of water protons. The signal intensity of these protons depends on many factors such as the values of the water relaxation times, T_1 and T_2 and the type of pulse sequence. Paramagnetic molecules catalyse the proton relaxation of aqueous solutions in which they are dissolved. The relaxation time of the water molecules decreases of a factor of the order of 10^6 when the water oxygen atom is co-ordinated to a highly paramagnetic ion. This in turn perturbs the signal intensity: decreases in T_1 enhance the signal intensity, while decreases in T_2 decrease the signal intensity [49,51]. Contrast agents, which provide contrast between diseased and normal tissues, are usually paramagnetic metal ions complexed with a chelating substance, which are capable of enhancing the signal intensity of NMR images. It is necessary that it efficiently reduces the water proton relaxation rate or enhances the relaxivity (the increase of the water proton relaxation rate per unit concentration of paramagnetic contrast agent) of the water protons compared to the relaxivity induced in such water protons by the paramagnetic substance alone, free in solution. Complexes of Gd^{3+} are the most used owing to the largest magnetic moment, with seven unpaired electrons, and long electron spin relaxation times of this lanthanide. Some contrast agents can bind non-covalently to plasma proteins (eg. human serum albumin) through van der Waals interactions, by hydrophobic domains, or by electrostatic interactions [51].

The first compound used as a contrast agent in MRI was $[\text{Gd}(\text{DTPA})]^{2-}$, but soon the higher thermodynamic and kinetic stability of $[\text{Gd}(\text{DOTA})]^-$ was currently preferred. Macrocyclic ligands, such as DOTA and TETA, have the great advantage of forming stable complexes, but their slow complexation rates constitute a serious setback in their use as contrast agent. All the complexes mentioned are water soluble and stable, but they are charged complexes and their solutions have



high osmolarity when injected intravenously, so some other ligands which could form neutral complexes were developed: NOTA, **30**, or NOTA derivatives [52-56] or DOTA and its derivatives as **31 - 33** [56-61]. In general, the search for new contrast agents is directed to functionalized derivatives of macrocycles, generally DOTA or NOTA, supposing that the stability constants of Gd^{3+} complexes are not altered in comparison to that of the parent macrocycles.

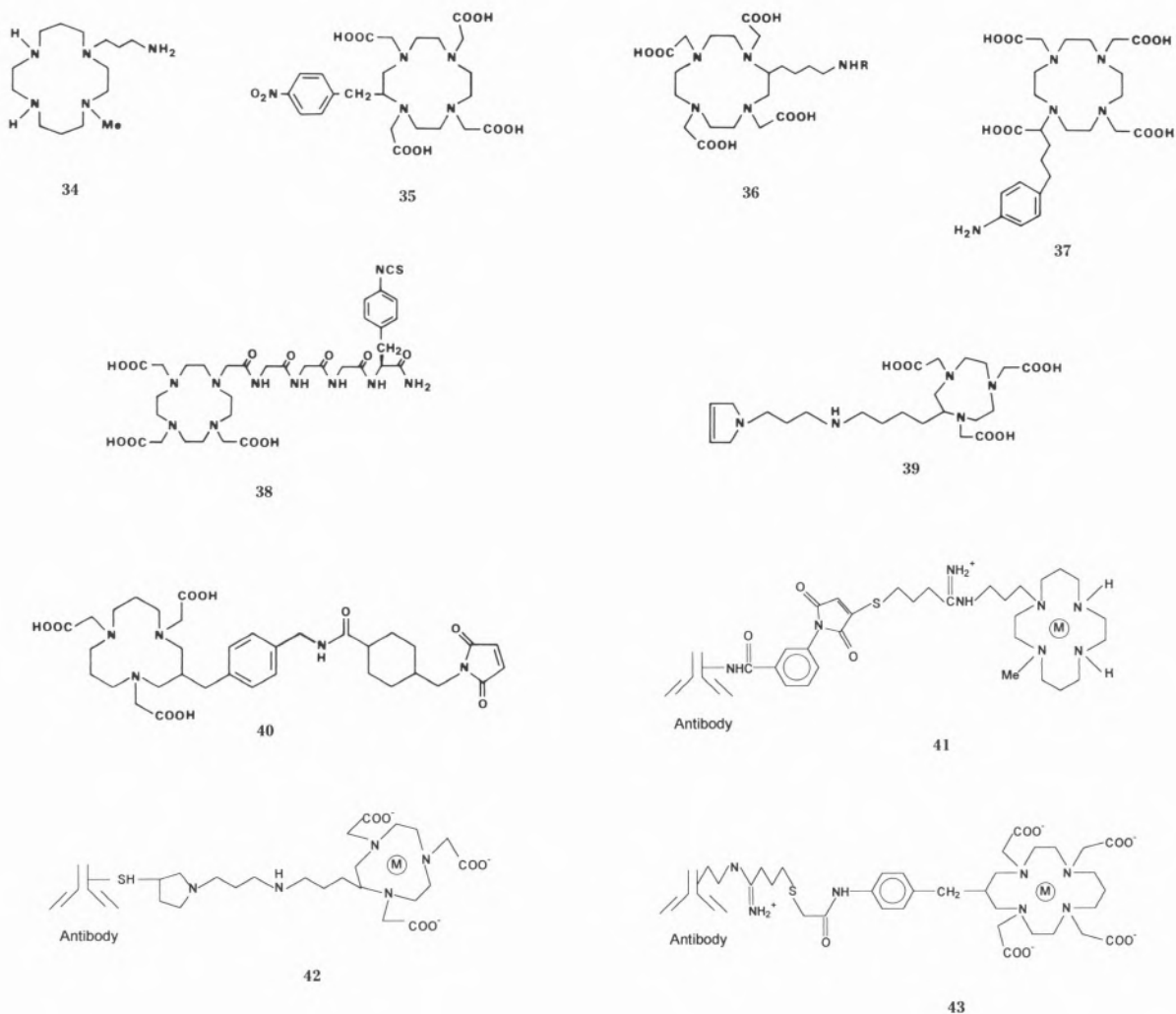
Nuclear medicine - radiopharmaceuticals

The radioisotopes used in nuclear medicine vary according to their purpose: the diagnosis (radioimmunosintigraphy) or the therapy (radioimmunotherapy). In diagnosis, the location of the radionuclide in the body is detected by extremely sensitive devices, available today, for which low radiation doses are needed. But if the therapy is the aim, a high dose of radiation is necessary, and consequently highly selective agents are needed which rapidly bind at the target site, and quickly clear from the body if unabsorbed. Isotopes used for imaging should emit only penetrating radiation (γ or β^+) of a single energy (with energies greater than 80 KeV). The half-lives must be sufficiently long to synthesise the radiopharmaceutical, inject the drug into the patient, and get images. Although $^{99\text{m}}\text{Tc}$ (γ emitter; $t_{1/2}$ 6.02 h; 141 keV) is the most widely used radioisotope in diagnostic,

it has a very short half-life which limits its use; best candidates are ^{111}In (γ emitter; $t_{1/2}$ 2.83 d; 171, 247 keV), ^{67}Ga (γ emitter; $t_{1/2}$ 3.25 d; 184 keV) and ^{64}Cu ($t_{1/2}$ 12.8 h; 511 keV). Radioisotopes used for therapy should emit only non-penetrating radiations (β , α , Auger e^-) to deliver a radiation dose sufficient to cause cell death through multiple double-strand cleavage of cellular DNA and usually have half-life in the range of 1-10 days to permit transportation to the tumour site. The best candidates are β^- emitting radioisotopes: ^{161}Tb ($t_{1/2}$ 166 h; 0.45-0.58 MeV) has good nuclear properties but is difficult to obtain; ^{67}Cu ($t_{1/2}$ 52 h; 0.40-0.58 MeV) with lower β^- energy may be suited to the elimination of small metastases or leukemias but is very expensive, and the best choice seems to be ^{90}Y (β^- ; $t_{1/2}$ 64 h; 2.25 MeV) [47,48].

The majority of the radiopharmaceutical applications requires the attachment of the radioactive metal ions to a ligand by complexation to control biodistribution. The first ligands used were naturally occurring molecules which exhibited specific *in vivo* properties, like cyanocobalamin. Nowadays, the most promising vehicles for

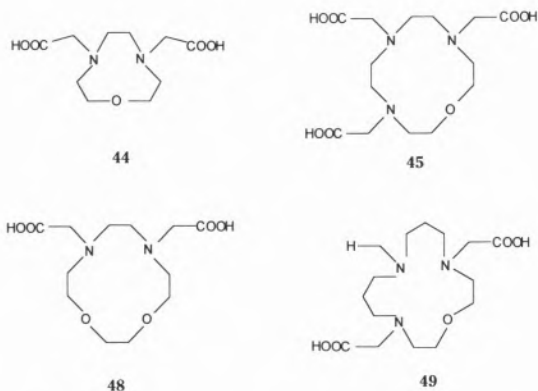
tumour therapy are conjugates or bifunctional ligands, which are expanding fast, since advances in genetic engineering have made possible not only to generate antibodies for specific antigens, but also to allow the incorporation of additional amino acids or amino acids sequences into the antibodies. The complex carrying the radioisotope is linked directly to the lysine residues of the antibody by simple reactions [47,48,50]. Until the middle-eighties the emphasis had been on the synthesis of C-functionalized derivatives of EDTA and DTPA, but their anionic complexes were not sufficiently stable at low pH or in the presence of serum cations to allow their successful use. More recently, functionalized macrocyclic ligands have been used, owing to their metal binding properties, forming more stable antibody conjugates. Some of those considered are derivatives bearing a C-substituted functional group or having one of the N-acetate groups modified for antibody attachment, such as derivatives of tetraazamacrocycles **34** [62], of DOTA **35-38** [63-70], of TETA **29** [65, 71-74], and of NOTA **39**, or other triazamacrocyclic derivatives **40** [66, 75,76]. **41**



[62], **42** [72,73] and **43** [75] are examples of some conjugate complexes. Recently, experimental therapy in tumour-bearing animals with a ^{90}Y , ^{212}Bi and ^{67}Cu labelled conjugate, by D. Parker *et al.* [64,68], O Gansow *et al.* [77,78] and DeNardo *et al.* [72,73] have obtained promising results for immunotherapy.

5. Present and future research

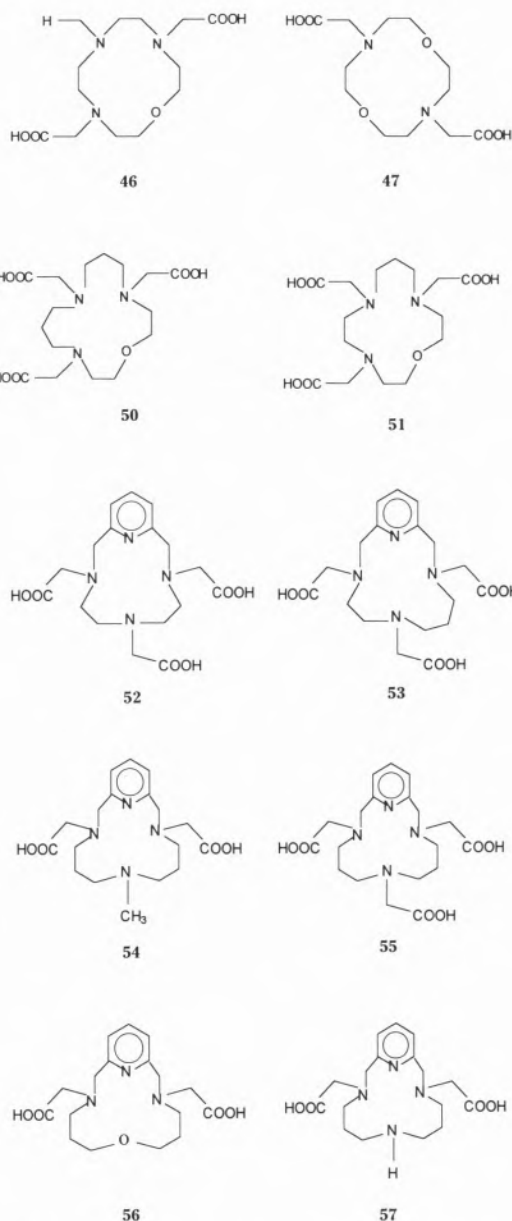
As mentioned several times in the precedent section, the principal drawback for the use of DOTA-TETA ligands and their derivatives in nuclear medicine is the slow complexation rates of their metal complexes. Stability constants of those complexes are in general higher than necessary for those applications. So the logic pursuit of new ligands having faster kinetics of formation of complexes led us to synthesise two new series: the first one, by the replacement of one or more of the nitrogen atoms of the tetraazamacrocyclic series by oxygen atoms, **44-51**; the second one, by the replacement of one of the nitrogen atoms of the tetraazamacrocyclic series by a pyridine ring, **52-57**.



The studies with the first ligand series are almost finished and, as a conclusion, we can say that there is a considerable decrease in the stabilities of the metal complexes formed as each nitrogen is replaced by one oxygen atom, as expected, and there are faster reaction kinetics; nevertheless, the gain in kinetics, which is not really exciting, does not compensate for the decrease in stability of the majority of the complexes [79-82].

The studies of the other series containing a pyridine in the macrocycle, are still in progress, but the results are more promising. All the ligands have been synthesised, but stability constants are not yet completely determined [83]. Other N-substituted groups were introduced, such as methyl and methylpyridine groups, to test the effect on complexation [84].

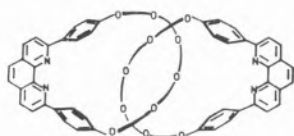
In general, the established conclusions for similar linear amines, like complexones EDTA, DTPA and so on, should not bear on macrocyclic compounds due the many constraints imposed by the macrocycle on



complexation. In fact, stability constants data of macrocyclic complexes are difficult to interpret without the support of structural data. So, in the last years, not only X-ray diffraction studies have been carried out [82,85] or are in course of publication [86], but also several spectroscopic studies in solution have been made using Uv-vis-near IR, EPR and NMR techniques [82,83,85]. Such a small research group has no possibilities to pursue enough studies in order that generalisations could be made, so lately some theoretical studies including molecular mechanics calculations came to our help too [86].

This chemistry field is so marvellous, that in general anyone who is introduced to it does not give it up. It is also so vast, if natural macrocycles and supramolecu-

lar chemistry are included, that we can move on it for ever! The aim would be fundamental co-ordination chemistry, practical applications, or the simple artistic pleasure of designing beautiful molecular architectures. Sauvage *et al.* [87] have written "The search for aesthetically attractive molecules has been a concern going back to the origin of chemistry. The criteria for beauty have obviously changed with time, being connected to analytical and synthetic tools. The interest in catenanes (**58**) and related systems originates to a large extent in their aesthetic appeal. In this respect, graphic arts and chemistry find a link".



58

Acknowledgments

The author thanks all co-authors of previous and present papers for their active collaboration and helpful discussions. Special thanks to Maria José Calhorda and Judite Costa who read the manuscript of this paper and have suggested many corrections and improvements of the text. The financial support from JNICT is gratefully acknowledged.

Note - Names of linear ligands abbreviated in this text:

- EGTA - Ethyleneglycol-bis(oxyethylenenitrilo) tetraacetic acid;
- DTPA - Diethylenetriaminopentaacetic acid;
- EDTA - Ethylenedinitrilotetraacetic acid.

References

1. L. F. Lindoy, *The Chemistry of Macrocyclic Ligand Complexes*, Cambridge University Press, Cambridge, 1989.
2. J. J. Christensen, D. J. Eatough, R. M. Izatt, *Chem. Rev.* **74** (1974) 351.
3. R. M. Izatt, K. Pawlak, J. S. Bradshaw, R. L. Bruening, *Chem. Rev.* **85** (1985) 271.
4. R. M. Izatt, K. Pawlak, J. S. Bradshaw, R. L. Bruening, *Chem. Rev.* **91** (1991) 1721.
5. G. W. Gokel, S. H. Korzeniowski, *Macrocyclic Polyether Syntheses*, Springer-Verlag, Berlin, 1982.
6. G. A. Melson, in *Coordination Chemistry of Macrocyclic Compounds*, ed. by G. A. Melson, Plenum Press, New York, 1979, 1-16.
7. V. L. Goedken, in *Coordination Chemistry of Macrocyclic Compounds*, ed. by G. A. Melson, Plenum Press, New York, 1979, 603-654.
8. J. van Alphen, *Rec. Trav. Chim. Pays-Bas* **55** (1936) 835.
9. N. F. Curtis, *J. Chem. Soc.*, (1960) 4409.
10. M. C. Thompson, D. H. Busch, *Chem. Eng. News* (1962) 57.
11. C. J. Pedersen, *J. Am. Chem. Soc.* **89** (1969) 2495, 7017.
12. J. E. Richman, J. T. Atkins, *J. Am. Chem. Soc.* **96** (1974) 2268; J. T.

- Atkins, J. E. Richman, W. F. Oettle, *Org. Synth.* **58** (1978) 86.
13. J. D. Lamb, R. M. Izatt, J. J. Christensen, D. J. Eatough, in *Coordination Chemistry of Macrocyclic Compounds*, ed. by G. A. Melson, Plenum Press, New York, 1979, 145-217.
14. G. Gokel, *Crown Ethers & Cryptands*, Monographs in Supramolecular Chemistry, The Royal Society of Chemistry, Cambridge, 1994.
15. P. G. Potvin, J.-M. Lehn, in *Synthesis of Macrocycles. The Design of Selective Complexing Agents, Progress in Macrocyclic Chemistry*, ed. by R. M. Izatt, J. J. Christensen, vol. 3, John Wiley & Sons, New York, 1987, pp. 167-239.
16. D. H. Busch, *Chem. Rev.* **93** (1993) 847.
17. B. Dietrich, J.-M. Lehn, J.-P. Sauvage, *Tetrahedron Lett.* (1969) 2885, 2889.
18. J.-M. Lehn, J.-P. Sauvage, *J. Am. Chem. Soc.* **97** (1975) 6700.
19. D. J. Cram, K. N. Trueblood, *Topics in Curr. Chem.* **98** (1981) 43.
20. J.-M. Lehn, *Struct. Bonding* (Berlin) **16** (1973) 1.
21. J.-M. Lehn, *Science* **227** (1985) 849.
22. I. O. Sutherland, *J. Chem. Soc., Faraday Trans. 1* **82** (1986) 1145.
23. B. Dietrich, *Pure & Appl. Chem.* **65** (1993) 1457.
24. F. C. J. M. van Veggel, W. Verboom, D. N. Reinhoudt, *Chem. Rev.* **94** (1994) 279.
25. H. Stetter, W. Frank, *Angew. Chem. Int. Ed. Engl.* **15** (1976) 686.
26. J.-M. Lehn, J. P. Sauvage, *Chem. Commun.* (1971) 440; *J. Am. Chem. Soc.* **97** (1975) 6700.
27. W. H. Müller, *Naturwissenschaften* **57** (1970) 248.
28. a) R. Delgado, J. J. R. Fraústo da Silva, *Talanta* **29** (1982) 815; b) S. Chaves, R. Delgado, J. J. R. Fraústo da Silva, *Talanta* **39** (1992) 249.
29. J. R. Ascenso, R. Delgado, J. J. R. Fraústo da Silva, *J. Chem. Soc. Perkin Trans. 2* (1985) 781.
30. R. Delgado, J. J. R. Fraústo da Silva, M. C. T. A. Vaz, *Inorg. Chim. Acta* **90** (1984) 185.
31. R. Delgado, J. J. R. Fraústo da Silva, M. C. T. A. Vaz, *Talanta* **33** (1986) 285.
32. J. R. Ascenso, R. Delgado, J. J. R. Fraústo da Silva, *J. Chem. Soc. Dalton Trans.* (1986) 2395.
33. M. F. Loncin, J. F. Desreux, *Inorg. Chem.* **25** (1986) 2646.
34. W. P. Cacheris, S. K. Nickle, A. D. Sherry, *Inorg. Chem.* **26** (1987) 958.
35. E. T. Clarke, A. E. Martell, *Inorg. Chim. Acta* **190** (1991) 37.
36. J. F. Desreux, *Inorg. Chem.* **19** (1980) 1319.
37. J. F. Desreux, M. F. Loncin, *Inorg. Chem.* **25** (1986) 69.
38. A. Riesen, M. Zehnder, T. A. Kaden, *Helv. Chim. Acta* **69** (1986) 2067.
39. M.-R. Spirelet, J. Rebizant, J. F. Desreux, M.-F. Loncin, *Inorg. Chem.* **23** (1984) 359.
40. M.-R. Spirelet, J. Rebizant, M.-F. Loncin, J. F. Desreux, *Inorg. Chem.* **23** (1984) 4278.
41. A. Riesen, M. Zehnder, T. A. Kaden, *J. Chem. Soc., Chem. Commun.*, (1985) 1336.
42. A. Riesen, M. Zehnder, T. A. Kaden, *Helv. Chim. Acta* **69** (1986) 2074.
43. M. K. Moi, M. Yanuck, S. V. Deshpande, H. Hope, S. J. DeNardo, C. F. Meares, *Inorg. Chem.* **26** (1987) 3458.
44. A. Riesen, M. Zehnder, T. A. Kaden, *Acta Cryst.* **C44** (1988) 1740.
45. B. Bosnich, C. K. Poon, M. L. Tobe, *Inorg. Chem.* **4** (1965) 1102.
46. N. Maitra, A. W. Herlinger, B. Jaselskis, *Talanta* **35** (1988) 231.
47. D. Parker, *Chem. Soc. Rev.* **19** (1990) 271.
48. S. Jurisson, D. Berning, W. Jia, D. Ma, *Chem. Rev.* **93** (1993) 1137.
49. D. Parker, *Chem. in Britain* (1994) 818.
50. V. Alexander, *Chem. Rev.* **95** (1995) 273.
51. R. B. Lauffer, U. S. Patent n. 4,880,008, 14/11/1989.

52. C. F. G. C. Geraldés, A. D. Sherry, R. D. Brown III, S. H. Koenig, *Magn. Reson. Med.* **3** (1986) 242.
53. R. H. Knop, J. A. Frank, A. J. Dwyer, M. E. Girton, M. Naegele, M. Schrader, J. Cobb, O. Gansow, M. Maegerstadt, M. Brechbiel, L. Baltzer, J. L. Doppman, *J. Computer Assist. Tomography* **11** (1987) 35.
54. E. Brücher, A. D. Sherry, *Inorg. Chem.*, **29** (1990) 1555.
55. S. Cortes, E. Brücher, C. F. G. C. Geraldés, A. D. Sherry, *Inorg. Chem.* **29** (1990) 5.
56. E. Brücher, S. L. Stefan, D. R. Allen, A. D. Sherry, *Radiochimica Acta* **61** (1993) 207.
57. M. M. Magerstädt, O. A. Gansow, M. W. Brechbiel, D. Colcher, L. Baltzer, R. H. Knop, M. E. Girton, M. Naegele, *Mag. Reson. Med.* **3** (1986) 808.
58. D. Meyer, M. Schaffer, B. Bonnemain, *Inv. Radiology* **23** (1988) S232.
59. D. D. Dischino, E. J. Delaney, J. E. Emswiler, G. T. Gaughan, J. S. Prasad, S. K. Srivastava, N. F. Tweedle, *Inorg. Chem.* **30** (1991) 1265.
60. S. Aime, P. L. Anelli, M. Botta, F. Fedeli, M. Grandi, P. Paoli, F. Uggeri, *Inorg. Chem.* **31** (1992) 2422.
61. K. Micskei, L. Helm, E. Brücher, A. E. Merbach, *Inorg. Chem.* **32** (1993) 3844.
62. J. Franz, G. M. Freeman, E. K. Barefield, W. A. Volkert, G. J. Ehrhart, R. A. Holmes, *Nucl. Med. Biol.* **14** (1987) 479.
63. M. K. Moi, C. F. Mears, S. J. DeNardo, *J. Am. Chem. Soc.* **110** (1988) 6266.
64. J. P. L. Cox, K. J. Jankowski, R. Katakai, D. Parker, N. R. A. Beeley, B. A. Boyce, M. A. W. Eaton, K. Millar, A. T. Millican, A. Harrison, C. Walker, *J. Chem. Soc., Chem. Commun.* (1989) 797.
65. A. Riesen, T. A. Kaden, W. Ritter, H. R. Mäcke, *J. Chem. Soc., Chem. Commun.* (1989) 460.
66. J. P. L. Cox, A. S. Craig, I. M. Helps, K. J. Jankowski, D. Parker, M. A. W. Eaton, A. T. Millican, K. Millar, N. R. A. Beeley, B. A. Boyce, *J. Chem. Soc. Perkin Trans. 1* (1990) 2567.
67. C. J. Broan, J. P. L. Cox, A. S. Craig, R. Katakai, D. Parker, A. Harrison, A. M. Randall, G. Ferguson, *J. Chem. Soc. Perkin Trans. 2* (1991) 87.
68. A. Harrison, C. A. Walker, D. Parker, K. J. Jankowski, J. P. L. Cox, A. S. Craig, J. M. Sansom, M. R. A. Beeley, R. A. Boyce, L. Chaplin, M. A. W. Eaton, A. P. H. Farnsworth, K. Millar, A. T. Millican, A. M. Randall, S. K. Rhind, D. S. Secher, A. Turner, *Nucl. Med. Biol.* **18** (1991) 469.
69. S. J. Kline, D. A. Betebenner, D. K. Johnson, *Bioconjugate Chem.* **2** (1991) 26.
70. M. Li, C. F. Mears, G.-R. Zhong, L. Miers, C.-Yi Xiong, S. J. DeNardo, *Bioconjugate Chem.* **5** (1994) 101.
71. M. K. Moi, C. F. Mears, M. J. McCall, W. C. Cole, S. J. DeNardo, *Anal. Biochem.* **148** (1985) 249.
72. C. F. Mears, *Nucl. Med. Biol.* **13** (1986) 311.
73. S. V. Deshpande, S. J. DeNardo, C. F. Mears, M. J. McCall, W. C. Cole, G. P. Adams, M. M. Moi, G. L. DeNardo, *J. Nucl. Med.* **29** (1988) 217.
74. G. Ruser, W. Ritter, H. R. Mäcke, *Bioconjugate Chem.* **1** (1990) 345.
75. P. J. Marsden, F. A. Smith, S. Mather, *Appl. Radiat. Isot.* **42** (1991) 815.
76. A. S. Craig, I. M. Helps, K. J. Jankowski, D. Parker, N. R. A. Beeley, B. A. Boyce, M. A. W. Eaton, A. T. Millican, K. Millar, A. Phipps, S. K. Rhind, A. Harrison, C. Walker, *J. Chem. Soc., Chem. Commun.* (1989) 794.
77. M. W. Brechbiel, C. G. Pippin, T. J. McMurry, D. Milenic, M. Roselli, D. Colcher, O. Gansow, *J. Chem. Soc., Chem. Commun.* (1991) 1169.
78. M. W. Brechbiel, O. Gansow, R. W. Atcher, J. Schlom, J. Esteban, D. E. Simpson, D. Colcher, *Inorg. Chem.* **25** (1986) 2772.
79. M. F. Cabral, J. Costa, R. Delgado, J. J. R. Fraústo da Silva, M. F. Vilhena, *Polyhedron* **9** (1990) 2847.
80. M. T. S. Amorim, S. Chaves, R. Delgado, J. J. R. Fraústo da Silva, *J. Chem. Soc. Dalton Trans.* (1991) 3065.
81. M. T. S. Amorim, R. Delgado, J. J. R. Fraústo da Silva, *Polyhedron* **11** (1992) 1891.
82. S. Chaves, R. Delgado, M. T. Duarte, J. A. L. Silva, V. Félix, M. A. A. F. de C. T. Carrondo, *J. Chem. Soc. Dalton Trans.* (1992) 2579.
83. J. Costa, R. Delgado, *Inorg. Chem.* **32** (1993) 5257.
84. J. Costa, R. Delgado, *XXth International Symposium on Macrocyclic Chemistry*, Jerusalem (Israel), July 2, 1995. Poster 25.
85. V. Félix, R. Delgado, M. T. S. Amorim, S. Chaves, A. M. Galvão, M. T. Duarte, M. A. A. F. de C. T. Carrondo, I. Moura, J. J. R. Fraústo da Silva, *J. Chem. Soc. Dalton Trans.* (1994) 3099.
86. V. Félix, C. Brito, J. Costa, T. Arcos, M. J. Calhorda, R. Delgado, M. T. Duarte, M. G. B. Drew, in preparation.
87. C. O. Dietrich-Buchecker, J.-P. Sauvage, *Chem. Rev.* **87** (1987) 795.
88. F. H. Allen, J. E. Davies, J. J. Galloy, O. Johnson, O. Kennard, C. F. Macral, D. G. Watson, *Chem. Inf. Sci.* **31** (1991) 204.

Biological Photosensitizers. Phototoxic Agents of the Future?

Fotosensibilizadores Biológicos. Pesticidas no Futuro?

RALPH S. BECKER^{1,2} AND ANTÓNIO L. MAÇANITA^{1,3}

1. INSTITUTO DE TECNOLOGIA QUÍMICA E BIOLÓGICA, UNL, R. DA QUINTA GRANDE, 2780 OEIRAS; 2. DEP. CHEMISTRY, UNIV. OF ARKANSAS, FAYETTEVILLE, AR, 7270, USA; 3. DEP. ENG. QUÍMICA, INSTITUTO SUPERIOR TÉCNICO, UTL, AV. ROVISCO PAIS, 1096 LISBOA CODEX, PORTUGAL

Plants are able to produce substances displaying antiviral, bactericidal, antifungal, insecticidal and herbicidal activity. The toxic action of some of these substances is triggered by absorption of solar light, which generates highly reactive electronic excited states. The observation that these compounds are part of the natural defense mechanisms of plants against parasites has, in the last decade, awakened a great interest in the possibility of development of a new type of pesticide: the photopesticide. Presently, several natural compounds, as well as synthetic ones, displaying phototoxic activity towards insects, viruses, fungi, bacteria, pests and others are known and some patents covering compounds and action pathways have been issued.

The phototoxicity mechanisms which are presently known include several excited state reactions, namely, (i) electron or proton transfer between an excited sensitizer and the substrates, (ii) energy transfer between the excited sensitizer and molecular oxygen in the ground state (3O_2) with formation of singlet oxygen (1O_2) and (iii) H-atom transfer or covalent bonding between the sensitizer and the substrate. Biological targets sensitive to photodynamic action include nucleic acids, amino acids, proteins, steroids, unsaturated lipids, nitrogen containing heterocyclic compounds and some vitamins.

During the last four years, our research was aimed at the selection of new compounds displaying photopesticide activity, based on the correlation between molecular structure and the photophysical, photochemical and phototoxic properties of these compounds. For this purpose, the photophysical as well as the phototoxic properties of several families of natural compounds (coumarins, chromones, furanocoumarins, furanochromones, flavones, β -carboline and thiophenes) were characterized and the results were rationalized on the basis of molecular orbital calculations. Compounds from the families of coumarins, furanocoumarins, chromones, flavones and α -oligothiophenes have been modified in order to optimize their **absorption of solar light, phototoxicity, target selectivity and long-term photo or biodegradability**. Out of fourteen synthesized compounds, five have revealed promising properties and are currently undergoing further studies.

As plantas produzem substâncias com acção tóxica sobre os sistemas biológicos, nomeadamente antiviral, bactericida, antifúngica, insecticida e herbicida. A acção tóxica de algumas destas substâncias envolve a formação, por absorção de luz solar, de estados electrónicos excitados altamente reactivos. A observação de que estes compostos fazem parte do mecanismo de defesa natural das plantas contra parasitas tem motivado enorme interesse na possibilidade de desenvolvimento de um novo tipo de pesticidas ao longo da última década: o fotopesticida. Presentemente são já conhecidos vários compostos naturais e também alguns sintéticos que apresentam actividade fototóxica para insectos, vírus, fungos, ervas daninhas e outros, existindo algumas patentes sobre compostos e modos de acção.

Os modos de fototoxicidade actualmente conhecidos envolvem várias reacções de estado excitado, nomeadamente, (i) transferência electrónica ou de protão entre um sensibilizador excitado e o substrato, (ii) transferência de energia entre o sensibilizador excitado e o oxigénio molecular tripleto (3O_2) com formação de oxigénio singuleto (1O_2) e (iii) transferência de átomo de hidrogénio ou a formação de ligações covalentes entre o sensibilizador e o substrato.

Os alvos biológicos sensíveis à acção fotodinâmica que se encontram identificados incluem ácidos nucleicos, aminoácidos, proteínas, esteróides, lípidos insaturados, heterociclos azotados e algumas vitaminas.

Ao longo dos últimos quatro anos, a nossa investigação teve como objectivo a selecção de novos compostos com actividade fotopesticida, baseada na correlação entre a estrutura molecular e as propriedades fotofísicas, fotoquímicas e fototóxicas destes compostos. Por esta razão, as propriedades fotofísicas bem como as fototóxicas das várias famílias de compostos naturais (cumarinas, cromonas, furanocumarinas, furanocromonas, flavonas, (β -carboline e tiofenos) foram caracterizados e os resultados foram racionalizados com base em cálculos orbitais moleculares. Compostos das famílias de cumarinas, furanocumarinas, cromonas, flavonas e (α -oligothiophenos foram modificados com vista a otimizar a sua absorção da luz solar, fototoxicidade, selecção de alvos e foto ou biodegradabilidade a longo prazo. De catorze compostos sintetizados, cinco revelaram propriedades promissoras e estão agora a ser sujeitos a estudos posteriores.

1. Introduction

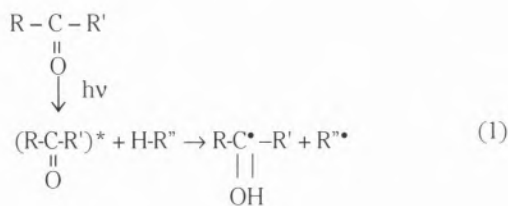
In the broadest sense, the term photosensitization, relative to biological systems, can be used to describe the consequences of the absorption of light by endogenous or exogenous compounds. Following such absorption, reactions generated by one or another excited state of the photosensitizer ensue.

The type of species affected by photosensitizers acting as photopesticides include arthropods, caterpillars, water fleas, fruit fly larvae, yellow mealworms, black imported fire ant, mosquitoes and mosquito larvae, boll weevil, cockroach, house fly, butterflies, cabbage butterfly larvae, black swallow tail larvae, blackfly larvae, fruit fly eggs, black cut worm larvae, alfalfa caterpillar, house and face flies, tobacco hornworm, potato beetle, European corn borer, *Maduca sexta* and *Euxoa Messoria*, as well as others. Furthermore, many photosensitizers can kill viruses, bacteria, algae, fungi, yeasts and nematodes. Finally, some are potent herbicides, and inhibit seed growth.

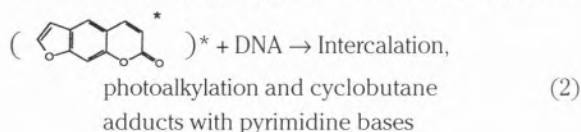
Photosensitization also is the mechanism by which photochemotherapy functions and is responsible for the adverse dermatological response of humans to several kinds of drugs including some antibiotics and non steroidal anti-inflammatories.

Several types of sensitization reactions can occur:

1) electron or hydrogen transfer between excited photosensitizers and substrate followed by ion-ion (sensitizer-substrate) or radical-radical (substrate-sensitizer) recombination. It is also possible to have electron transfer to O_2 to give O_2^- .



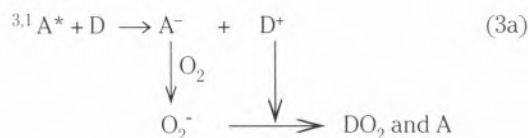
2) covalent bonding of the sensitizer to the substrate



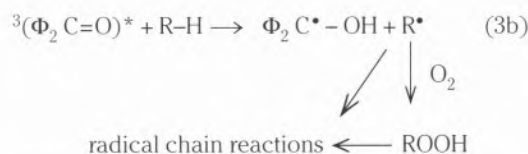
3) electron or hydrogen atom transfer as in item (1) to give radical ions and radicals respectively, which react with ground state oxygen (O_2) to give oxygenated products (called type I reaction involving oxygen).

4) excited sensitizer interacts with ground state O_2 to form excited state oxygen, 1O_2 which reacts with substrates (called type II reaction involving oxygen).

The latter two cases requiring O_2 leading to photosensitizers oxidations, have been classified by the term "Photodynamic Action". An example of the reaction known as type I involving electron transfer (see item (3) above) is



where D means electron donor, A is an electron acceptor and here, as elsewhere, a superscript 1 and * means an excited singlet state and a superscript 3 and * means an excited triplet state. Also, for reactions of type I involving H-atom transfer:



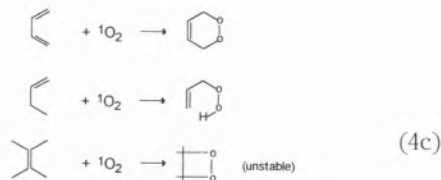
Reactions known as type II initially involve energy transfer [see (4) above]:



where S is a sensitizer and the 3O_2 (${}^3\Sigma_g^-$) and 1O_2 (${}^1\Delta_g$) are the ground triplet and excited singlet state respectively of O_2 . The excited 1O_2 then further reacts as:



Examples of the latter reaction giving oxidized products include:



Singlet oxygen (1O_2) is particularly damaging since it has 23 kcal/mole of excess energy compared to the usual ground state (triplet) oxygen and it can react without spin restrictions with most molecules which are ground state singlets.

The process ${}^3O_2 \rightarrow {}^1O_2$ (${}^3\Sigma_g \rightarrow {}^1\Delta_g$) is highly forbidden so direct excitation of the ground state of O_2 is extremely improbable, as is the decay of the excited singlet oxygen once it is formed. For example, the lifetime of 1O_2 in carbon tetrachloride is as long as ~4s. Consequently 1O_2 is produced indirectly, via a photosensitizer of which there are many: dyes, aromatic hydro-

carbons, ketones, psoralens, porphyrins, terthiophene and other oligothiophenes, furanochromones and polyacetylenes, among others. The efficiency of energy transfer depends on the photosensitizer and the solvent. The lifetime of $^1\text{O}_2$ is also solvent dependent, for example it is $\sim 4\text{s}$ in carbon tetrachloride as noted above, $3\text{--}4\ \mu\text{s}$ in water, ~ 50 in deuterated water, and $20\text{--}25\ \mu\text{s}$ in cationic and anionic micelles. There is still a question about membrane passage. In some model systems it ($^1\text{O}_2$) may penetrate relatively easily but in others there is notable quenching. The important question of course regards biological membranes and data on penetration of these by $^1\text{O}_2$ is not well established.

2. Nature of Excited Electronic States¹

Before continuing, it will be useful to briefly discuss the nature and properties of electronic excited states in molecules. Figure 1 presents a schematic energy diagram¹. The two electronic states important to us are the lowest energy singlet (short lived) and triplet (long lived) states.

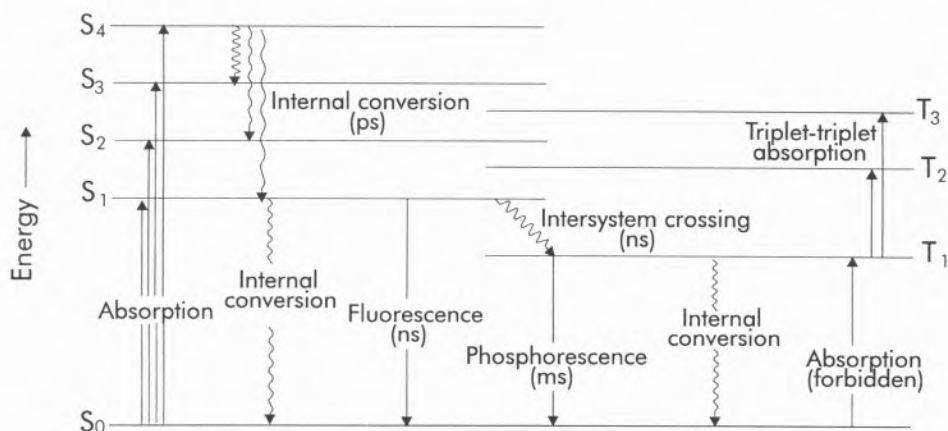
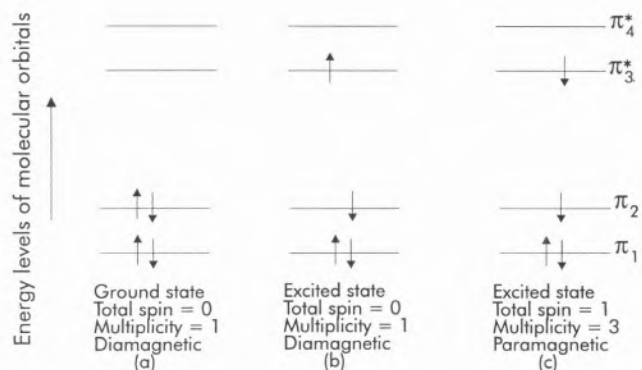


Figure 1. Schematic Energy Diagram: S is singlet, T is triplet. The S₀ state is the ground state and the subscript numbers identify individual states



The terms singlet and triplet arise from the quantity $2S+1$ (where S is the sum of the individual spins) which defines the term multiplicity: singlet and triplet. For example, when the excited electron has the same spin as it had before excitation, $S=+1/2-1/2=0$ and $2S+1=1$, a singlet results, Figure 2¹.

Note the very large difference in the lifetime of the fluorescence and phosphorescence - even in fluid solution the S₁ lifetime is about three orders of magnitude shorter than T₁. In general, intersystem crossing and fluorescence are quite competitive although there are notable exceptions. For example, the presence of high atomic number centers as metal atoms/ions in porphyrins or iodine in general, notably increases intersystem crossing at the expense of fluorescence. Also note the very fast lifetime of internal conversion from S_n to S₁ (S_n = S₂, S₃, S₄, etc.) compared to fluorescence or intersystem crossing. This gives the quite unique result that excitation into *any* S_n state "always" results in emission only from S₁ (there are a very few exceptions).

Also it is almost invariably true that the triplet state is occupied indirectly via the singlet state (commonly S₁) since the S₀ → T₁ absorption directly to T₁ is highly

spin forbidden. This fact dictates that the triplet state has a long lifetime. In fact, the longer it is, the better the chance is that it will encounter a biomolecule (to react with) or oxygen (to produce $^1\text{O}_2$) before it decays back to the ground state. These processes are much less likely from the excited singlet state S₁, which has a much shorter lifetime. We will say more about this shortly which is particularly important for our consideration.

Figure 2 - π-Electron orbitals for butadiene. In the normal state (a) the two lowest orbitals are occupied by two electrons of opposite spin yielding a singlet state. In the excited state (b) one of the electrons has been raised to the next higher level without change in spin to yield an excited singlet state. In state (c) excitation is accompanied by a change in spin of one of the electrons to yield an excited triplet state. The energy of the state derived from the orbitals in (c) is less than that derived from the orbitals in (b).

3. Important Photophysical/Chemical Characteristics

The first and one of the most important requirements of a photosensitizer/pesticide is that it absorbs light in the region where the sun has radiant energy. Of course this is maximized in the visible but a quite appreciable quantity of ultraviolet light is also available. Figure 3 gives an example of the comparison of the sun with some laboratory sources in the ultraviolet regions. On a typical summer day in the mid-eastern part of the United States near the seashore, the total ultraviolet is $\sim 4200 \mu\text{w}/\text{cm}^2$ and of this, about $1100 \mu\text{w}/\text{cm}^2$ is below 350 nm.

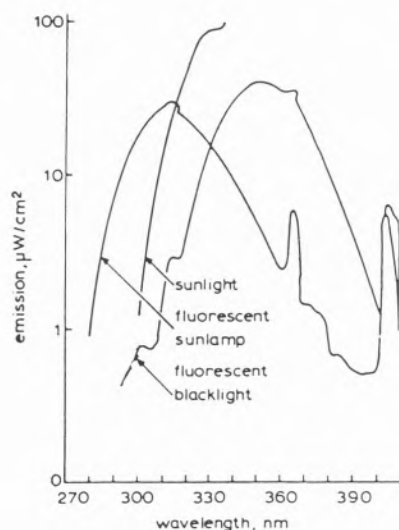


Figure 3. Ultraviolet distribution of Fluorescence Sunlamp, blacklight and sunlight.

A second important aspect is that the absorbed energy not be dissipated by radiationless processes since all of the reactions given early (1)-(4) depend on the existence of an excited state. In the reaction where electron transfer occurs, either an excited singlet or triplet state could be the reactive species. However, for the reactions involving H-atom transfer or the production of $^1\text{O}_2$, the triplet state is by far the most common state required for efficient reaction. Consequently, a third aspect of significant importance is the triplet quantum yield or efficiency of occupation of the triplet state by the sensitizer where ϕ_T is defined as:

$$\phi_T = \frac{\text{number of quanta in } T_1}{\text{number of quanta absorbed to } S_n}$$

In general it is desirable to have this triplet yield as large as possible.

A fourth important aspect concerns the lifetime of the triplet state. The reactions involving the triplet state depend on an encounter with a substrate. Then, in order to improve this possibility, it is desirable to have as long a lifetime as possible so the encounter can occur before the triplet state decays back to the ground-state.

Some comparative examples of the above ideas can be seen by looking at a class of compounds called verdins which are porphyrin-like macrocyclic 2, (see figure 4 for one example, and others), that vary by having none or a different metal center and peripheral substitutions². These all absorb near 700 nm.

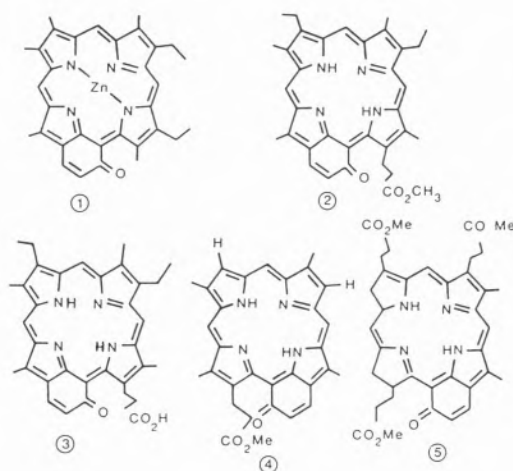


Figure 4. Structures of verdins: (1) ZnMPV; (2) MVME; (3) MVA; (4)DVME; (5) CVTME²

Three examples, for comparison are given below:

Table 1 - Triplet lifetimes (τ_T) and Quantum Yields (ϕ_T) and Singlet Oxygen Quantum Yields (ϕ_Δ) of ZnMPV, MVME and CVTME (see fig. 4)²

	τ_T (μs)	ϕ_T	ϕ_Δ
ZnMPV	30	0.16	0.17
MVME	6	0.08	0.10
CVTME	48	0.120	0.14

Of these compounds, one would presume ZnMPV and CVTME would be the better candidates as photosensitizers and in fact, ZnMPV has been shown to be a good photosensitizer (others not tested)².

Recall that one of the photosensitizer reactions (1) involves electron or H atom transfer. In the reaction shown as an example, the nature of the excited state of the photosensitizer was not defined: however commonly it is a triplet state. Furthermore, not just any triplet state, but one known as an $n\pi^*$ versus a π,π^*

triplet state. In the former of these, the state results from an initial excitation of a electron that is a part of a non-bonding electron pair, particularly for example from a carbonyl oxygen (C=O), figure 5.

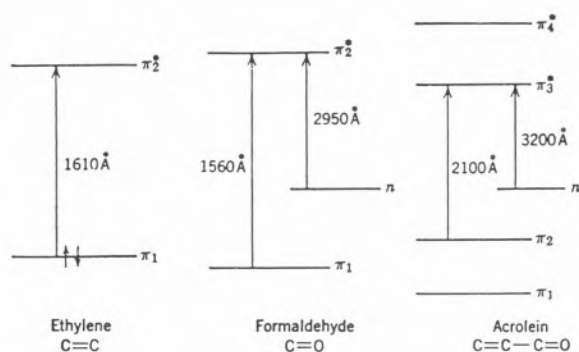
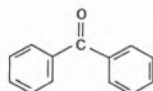
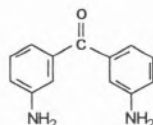


Figure 5. Schematic molecular orbital energy levels of ethylene and carbonyl compounds showing $n \rightarrow \pi^*$ excitation.

This then gives rise to an n, π^* singlet which gives an n, π^* triplet state as the lowest excited state. It is a special circumstance that an n, π^* triplet state also has (bi-) radical chemical character because of the relatively large spatial separation of the unpaired electrons in this state. Thus such a triplet state is highly reactive and for example can extract a H-atom from a donor. On the other hand, π, π^* triplet states do not have the (bi-) radical characteristics and do not function or are not capable of extracting a H-atom. Even similar molecules can have different lowest triplet states and thus have very different H-atom extraction capabilities. For example benzophenone



when irradiated can extract H-atoms but its amino derivative



can not. The reason is that benzophenone has a lowest n, π^* triplet while its substituted analog has a lowest π, π^* triplet state. So, then this is an important photophysical consideration to be known if a H-atom extraction is a desired goal, that is, the nature of the lowest triplet state. In this case also, it is important that the n, π^* triplet state has sufficiently high energy to extract a H-atom; that is, an n, π^* triplet state of relatively high energy is required to perform this kind of photochemistry.

4. Formation Efficiency of Singlet Oxygen by Sensitizers

The formation of 1O_2 is also an important issue since it is so effective in causing ultimate killing. Recall that 1O_2 dominantly comes via the reaction:



We have not thus far discussed aspects of the efficiency of this reaction. It is clear that the efficiency commonly denoted S_Δ depends on the nature of the sensitizer and on the nature of the solvent. Of course if S_Δ is solvent dependent so will be ϕ_Δ where:

$$\phi_\Delta = S_\Delta \times \phi_T \quad (6)$$

where ϕ_Δ is the yield of 1O_2 produced from a triplet state with yield ϕ_T .

Table 2 gives S_Δ and ϕ_Δ data for some molecules.

Table 2 - Singlet Oxygen Quantum Yields (ϕ_Δ) and Energy Transfer Efficiencies (S_Δ) for some Representative Molecules

Compound	ϕ_Δ (solvent) ^(b)	S_Δ (solvent) ^(a)
1. acetophenone	0.35 (Bz), 0.52 (AcN)	0.35 (Bz)
2. benzophenone	0.39 (Bz), 0.31 (AcN)	0.39 (Bz)
3. all-trans retinal	0.66 (Cx), 0.20 (MeOH)	-
4. psoralen	0.012 (Bz)	0.34 (Bz)
5. 5-methoxypsoralen	0.021 (Bz)	0.32 (Bz)
6. 8-methoxypsoralen	0.004 (Bz)	0.40 (Bz)
7. 4,5',8-trimethoxypsoralen	0.084 (Bz)	0.41 (Bz)
8. Rose Bengal	0.74 (Water)	-
9. Erythrosin B	0.63 (Water)	-
10. Eosin Y	0.57 (Water)	-
11. protoporphyrin DME ^(c)	0.57 (Bz)	0.71 (Bz)
12. mesoporphyrin DME	0.57 (Bz)	0.70 (Bz)
13. terthiophene	0.75 (Bz)	0.78 (Bz)
14. quaterthiophene	0.71 (Bz)	0.97 (Bz, Dx)
15. quinquethiophene	0.53 (Bz, Dx)	0.90 (Bz, Dx)

(a) Ref. 3 for compounds 1-3, ref. 4 for compounds 4-7, ref. 5 for compounds 8-10, ref. 6 for compounds 11-12, refs. 7 and 8 for compounds 13-15.

(b) Bz is benzene, AcN is acetonitrile, Cx is cyclohexane, MeOH is methanol and Dx is dioxane.

(c) DME is dimethyl ester.

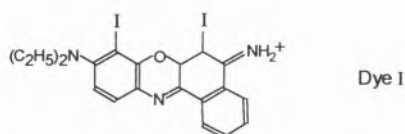
5. Structural Considerations of Photosensitizers

The foregoing requirements are photophysical in nature but to be an effective photosensitizer, the mole-

cule in its ground state must be near or at the desired target site. This entails some design aspects of the molecule to enhance the probabilities of it being where it should be or, that it even enter the specimen of concern such as a bacteria. Also, we shall see that special features of the excited state not yet considered, such as atomic charge changes, can also have an important consequence.

First consider structural aspects of the ground state. In a simple case, the changing of a substituent such as -OH to -OCH₃ in a coumarin or a psoralen, which does not affect much the photophysical properties of the compounds, significantly alters the partition between water and the potential region of a cell where the photosensitizer may be found and, consequently its killing power.

Another example is a dye shown below in the acid form (=NH₂⁺)⁹.



This dye has a ground state pK_a of 5.3 and shows only a low photoactivity/toxicity to various cells in a particular medium (pH=7.4). Because of the pK_a value it exists principally in the base form, in that medium. However, if the pH of the medium is decreased there is a significant increase in phototoxicity. This very likely is largely due to the fact that the acid form now becomes dominant in the medium and, since this form is soluble, it can be taken up by the cells whereas the base form has low solubility and cannot be taken up as readily. On the other hand, another similar dye with only one iodine atom is quite phototoxic at the original same pH of 7.4 for the medium, despite having a nine fold lower ϕ_A than the di-iodinated dye above. It turns out that the pK_a for the monoiodinated dye is 6.6 and therefore under the pH conditions of the medium the monoiodinated dye is soluble because it is significantly more in the acid form (rather than the base form).

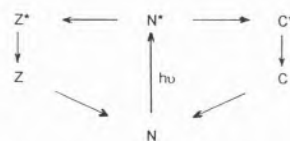
A special aspect not considered so far is the consequence of excitation on molecular properties such as charges on the atoms and any consequence derived from any changes in these properties. We shall consider one type case in particular and that is the change in the formal charge on atoms, particularly nitrogen and oxygen atoms. It is possible to measure the pK_a in the ground state and the excited state. In particular we will be concerned with the ground state (S_0) and the first excited singlet state (S_1). Table 3 gives a few examples of what can happen.

Table 3 - pK_a Values in S_0 and S_1 States

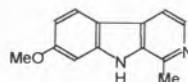
Compound	pK_a (S_0)	pK_a (S_1)
phenol (Ph)	10.0	3.8
m-bromoPh	9.0	2.8
p-ethyl Ph	10.0	4.3
o-methoxy Ph	10.0	5.2
p-methoxy Ph	10.0	4.7
2-naphthol	9.5	3.1
benzoic acid	4.2	9.5
acridine	5.5	10.6
Dye 1	6.6	11.6
Dye 1 less iodine	10.0	15.0
harminecation	7.7	13.3

Note that if a hydroxyl group is present, there is a large change in the pK_a in the direction of making the compound a stronger acid (decrease of pK_a) in S_1 , compared to S_0 , while for nitrogen atoms the pK_a increases making the compound a stronger base in the excited state. Note that for acids such as benzoic acid they become much less acidic in S_1 compared to S_0 . This obviously has very important consequences since the molecule in S_1 may not exhibit the same chemical behaviour as in S_0 and therefore any photosensitization/toxicity thought to be attributed to the original molecule may not be correct at all. Just recall briefly that if there is a change in pK_a there must be a change in charge on the nitrogen or oxygen atom to induce this change in pK_a . There are numerous examples of this but the (β -carboline, norharmine and harmine (see below) are representative of several features of this problem which we shall examine shortly.

For harmine, the situation is very complex since excitation in methanol, where only the base form exists in the ground state, results in a fluorescence which can be seen to have three components¹⁰: the neutral base form, cationic/acid and zwitterion form. This means of course that the latter two tautomers were all created in the S_1 state of the base form during the lifetime of S_1 - fast! (~ 3 ns). This does *not* occur in benzene or other nonprotic solvents. The mechanism is:



where N is the neutral/base form, C is the cation/acid and Z is the zwitterion of harmine, where the harmine molecule is:



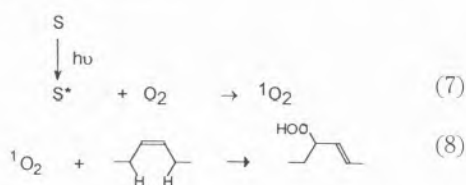
If we calculate the change in the charge on the nitrogens N_1 and $N_2(-H)$ in the S_0 and S_1 states, we get

N_1	0.10 <i>increase</i> in negative charge
$N_2(-H)$	0.15 <i>decrease</i> in negative charge

This of course means there would be a concurrent change in pK_a , this change in charge being an *increase* in pK_a for N_1 and a decrease in pK_a for $N_2(-H)$. These changes explain the existence of C^* and Z^* in/from the S_1 state of N^* . In fact, the charge changes must be large to form the C^* given the pK_a of the ground state of methanol from which a H^+ must be extracted to make C^* . The consequences are biologically significant. In a biological system having typical pH's of 6-8, *both* the neutral and cation would be in equilibrium in the ground state S_0 but the dominant emitting species from S_1 would be the cation. Thus, the excited species of importance may well be C^* which severely complicates the nature of the species and mechanism responsible for a photosensitization reaction. Similar complications can exist for other molecules containing a -OH group, such as 5-hydroxypsoralen vs 5-methoxypsoralen.

6. Some Mechanisms of Action of Photosensitizers in Biological Systems

The biochemical functional groups which are attacked by photosensitizers include proteins, carbohydrates, steroids, amino acids, fatty acids, nucleic acids, thiols, sulfides and disulfides. Photodynamic action which utilizes O_2 in some form and at some stage are of the type I or type II reactions, as noted in the Introduction. A specific reaction relative to a fatty acid (unsaturated lipid) would be:



This can result in an alteration of a membrane structure, changing the permeability and resulting in lysis and likely onward to cell death.

In the case of nucleic acids, guanine residues are the ones preferentially destroyed. Results depend at least in a large part on whether the photosensitizer intercalates or not. Typically if it does not, it can cause alteration in single stranded DNA which can further result in chain breaks. If it can intercalate, it can sensitize photo-modification of guanine in both single and double stranded DNA. Conformational alteration also occurs causing major changes in biological activity. Also, the psoralens intercalate into the double helix of DNA and with light, form cyclobutane adducts with pyrimidine bases. The

psoralens cause both mono and di-adducts (crosslinks) whereas the angular ones (as angelicin) give only monoadducts.

Some other examples include the photo-oxidation of ascorbic acid, the plant hormone indole-3-acetic acid, α -ketoglutaric acid, phytol, squalene, flavine and vitamin B12. Vitamin E is interesting by contrast in that it very largely causes 1O_2 to be physically quenched to its ground state (and thus it is deactivated giving no photo-oxidation).

In the case of proteins the photodynamic action is largely directed to degradation of side chains containing cysteine, tryptophan, histidine, tyrosine and methionine.

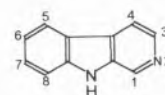
In other cases enzymes can be inactivated including those critical to fatty acid metabolism, Krebs cycle and glycosis reactions. Specific enzymes include oxidases, dehydrogenases, ATP ase and cytochrome -450 among others.

Morphological alteration can occur in a wide variety of insects¹¹. This includes modifications of larvae, unsuccessful emergence from the puporium, modification of various parts of emerged adults such as wings, retardation of growth and a shortened life span. Other effects include a prolonged larvae period, feeding inhibition, the number of eggs laid by a female over a life span and the viability of the eggs laid.

7. Other Natural and Synthetic Biosensitizers

A. β -Carbolines

The β -carbolines have the basic structure

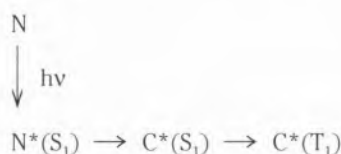


which is in fact the parent of the series (norharmine). Others are derived by substitution in various locations. Most or many are phytochemicals but relatively recently, an interesting different group were found in tunicates (*Endistoma olevaceum*). These compounds contained bromine, hydroxy, pyrrol-2-yl, 1-pyrrolin-2-yl and other substitutions. These showed antimicrobial activity in the dark.

The simple 1- CH_3 substituted (harmine), the 1- CH_3 , 7- OCH_3 substituted (harmine) and harmaline (3,4 dihydroharmine) and the parent norharmine have been examined by us¹⁰ in quite some detail although the work regarding flash experiments is not complete. Briefly, fluorescence studies show that upon excitation a single excited tautomer (N^*) exists in a solvent as benzene (and is generally true in *aprotic* solvents) but in a *protic* solvent as methanol, *three excited* species are in equilibrium: neutral (N^*), cation (C^*) and zwitterion (Z^*) all of which thermally decay eventually to the

ground state of the neutral (N). Laser flash spectroscopic studies¹² thus far show that in aprotic solvents only, the triplet state of the neutral form is observed. In the presence of a protic solvent, norharmine and harmine have a transient which is the *triplet state of the cation* (vs neutral triplet seen in aprotic solvents). The situation in harmine is not clear. The ϕ_T of norharmine is about 0.36 in a hydrocarbon solvent and the ϕ_A is also about 0.34 in a hydrocarbon solvent and a protic solvent methanol. However, recall that in methanol it is the triplet state of the *cation* that is observed in the flash experiments. For harmine, the ϕ_A was also about 0.34 in a hydrocarbon solvent. All of the true β -carboline cations (from the hydrochloride salt) show *only a cation tautomer* upon excitation.

In general, the large changes in pK_a between the ground and excited states occur between S_0 and S_1 but not between S_0 and T_1 . Thus we expect that the excited cations $C^*(S_1)$ would be formed during the lifetime of $N^*(S_1)$ and then the $C^*(S_1) \rightarrow C^*(T_1)$ process would occur. Nonetheless the process $N^*(S_1) \rightarrow N^*(T_1)$ could still occur in competition with $N^*(S_1) \rightarrow C^*(S_1)$ in methanol and then the process $N^*(T_1) \rightarrow C^*(T_1)$ could follow. It would appear that the rate constant for $N^* \rightarrow N^*(T_1)$ is in the vicinity of 10^8 s^{-1} . In general, we expect the reactions $N^*(S_1) \rightarrow C^*(S_1)$ to be fast particularly in neutral water where the rate constant is $\sim 1.5 \times 10^9 \text{ s}^{-1}$. Therefore we believe that $C^*(T_1)$ arises from the reaction sequence

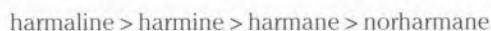


rather than $C^*(T_1)$ coming from $N^*(T_1)$. Particularly in water we see both $C^*(S_1)$ and zwitterion ion, $Z^*(S_1)$ produced. The $Z^*(S_1)$ does not (re)form either the $C^*(S_1)$ or $N^*(S_1)$, nor does $C^*(S_1)$ form either $N^*(S_1)$ or $Z^*(S_1)$ when OH^- concentration is very small (but can if the OH^- concentration is sufficiently high).

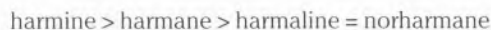
The one molecule not considered above is harmaline. It has proven to be very different regarding its fluorescence quantum yield (ϕ_F) which is some 15-20 fold lower than the others. However as the true cation, its ϕ_F is equal and even greater than two of the three other β -carbolines. No flash data is available.

There has been some evaluation of the phototoxicity of the β -carbolines in particular by the non-eudistomins^{13,14}. In general, harmine has been shown to bind readily to double stranded DNA. β -carbolines in general are known to inactivate several bacteria, viruses and yeasts^{15, 16}. Overall observations indicated DNA as the target for the β -carbolines (especially single strand DNA or RNA). Later, some especially interesting studies were done employing some bacterial mutants of wild *E.coli*¹³.

Firstly all β -carbolines as described above produced singlet oxygen with the order being:



Also, they all produced H_2O_2 in the order:



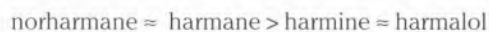
There is some question about the accuracy of this order because all the measurements were at the same initial concentration yet the intensity and width of absorption over the wavelength of irradiation (UV-A) by each of the compounds is different. Others¹⁷ have shown that the same compounds produce singlet oxygen in a different order and also that they produce superoxide ion O_2^- .

Despite the above possible complication, it could be shown that harmaline plus UV-A results in generation of H_2O_2 and subsequent toxic oxygen products that attack DNA along with other cellular components. The inactivation by harmaline was shown to be oxygen (plus UV-A) dependent. For harmane, cellular inactivation was induced by both oxygen independent and dependent mechanisms and the membrane was likely the target. For harmine, the cellular damage was oxygen dependent and the membrane was also the target. Finally for norharmine, the major source of inactivation was oxygen dependent. One compound not mentioned is harmalol which is harmaline with an -OH group replacing the -OCH₃ group. This compound was inactive. This observation of lack of activity is consistent with other cases where an -OH group is substituted on a aromatic moiety (for example, 5-hydroxypsoralen⁶). Overall the phototoxicity was:



based on inactivation data.

These same β -carbolines were also tested regarding their photopesticide activity on *trichoplusia ni* (the cabbage looper). Killing power was in the order:



and again harmolol was not active.

It is clear from our photophysical data that triplet states of the neutral tautomer are formed for all of norharmine, harmane and harmine in a *hydrophobic* hydrocarbon (lipid-like) environment¹². Also, singlet oxygen is formed with about the same efficiency for norharmine and harmine which must also be true for harmane. In a hydrophilic environment (methanol) triplets are also formed *but* they are of the cation versus neutral in a hydrophobic environment (clearly for harmane and norharmine). Also, recall singlet oxygen

was produced for norharmane in methanol with about the same efficiency as in a hydrocarbon - the question is, in methanol was singlet oxygen produced by the cation or the neutral triplet. At this time it is not clear given the fact that even in methanol fluorescence emission is still principally that of the neutral free base. Also, we have to be concerned about competitive rate constants involving: (1) several intramolecular processes (2) H^+ extraction and, (3) reaction with O_2 (to produce 1O_2).

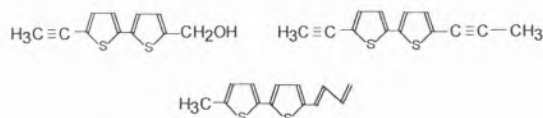
It is clear that only the neutral triplet is present in a hydrocarbon, lipid-like environment. The phototoxicity data indicated the membrane as a prime target where one would expect a more hydrophobic, lipid-like environment and these molecules do dissolve well in such media. Therefore it would be likely that one of the primary killing modes results from excitation of the neutral free bases in the membrane producing N^* which then, in collisions with oxygen, transfer energy to make 1O_2 which is the direct phototoxic agent. This is consistent with the fact that there is an oxygen dependency for cellular inactivation for all the compounds tested on the mutant *E. coli*¹³. Also however at pH values near 7, considerable amount of ground state cation exists. This than can enter the cell, migrate to an interface (of both lipophilic and hydrophilic character) and be excited by light to produce C^* which could then produce 1O_2 which in turn diffuses into the membrane (from the interface where it was produced).

B. α -Oligothiophenes

The α -oligothiophenes (often and here called α n's) have the structure:



where $n=3$ (trithiophene) is natural occurring in marigolds and an African tropical plant called cabbage tree - it is a yellow compound just like marigold flowers. Also, there are naturally occurring derivatives of $n=2$ (bithiophene) in marigolds, and Helenieae, Helientheae and Cynareae of Asteraceae. Some of the structures are:



Note these all contain unsaturated substituents and, as far as we know, no unsubstituted bithiophene exists in nature. Both $n=3$ and $n=2$ compounds occur in flowers, leaves and roots. Trithiophene ($n=3$), also called α -therthienyl, is a particularly effective photopesticide (kills mosquito larvae and bacteria) and it is commonly used as a standard photosensitizer.

The photophysical and photochemical behaviour as well as the ability to form 1O_2 has been examined in a comprehensive way by us on $\alpha 2$ to $\alpha 7$ ^{8,18}. Table 4 presents some of the essential information pertinent to our concern. Note that for $\alpha 3$ to $\alpha 7$, the compounds are colored from yellow to orange as can be seen by the fact that the absorption maximum steadily shifts to longer wavelengths as n increases. Also note other interesting features: ϕ_F increases and ϕ_T decreases reaching a plateau near $\alpha 5$. Also note that ϕ_Δ increases from $\alpha 2$ to $\alpha 3$ and then decreases as n increases. Finally the triplet state lifetime τ_T progressively shortens as n increases. Others⁷ have obtained ϕ_Δ for $\alpha 3$ to $\alpha 6$ similar to ours.

Table 4 - Some Data of Interest on α -Oligothiophenes

Cpd	Abs. λ (max)nm	ϕ_F	ϕ_T	τ_T (μ s)	ϕ_Δ ^(a)
$\alpha 2$	303	0.017	0.94	146	0.69
$\alpha 3$	354	0.006	0.93	108	0.81
$\alpha 4$	392	0.18	0.67	48	0.72
$\alpha 5$	417	0.36	0.6	29	0.56
$\alpha 6$	436	0.44	--	≥ 17	0.36 ^(b)
$\alpha 7$	441	0.34	≈ 0.6 ^(d)	≥ 15	^(c)

(a) ϕ_Δ is in benzene and most other data is in dioxane except τ_T of $\alpha 6$ (benzene);

(b) Ref. 7;

(c) We estimate a value of ≈ 0.25 in benzene;

(d) in benzene

We also have obtained some preliminary results regarding the effectiveness of α -oligothiophenes in killing fungi¹⁹. All showed ability to kill but there was a clear maximum of this ability at $\alpha 3$, with $\alpha 2$ less (and $\alpha 4$ - $\alpha 7$ also still less). In addition, we determined octanol-water partition constants (K_{ow}) for all compounds, in order to evaluate the relative bio-accumulation of those (Table 5).

Table 5 - Octanol-Water Partition Constants of α -Oligothiophenes¹⁹

Compound	K_{ow}
$\alpha 1$	220
$\alpha 2$	2800
$\alpha 3$	18500
$\alpha 4$	100000
$\alpha 6$	500000
$\alpha 7$	1000000

If the mole fraction present in the hydrophobic portion was multiplied by the ϕ_Δ of each αn , then the general shape of the killing curve (from a plot of killing ability vs number of rings n) could be reproduced by plotting the foregoing product mole fraction $\times \phi_\Delta$ as a function of n (see Fig. 6).

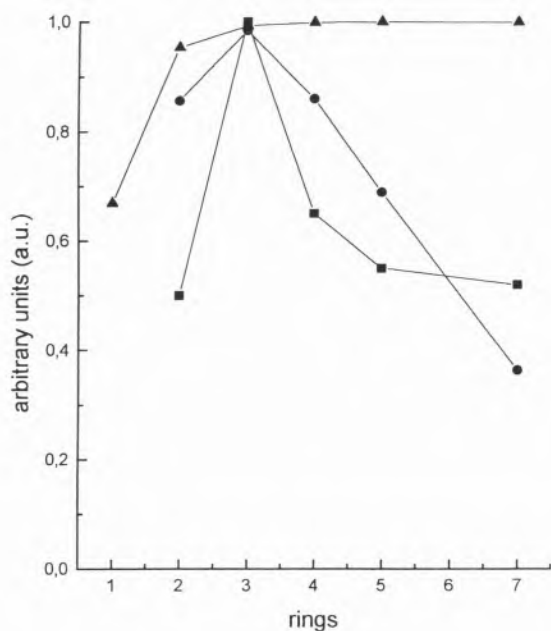
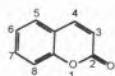


Figure 6. Plot of mole fraction of α -oligothiophenes in hydrophobic medium (from Kow data) (▲) product of mole fraction times singlet oxygen quantum yield (●) and killing power of oligothiophenes (■), all versus the number of rings, n .

In any case, the strong implication is that both the solubility in a hydrophobic phase in the products and ϕ_{Δ} are important with regard to killing power. If instead of ϕ_{Δ} , the ϕ_T is used it is not possible to reproduce the relative location of the killing power of $\alpha 2$ compared to the rest (it is predicted to be about equal to that of $\alpha 3$). The data above regarding the comparative use of ϕ_{Δ} and ϕ_T indicate that phototoxicity very probably directly involves singlet oxygen produced via energy transfer from the triplet state of the oligothiophenes.

C. Coumarins and Thione Coumarins

Coumarins have the basic structure:



where substitutions can be made to all positions. They are not only important in themselves but also because they constitute the principal moiety present in psoralens - see section D. The thione coumarins are those where $-C=O$ has become $-C=S$, sulfur replacing oxygen. As we will see, this has a dramatic effect on the photophysical properties and the UV-A and visible light photobiological activity by comparison to the coumarins ($-C=O$).

Studies of the spectroscopy and photophysical properties of several coumarins have appeared recently

and well as for the thione coumarins²⁰⁻²².

The photophysical behaviour of coumarin is largely dictated by a high degree ($\geq 98\%$) of internal conversion from S_1 where S_1 is a n,π^* state, which remains the lowest state in any solvent. The lifetime of S_1 is dictated by the rate constant of the non-radiative/internal conversion process $\geq 1 \times 10^9 \text{ s}^{-1}$. Various substitutions and their number have substantial effect on the fluorescence quantum yield, ϕ_F , triplet formation quantum yield, ϕ_T , and internal conversion. For example, for 3-chlorocoumarin, ϕ_F has a maximum value of 0.02 in dioxane- H_2O (1:4) mixtures and the non-radiative path from $S_1 \rightarrow S_0$ (vs. $S_1 \rightarrow T_1$) is dominant as before. On the other hand, 7-methoxy-4-methyl substitution results in substantial fluorescence in the same dioxane:water mixture as above (0.62 yield). Finally the presence of all three substituents, chloro, methyl and methoxy result in reasonable fluorescence in the dioxane:water mixtures (0.83 yield). In other solvents as cyclohexane and dioxane, fluorescence of the three-substituted compounds is many times more intense than for the other compounds. The cause of all this is a function of what excited state is lowest ($n\pi^*$ vs. π,π^*) and what degree of mixing between the $\pi^*\pi$ and lower n,π^* exists. In the case of coumarin, the lowest excited state is $^1(n,\pi^*)$ and this remains true, independent of the solvent although some $^1(\pi,\pi^*)$ does mix into the lower $^1(n\pi^*)$ in the case of water or a high percentage of H_2O in solvent mixtures. In the other extreme, the trisubstituted coumarin has a $^1(\pi,\pi^*)$ state lowest in water containing solvent mixtures. The other substituted coumarins have an $^1(n,\pi^*)$ state lowest in all solvents but various degrees of mixing of $^1(\pi^*,\pi^*)$ into $^1(n,\pi^*)$ occur depending on solvent polarity (increased polarity, increased mixing) and the nature and number of substituents.

The yield of triplet formation in coumarin appears to be low in a nonpolar solvent (~ 0.03). For the trisubstituted case, the ϕ_T is low in a non-polar aliphatic hydrocarbon solvent, higher in benzene and maybe as high as 0.2 in dichloromethane. The ϕ_T of other substituted compounds is not known. In any event it is clear that only substituted coumarins have a chance to be good photosensitizers and likely, those with multi-substitution would have the best chance since the effectiveness as a biosensitizer is largely dependent on the presence of triplet states and the higher the ϕ_T the better.

Before we discuss some biological data, we will consider the thione coumarins. These compounds as others (see below) were synthesized with the specific goals (1) to shift the absorption spectrum as far as possible into the visible region (or UVA), (2) to increase the quantum yield of triplet formation, ϕ_T and (3) to increase the quantum yield of singlet oxygen formation, ϕ_{Δ} . In Figure 7, the absorption spectra of coumarin and thione coumarin and some other representative photosensitizers (chromone, psoralen and flavone) and their synthetic thione analogues are shown.

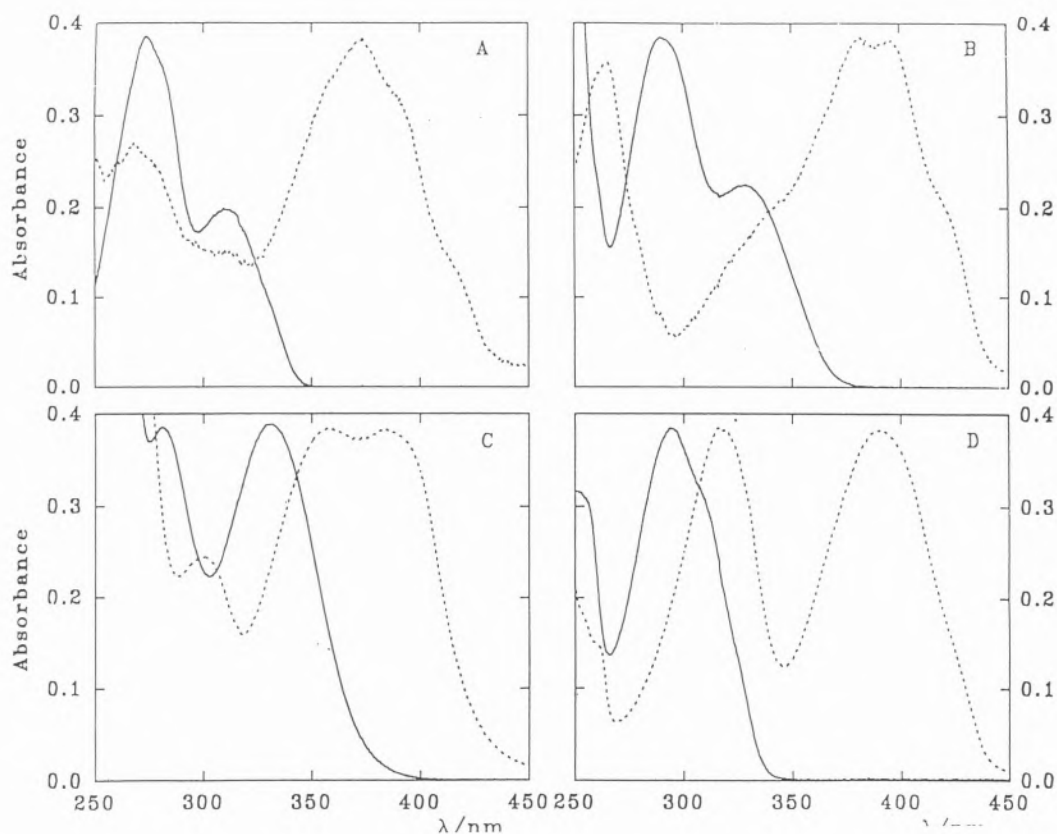


Figure 7 - Absorption spectra of (—) the natural compounds and (---) their thione analogues in methanol: A coumarin and thionecoumarin; B psoralen and thionepsoralen; C khellin and thionekhellin; D flavone and thioneflavone.

Note the dramatic effect of the insertion of sulfur in place of oxygen in the ketone/carbonyl group on the absorption range. Clearly, the thione absorption strongly overlaps with natural (sun) light emission, in contrast with that of their natural counterparts.

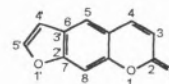
In contrast to coumarin, the thione coumarin has $\phi_T \sim 0.75$ (vs. 0.03-0.04 for coumarin). Although we do not have quantitative data on all of the thiones of the substituted coumarins discussed above, it is clear based on the other cases of $-C=S$ compared to $-C=O$ including the psoralens²⁰, that they will have higher ϕ_T values than their carbonyl counterparts discussed earlier.

Some relatively newer data^{23,24} on coumarins and thione coumarins have compared the effectiveness of these as phototoxins using mutant *E. coli*²³ and fungi²⁴. In the case of the *E. coli*, the thione coumarin was highly active with UV-A where coumarin could not even be activated. For the case of fungi, *F. culmorum*, growth could be effectively photoinhibited by UV-A irradiation of thione coumarin and several differently substituted ones²⁴. Coumarin was inactive and the other substituted coumarins were not active as their thione counterparts. Moreover, and importantly, the thione coumarins were phototoxic

with visible light whereas coumarins themselves in general were not at all phototoxic (see also Table 6).

D. Psoralens and Thione Psoralens

Seemingly significant information is available on several psoralens regarding the photophysical properties. However, there are some substantial problems with some of the ϕ_T data in terms of inconsistency, the use of an absorption coefficient for one solvent being assumed in another, and solvent dependence (particularly involving water and water-containing solutions). In the case of the parent psoralen²⁵,



it has been shown the ϕ_T varies significantly with solvent polarity for example as measured by $E_T(30)$, being 0.01 in hexane and 0.55 in water. Also, in water-containing solutions such as dioxane: H_2O , ϕ_T varied from 0.06 (2.75 M H_2O) to 0.49 (49.5 M H_2O). Similar results also occur for 5-methoxypsoralen²⁶: in dioxane ($T=0.09$) whereas in pure water ϕ_T 0.01; however at intermediate water concentrations the ϕ_T maximized (0.30) in the 5.5-11 M H_2O region then decreased ($\phi_T = 0.03$ in 33 M H_2O). The 8-methoxypsoralen also has a solvent dependence for ϕ_T

being 0.08 in dioxane, which increases in value to about 20% water and then decreases to 0.01 in 70% water²⁷.

Later results²⁰ in other solvents found for psoralen, that $\phi_T = 0.1$ in methanol, for 8-methoxypsoralen $\phi_T \leq 0.02$ in benzene and for 4,5,8-trimethylpsoralen, $\phi_T = 0.26$ in methanol.

It can be seen that the nature of the environment is very important in determining ϕ_T for psoralens. Thus, since a large portion of the phototoxic potency depends on the occupancy of the triplet state, variable response from the psoralens could be expected depending on the environment in the site of action/target. Psoralens have been studied extensively regarding photochemical activity and photobiological effects²⁸ but much of the attention has been on the [2+2] cycloaddition to DNA and the constituent bases. In vivo, reactions are not only with DNA but proteins and lipids.

Recall that several mechanisms exist for phototo-

xic reactions including reaction with singlet oxygen obtained (by energy transfer from triplet state psoralens), electron transfer to O_2 form to O_2^- (superoxide ion) and direct interaction of excited psoralens with biomolecules. Also recent, *in vitro* photolysis of psoralen (and the 8-methoxy derivative) has shown the formation of a number of one and two ring compounds containing carbonyl and hydroxyl substitutions²⁹. It is not known if these are also produced in vivo but if they are, they could also act as phototoxic agents.

Recent results³⁰ (as well as earlier ones) have shown that in particular 8-methoxypsoralen is very mutagenic based on the sensitivity of a series of mutant *E. coli* to inactivation by various phototoxins. The corresponding thione was also phototoxic although the mechanisms seemed more diverse than for 8-methoxypsoralen itself.

Very recent studies on a fungi, *Fusarium culmorum*, (Table 6)²⁴ showed that the parent psoralen and

Table 6 - Photo-inhibition of *Fusarium culmorum* after 3 days growth on silica gel plates as evaluated from the diameter of the inhibition zones, under UVA and VIS light.

Natural Compounds	Photo Inhibition (cm)		Thione Compounds	Photo Inhibition (cm)	
	UVA ^a	VIS ^b		UVA ^a	VIS ^b
Coumarins					
Coumarin	0	0	Thionecoumarin	1.3	0.5
6-Methylcoumarin	0	0	6-Methylthionecoumarin	1.4	1.0
7-Methoxycoumarin	1.3	0	7-Methoxythionecoumarin	1.0	1.4
7-Methoxy-4-methylcoumarin	1.5	0			
7-Hydroxy-4-methylcoumarin	0	0			
3-Chlorocoumarin	0.7	0	3-Chlorothionecoumarin	1.3	1.3
3-Chloro-7-hydroxy-4-methylcoumarin	0	0			
3-Chloro-7-methoxy-4-methylcoumarin	1.1	1.1			
Coumaphos	0	0			
Furanocoumarins					
Psoralen	1.9	0 ^c (2.0)	Thionepsoralen	1.9	1.4
4,5',8-Trimethylpsoralen	1.9	0 ^c (1.8)	4,5',8-Trimethylthionepsoralen	2.1	1.6
5-Methoxypsoralen	3.5	0 ^c (2.0)	5-Methoxythionepsoralen	3.4	1.7
8-Methoxypsoralen	3.6	0 ^c (2.2)	8-Methoxythionepsoralen	3.0	1.5
Furanochromones					
Khellin	1.4	0	Thionekhellin	0	0
Visagin	2.0	-			

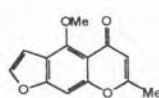
a - Philips lamps; b - Osram lamps; c - Xenon lamp with cut-off filter

three differently substituted ones were quite phototoxic with UV-A light.

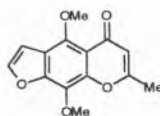
Furthermore, the thione analogs of all of these are essentially equally phototoxic with UV-A light. However, when *visible light* only was employed, none of the *psoralens* (same four as before) could be photoactivated and therefore they were not phototoxins. In contrast, *visible light* irradiation of the *thione* analogs *did* cause significant toxic activity and therefore the thiones are effective phototoxins with visible light.

E. Chromones, Furanochromones and their Thionederivatives

Visnagin and khellin, are natural photosensitizers occurring in species of *Ammi* (Apiaceae), which present structural similarities with 5-methoxypsoralen and 5,8-dimethoxypsoralen.



Visnagin



Khellin

Extracts of these plants and compounds purified from the extracts have long standing medicinal applications, and particularly visnagin and khellin have been referred to as being phototoxic to cells and micro-organisms.

Photoactivity tests of these furanochromones towards *Fusarium culmorum*^{24,31} as biological target (Table 6) showed that visnagin was significantly more phototoxic than khellin, as previously found in studies with other target organisms.

The radiative, k_f , and the internal conversion, k_{ic} , rate constants of visnagin and khellin strongly depend on the solvent, namely on its hydrogen bonding ability and polarity³¹. For both compounds the $S_1 \leftarrow S_0$ transition is predicted to be n,π^* in the gas phase and the energy difference between the $S_2(\pi,\pi^*)$ and the $S_1(n,\pi^*)$ states is predicted to be smaller in khellin. These results are compatible with the total absence of fluorescence of visnagin in nonpolar solvents (cyclohexane or dioxane) and the very weak fluorescence of khellin in the same solvents. The lowest energy band observed in the absorption spectra is assigned to the $S_2 \leftarrow S_0 \pi,\pi^*$ transition in accordance with the solvent bathochromic shifts and the extinction coefficient values. The appearance of fluorescence with the addition of water is due to the solvent induced $n\pi^*-\pi\pi^*$ mixing and/or inversion.

In a plot of k_{ic} as a function of the water fraction two trends of variation are observed: at the earlier stages of water addition, k_{ic} decreases, passes through a minimum and then increases with further addition of water.

The sharp decrease of k_{ic} with the initial addition of water is comparable to our previous findings with coumarins²¹ and psoralens²⁷, where the two first singlet states also are $n\pi^*$ and $\pi\pi^*$ states. This was rationalized on the basis of a decrease of the "proximity effect" of the $n\pi^*$ and the $\pi\pi^*$ states with addition of water²².

The reasons for the increase of k_{ic} at higher water concentrations are not straight forward if we consider that this effect is one order of magnitude larger in khellin than in visnagin. It is also present in the case of psoralens but it is absent in the case of coumarins. However, a plot of k_{ic} as a function of the emission wavelength, instead of the v/v fraction of water, for visnagin, khellin, 4-methyl, 3-chloro, 7-methoxy coumarin and 5-methoxy psoralen shows that the response of k_{ic} to the difference in the energies of S_1 and S_0 , is identical for all four compounds. That is, k_{ic} increases with the decrease of the S_0-S_1 energy gap, according to the "golden rule" for radiationless transitions.

The increase of k_{ic} at high water concentrations implies that the quantum yield of the triplet formation (ϕ_T) is a decreasing function of the water content for both compounds. Despite the similarity of the triplet formation quantum yields in non protic solvents, ϕ_T of visnagin is larger than that of khellin in the range of water concentrations expected in the vicinity of biological targets. Therefore, it is possible that the lower phototoxicity of khellin is due to its lower triplet formation quantum yield. Note that here, as well as with other compounds such as psoralens, where the photophysical properties are strongly solvent dependent, we must have some clue of the polarity and/or water content of the target environment in the organism in order to establish whether there is some correlation between ϕ_T and the photobiological activity.

The thione derivative of khellin is inactive towards *F. culmorum* (see Table 6), in contrast with the thionecoumarins and thionepsoralens. The most probable reason for this absence of activity is the dramatic decrease of triplet lifetimes upon substitution (Table 7)²⁰.

Table 7 - Triplet-Triplet Absorption Wavelength Maxima, $\lambda(T_n \leftarrow T_1)$, and Triplet Lifetimes of Furanochromones and Thione Analogues in Methanol, at 295 K²⁰.

Compound	$\lambda(T_n \leftarrow T_1)/\text{nm}$	$\tau_T/\mu\text{s}$
chromone	630	0.20
thionechromone	460	0.23
visnagin	380	25
thionervisnagin	-(a)	-
khellin	355	70
thionekhellin	-(a)	0.1

(a) no T-T absorption spectrum could be obtained

Flavones constitute a very important group of natural compounds belonging to the chromone family. Up to now we have tested 8 of these compounds, none of them displaying phototoxic activity. Despite this, some of their thione derivatives are photoactive towards *F. culmorum*. This result opens the interesting possibility of synthesizing phototoxic thione derivatives which, after accomplishing their job, revert back to the original non photoactive natural compounds, under natural hydrolyzing conditions.

8. Conclusions

It can be seen that a great number of naturally occurring and synthetic compounds could be potential biological photosensitizers, directly or via the production of singlet oxygen. Certain fundamental requirements are important regarding photophysical characteristics of good photosensitizers: (1) in general a large population of the triplet state should be present, (2) the energy of the triplet should be high enough to induce any of several types of photoreactions, as described in this review, and/or formation of singlet oxygen and (3) the lifetime of the triplet state should be relatively long.

Even if all of the foregoing characteristics were optimum, it is still necessary that the phototoxin be able to penetrate to a biological molecular target site. Thus, chemical and structural aspects of the molecule must be considered in any design of a phototoxin.

A wide variety of biological systems have been examined as targets including fungi, insects, viruses, algae, yeasts, larvae, bacteria, humans (in the form of photochemotherapy) and others. There is developing a considerable body of data regarding the molecular level of action of phototoxins which include photo-oxidation, side chain degradation, cyclobutane adduct formation (in DNA), among others.

Notable successes have been obtained employing several classes of compounds as phototoxins, for example, thione compounds of natural and synthetic coumarins, psoralens, chromones and furanochromones. The improvements include (1) significant *absorption of sunlight* without loss of photoactivity per excited molecule, (2) increase in the *quantum yields of triplet and the singlet oxygen formation* (most phototoxic mechanisms involve the triplet state directly or indirectly), (3) good *efficiency* (they are photoactive against *F. culmorum*, which has been referred to as difficult to control) and (4) probable *bio or photodegradability* (thiones are efficiently hydrolyzed back to their natural parent compounds under varying environmental conditions). Therefore, although there are still several open questions regarding the photoactivity mechanisms, such as the location of the photosensitizer in the fungus and the kinetics of photo/thermal degradation of these compounds, we think that these results are encouraging for the possible utilization of thione analogues of natural

compounds in the control of phytopathogenic fungi.

Also, some of the oligothiophenes are quite biologically active and newly available photophysical data should help shed new light on the mechanism of their action.

Finally, new and developing photophysical information on a variety of β -carboline and flavones should provide valuable leads towards the determination of the modalities of their phototoxic action.

References

1. R. S. Becker *Theory and Interpretation of Fluorescence and Phosphorescence*, Wiley-Interscience, New York, N.Y., 1969.
2. R. S. Becker, S. Das, S. Chakravorti and A. Morgan, *J. Photochem. Photobiol., Section B: Biology*, **10** (1991) 345.
3. S. K. Chattopadhyay, C. V. Kumar, P. K. Das, *J. Photochem.* **18** (1984) 293; **30** (1985) 81.
4. C. N. Knox, E. J. Land and T. G. Truscott, *Photochem. Photobiol.*, **43** (1986) 359.
5. J. J. M. Lamberts and D. C. Nekkers, *Tetrahedron*, **41** (1985) 2183.
6. J. P. Keene, D. Kessel, E. J. Land, R. W. Redmond and T. G. Truscott, *Photochem. Photobiol.*, **43**.
7. D. Oelkrug, H. S. Egelhoff and F. Wilkinson; *J. Fluores.*, **5** (1995) 165.
8. R. S. Becker, J. Seixas de Melo, A. L. Maçanita and F. Elisei, *J. Phys. Chem.* (1995), submitted for publication.
9. R. S. Becker, S. Chakravorti and S. Das, *Photochem. Photobiol.* **51** (1990) 533.
10. A. Dias, A. P. Varela, M. da Graça Miguel, A. L. Maçanita and R. S. Becker, *J. Phys. Chem.* **96** (1992) 10292.
11. G. D. Pimprikar and M. J. Coign, "Light Activated Pesticides", ed. J. K. Heitz and H. R. Downum, ACS Symposium 339, Washington, DC, 1987, 34-155.
12. R. S. Becker, F. Elisei and A. L. Maçanita, unpublished results.
13. R. A. Larson, K. A. Tuveson, M. R. Berenbaum, *Photochem. Photobiol.* **48** (1988) 665.
14. J. B. Hudson, A. Graham, R. Fong, L. L. Hudson and G. H. N. Towers, *Photochem. Photobiol.* **44** (1984) 483.
15. D. J. McKenna and G. H. N. Towers, *Phytochem.* **20** (1981) 1001.
16. J. B. Hudson and G. H. N. Towers, *Photochem. Photobiol.* **48** (1988) 289.
17. K. H. Chae and H. S. Ham, *Bull. Korean Chem Soc.* **7** (1986) 478.
18. R. S. Becker, J. Seixas de Melo, A. L. Maçanita and F. Elisei, *Pure and Appl. Chem.* **67** (1995) 9.
19. A. Lopes, M. L. Borges, J. S. Melo, I. Pais, O. Matos, F. Elisei and R. S. Becker, *Proc. of the XVllth International Photochemistry Conference*, London (1995) pp.
20. R. S. Becker, S. Chakravorti, C. A. Gartner and M. G. Miguel, *J. Chem. Soc., Faraday Trans.* **89**, (1993) 1007.
21. J. S. de Melo, R. S. Becker and A. L. Maçanita, *J. Phys. Chem.* **98** (1994) 6054.
22. J. S. de Melo, R. S. Becker, F. Elisei and A. L. Maçanita, submitted.
23. R. W. Tuveson, G. Wong and R. S. Becker, *Photochem. Photobiol.* **56** (1992) 34.
24. M. L. Borges, O. C. Matos, I. Pais, J. S. de Melo, C. P. Ricardo, A. L. Maçanita and R. S. Becker, *Pestic. Sci.*, **44** (1995).
25. T. S. e Melo, M. Bazin, J. C. Ronford-Haret, R. Santus, *Photochem. Photobiol.*, **58** (1993) 19.

26. T. S. e Melo, A. L. Maçanita, M. Prieto, M. Bazin, J. C. Ronford-Haret and R. Santus, *Photochem. Photobiol.* **48** (1988) 429.
27. T. S. e Melo, L. Ribeiro, A. Maçanita, M. Bazin, J. C. Ronford-Haret and R. Santus, *Int. Conf. Luminescence*, Lisbon, 1990.
28. F. Dall'Acqua, S. Caffieri, G. Rodighiero in Primary Photo-Processes in *Biology and Medicine*, NATO ASI series, Plenum Press, N.Y., PP260-272, 1985.
29. K. A. Marley and R. A. Larson, *Photochem. Photobiol.* **59** (1994) 503.
30. R. W. Tuveson, G. Wong and R. S. Becker, *Photochem. Photobiol.* **56** (1992) 34 and references therein.
31. Marta L. Borges, L. Latterini, F. Elisei, R. S. Becker and A. L. Maçanita, to be published.

